DISS. ETH NO. 26521

FUNCTIONAL ANALYSES OF CANDIDATE QTL GENES INVOLVED IN FUNGAL VIRULENCE

A thesis submitted to attain the degree of

DOCTOR OF SCIENCES of ETH ZURICH

(Dr. sc. ETH Zurich)

presented by

LUKAS MEILE

MSc ETH Biology, ETH Zurich

born on 25.05.1989

citizen of Mosnang (SG)

accepted on the recommendation of

Prof. Dr. Bruce McDonald,
Prof. Dr. Olivier Voinnet,
Prof. Dr. Antonio Di Pietro

2019

Contents

Summary

Plant pathogenic fungi impose a major threat to agricultural food production. The control of fungal crop diseases is challenging because many pathogens can rapidly evolve virulence on resistant crop varieties. Despite the great threat, little is known about the molecular components involved in the interaction between plants and pathogens. This is especially true for non-model pathogens. The aim of this doctoral thesis was to improve our understanding of the genetic basis of virulence and host adaptation, which will be required to generate new innovations for disease control and to increase the spectrum and durability of genetic resistance.

The ascomycete fungus *Zymoseptoria tritici* is the causal agent of septoria tritici blotch (STB), the most damaging disease of wheat in Europe. *Z. tritici* populations exhibit high levels of genetic and phenotypic diversity and a high degree of strain-host specificity. To understand the genetic basis of quantitative strain-specific virulence in *Z. tritici*, functional validation of candidate genes present in a previously identified quantitative trait locus (QTL) was undertaken. By performing gene deletion and allelic replacement experiments, a small secreted protein was identified as key determinant of the quantitative virulence difference between two *Z. tritici* strains. This protein, Avr3D1, fulfilled the hallmarks of a classic effector, including a high cysteine content and *in planta*-specific expression, and was found to act as an avirulence factor involved in a minor gene-for-gene interaction. The corresponding wheat resistance gene, possibly *Stb7* or *Stb12*, was present in four out of 17 wheat lines.

Avr3D1 was present in all the genomes of 135 investigated strains, was highly diverse and showed signs of diversifying selection, indicating an important role in pathogen fitness in susceptible hosts; however, such a role remains to be identified.

The characterization of several protein isoforms of Avr3D1 revealed a continuous range of avirulence activity and several candidate residues that additively contributed to escape from recognition. A homologue of Avr3D1 identified in a sister species of *Z. tritici*, which does not infect wheat, triggered a strong immune response in wheat, raising the possibility that this avirulence factor also contributes to nonhost resistance.

Avr3D1 is located in a highly plastic region of the genome, featuring a lack of synteny caused by presence/absence polymorphisms of various transposable elements (TEs) but also of genes adjacent to *Avr3D1*. This observation is in line with the two-speed-genome model, which suggests that effector genes located in these dynamic regions benefit from an accelerated evolution, which is a driver of host adaptation. We investigated whether the location of effector genes in genomic regions rich in TEs might also have functional consequences mediated by the heterochromatic nature of these regions. The genomic environment of *Avr3D1* and additional effector genes was indeed found to influence their high transcriptional inducibility. Several histone modifications contributed to effector gene silencing in the absence of the host. Host colonization led to effector gene de-repression, which was associated with a decrease in histone H3 lysine 9 and lysine 27 trimethylation levels. Engineering the *Z. tritici* genome with fluorescent reporter genes revealed that effector gene de-repression is regulated at the single-cell level and likely requires gene-specific transcription factors.

Our results indicate that the high virulence diversity observed in pathogen populations could be largely based on avirulence factor diversity. We further highlight the high complexity of effector gene regulation, which features host-triggered

chromatin remodeling and cell-specific expression profiles. Hence, we provide new insights into the regulation and diversity of virulence in fungal plant pathogens.

Zusammenfassung

Pflanzenpathogene Pilze stellen ein grosses Problem für die Landwirtschaft dar, da sie immense Ernteausfälle verursachen können. Gegenmassnahmen sind häufig nur bedingt wirksam, unter anderem weil verfügbare resistente Sorten wegen der hohen Anpassungsfähigkeit vieler Krankheitserreger schnell anfällig werden können. Angesichts der Gefahr für die Landwirtschaft und Ernährungssicherheit, die von Pflanzenkrankheiten ausgeht, ist ein besseres Verständnis der molekularen Interaktionen zwischen Pflanzen und ihren Krankheitserregern von grossem Interesse, weil dieses Wissen ein Grundstein für die Entwicklung neuer Konzepte und Technologien für die Krankheitsbekämpfung darstellen kann. Aus diesem Grund war es das Ziel dieser Doktorarbeit, zu verstehen, welche Gene von pflanzenpathogenen Pilzen Schlüsselfunktionen für die Infektion haben und wie sich solche Pilze an resistente Sorten anpassen können.

Zymoseptoria tritici ist ein Pilz, der die Septoria-Blattdürre des Weizens verursacht. Verschiedene Stämme dieses Pilzes können extrem vielfältig sein, sowohl in Bezug auf ihre Genetik als auch auf ihren Phänotyp. In der Regel kann ein bestimmter Stamm nur bestimmte Weizensorten befallen, im Gegenzug ist selbst eine resistente Sorte üblicherweise nicht gegen alle Pilzstämme resistent. Ausserdem gibt es, je nach Stamm, zahlreiche Abstufungen zwischen Resistenz und Anfälligkeit. Um diese Spezifität zwischen Pilzstämmen und Weizensorten besser zu verstehen, habe ich im Zuge dieser Doktorarbeit in *Z. tritici* nach Genen gesucht, die einen sortenspezifischen Einfluss auf die Virulenz haben. Dazu habe ich die Funktion von verschiedenen Genen in einem bereits bekannten quantitativen «Trait Locus» für Virulenz validiert. Dabei hat sich gezeigt, dass ein kleines Protein, welches als

potentielles Effektor-Protein identifiziert wurde, grösstenteils verantwortlich war für den Unterschied in der Virulenz zwischen zwei *Z.tritici*-Stämmen. Dieses Cystein-reiche Protein, bezeichnet als Avr3D1, ist ein Avirulenzfaktor, der in bestimmten Weizensorten eine partielle Resistenzreaktion hervorruft. Das entsprechende (und bisher noch nicht isolierte) Resistenzgen war in vier von 17 Weizensorten vorhanden und es handelt sich dabei womöglich um *Stb7* oder *Stb12*.

Avr3D1 konnte in sämtlichen 135 untersuchten *Z. tritici*-Stämmen identifiziert werden. Die kodierende DNA-Sequenz dieses Gens ist sehr variabel und stand offenbar unter diversifizierender Selektion, was darauf hindeutet, dass Avr3D1 wahrscheinlich eine wichtige Funktion für *Z. tritici* besitzt. Bei der Charakterisierung von verschiedenen Avr3D1-Isoformen zeigte sich ein kontinuierliches Spektrum von Avirulenz-Aktivität. Es konnten auch verschiedene Protein-Reste identifiziert werden, die kumulativ dazu beitragen, dass Avr3D1 nicht (vollständig) vom entsprechenden Resistenz-Protein erkannt werden kann. Ein homologes Protein, das in einer verwandten Spezies, welche auf Weizen nicht virulent ist, identifiziert wurde, löste in Weizen eine starke Resistenzreaktion aus, woraus sich schliessen lässt, das Avr3D1 möglicherweise auch an Nichtwirtsresistenz beteiligt ist. Das Gen *Avr3D1* befindet sich in einer instabilen Genom-Region, welche von einem hohen Grad an Transposon-An-/Abwesenheitspolymorphismus geprägt ist. Solche Regionen sind oft mit Effektor-Genen assoziiert, womöglich weil sie deren Evolutionsrate günstig beeinflussen für eine optimierte Anpassung an verschiedene Wirtspflanzen. Wir haben untersucht, ob diese Transposon-assoziierten Regionen mit Blick auf ihre typische Heterochromatin-Struktur auch einen Einfluss auf die Transkriptionsregulierung von Effektor-Genen haben. Abhängig von der genomischen Umgebung trugen mehrere post-translationale Histon-Modifikationen dazu bei, dass die Transkription verschiedener

Effektor-Gene in axenischer Kultur epigenetisch unterdrückt wurde. Während einer Infektion hingegen wurden die Effektor-Gene aktiviert, was mit einer Änderung des Ausmasses dieser Histon-Modifikationen einherging.

Zusammenfassend legen diese Resultate nahe, dass die hohe Virulenz-Diversität, die typischerweise mit Pflanzenpathogenen assoziiert ist, möglicherweise grösstenteils auf der Sequenz-Diversität von Avirulenzfaktoren basiert. Es hat sich auch gezeigt, dass die Regulation von Effektor-Genen ein hohes Mass an Komplexität aufweist und unter dem Einfluss von Wirtspflanzen-induzierten Chromatin-Neukonfigurationen steht. Diese Arbeit erlaubt somit neue Einblicke in die Regulation und die Diversität der Virulenz von pflanzenpathogenen Pilzen.

General introduction

General overview

Plants, including food crops, are under constant disease pressure. Fungal plant diseases pose a great and increasing threat to food security (Fisher *et al.*, 2012; Bebber & Gurr, 2015). In addition to fungicides, the control of fungal diseases mainly relies on genetic resistance. Due to worldwide emerging fungicide resistance in recent years, the development of new control strategies including new sources of genetic resistance is expected to be essential for future food security (Fisher *et al.*, 2012; Michelmore *et al.*, 2017). Although genetic resistance is generally regarded as a cheap and safe crop protection approach (Michelmore *et al.*, 2017), it can be overcome, especially by pathogens with a high evolutionary potential (McDonald & Linde, 2002). A well-known example of how emerging races of pathogens that defeat host resistance can threaten crop production is the wheat stem rust fungus *Puccinia graminis f.sp. tritici* (*Pgt*). Several *Pgt* races within the Ug99 lineage, which emerged 20 years ago in Uganda, became virulent on most wheat cultivars grown worldwide and new virulent races continue to emerge (Njau *et al.*, 2010; Singh *et al.*, 2011; Chen *et al.*, 2017). In addition to the emergence of new virulent races, the defeat of host resistance is also associated with an extension of the host range of certain pathogens and, consequently, with the emergence of new diseases. For example, the wheat blast disease, which recently caused severe damage in East Asia, is thought to have emerged through a combination of using less resistant wheat cultivars and of overcoming the remaining genetic resistance by the pathogen (Inoue *et al.*, 2017). To fight emerging diseases and increasing disease severity and to

improve the durability of genetic resistance, a profound understanding of pathogenesis, host evasion and pathogen evolution is needed.

Molecular components of host-pathogen interactions

Plants and symbiotic organisms establish an intimate relationship, in which both interactors deploy specialized molecular weapons. Only in rare cases these interactions culminate in disease (Heath, 2000; Thordal-Christensen, 2003). The main reason for this is the robust plant immune system, which prevents the infection by most potential pathogens. Pathogens need to circumvent this immune system in order to successfully complete their life cycle (Jones & Dangl, 2006; Cook *et al.*, 2015). In some cases, microorganisms are strongly specialized and can only infect one plant species, while others have a broader host range and infect several plant species that are not closely related (Heath, 2000; Thordal-Christensen, 2003).

Plants detect colonizing microorganisms through receptor proteins that respond to conserved microbial and plant molecules that are released or exposed during infection. These molecules are known as microbe-associated molecular patterns (MAMPs) if they are of microbial origin and as damage associated molecular patterns (DAMPs) if they are of plant origin. In both cases, their recognition triggers a basal defence response against adapted and nonadapted pathogens (Jones & Dangl, 2006; Sánchez-Vallet *et al.*, 2015; Ayliffe & Sørensen, 2019). Success in infection comes along with abolishing the immune response, which is frequently achieved by the secretion of so-called effectors. Effectors are secreted molecules of different classes, which facilitate host colonization by interfering with the host metabolism or immune system (Hogenhout *et al.*, 2009; Lo Presti *et al.*, 2015). Effectors of proteinaceous nature are frequently of small size and rich in cysteines (Duplessis *et*

al., 2011; van der Does & Rep, 2017). Frequently, numerous disulphide bridges in the tertiary structure of effectors provide stability under the non-optimal conditions of the apoplast. Although effector proteins are frequently not conserved among different species, different independently evolved effectors have sometimes been shown to converge onto the same host targets or even to share structural similarities (Mukhtar *et al.*, 2011; de Guillen *et al.*, 2015; Fiorin *et al.*, 2018). Although the functions of most effectors remain enigmatic, several well-characterized effectors are known to be involved in preventing the induction of the immune response. Various pathogens have been shown to prevent the detection of chitin a major component of the fungal cell wall, as a critical step for host colonization (Sánchez-Vallet *et al.*, 2015). Strategies to prevent chitin-triggered immunity have evolved independently in different fungal pathogens. For example, several fungal species secrete LysM effectors to sequester chitin oligomers (Jonge *et al.*, 2010; Sánchez-Vallet *et al.*, 2013; Kombrink *et al.*, 2017), while the pathogen *Moniliophthora perniciosa* secretes an inactive chitinase for the same purpose (Fiorin *et al.*, 2018). Another fungal core effector, NIS1, was recently shown to target host immune kinases associated with plant receptors (Irieda *et al.*, 2019). Several effectors inhibit plant papain-like cysteine proteases to suppress the defense response of the host (Hörger & van der Hoorn, 2013; Misas Villamil *et al.*, 2019). These examples of effectors involve targeting general components of the host immune system. However, effector function can also be highly specialized towards only certain hosts and the compatibility between the effector and the host target is proposed to define the outcome of the interaction (Ayliffe & Sørensen, 2019). Some necrotrophic pathogens hijack the immune response by secreting host-specific necrotrophic effectors that target specific receptors, promoting host cell death and pathogen proliferation (Friesen *et al.*, 2008; McDonald & Solomon, 2018).Similarly, host adaptation of the oomycetes

Phytophthora infestans and *Phytophthora mirabilis* was shown to be linked with specialization of a cystatin-like effector towards its associated target in compatible hosts (Dong *et al.*, 2014).

To defend themselves against pathogens, plants have evolved systems to specifically recognize effectors and subsequently induce an immune response. In a particular host, resistance against certain strains of a pathogen is commonly achieved by plant resistance proteins that specifically recognize certain isoforms of effector proteins, known as avirulence factors (van Kan *et al.*, 1991; Rouxel & Balesdent, 2010). This specific recognition of strains harbouring avirulence factors leads to variability of virulence phenotypes within one pathogen species and has been broadly investigated as a strain-specific barrier (Skamnioti & Ridout, 2005; Bent & Mackey, 2007). The recognition of avirulence factors by resistance proteins can be direct through protein-protein interactions or indirect through the recognition of modified effector targets. The indirect recognition has become known as the guard model (Jones & Dangl, 2006). These two different ways of recognition have distinct implications on how pathogens evade host recognition. The direct recognition of avirulence factors allows the pathogen to modify the sequence of the avirulence factor to escape recognition while preserving the intrinsic effector function. On the other hand, for avirulence factors detected through the guard model, recognition is linked to effector function and escaping recognition would require the loss of effector function, for example by deletion of the avirulence factor (Zhang *et al.*, 2015). As a consequence, avirulence factors detected through the guard model are generally thought to exhibit presence/absence polymorphisms in pathogen populations while directly recognized avirulence factors are more prone to sequence polymorphisms as

a result of selection for escape from recognition (Van der Hoorn *et al.*, 2002; Bent & Mackey, 2007).

A new emerging concept suggests that resistance against adapted and nonadapted pathogens is a continuum and that accumulation of avirulence factors also plays a major role in nonhost resistance (Schulze-Lefert & Panstruga, 2011; Ayliffe & Sørensen, 2019). Accordingly, AvrPm3 recognition by wheat was shown to contribute to host specificity of powdery mildew pathogens isolated from *Dactylis* and rye (Bourras *et al.*, 2019) and loss of a single avirulence factor in *Pyricularia oryzae* contributed to its capacity to infect wheat (Inoue *et al.*, 2017). From the plant side, several typical resistance proteins have been identified to be involved in nonhost resistance in *Brachypodium distachyon* against wheat stripe rust (Bettgenhaeuser *et al.*, 2018; Gilbert *et al.*, 2018). Collectively, these examples indicate that effector recognition contributes to nonhost resistance to nonadapted pathogens.

Host specialization also comes along with a tight regulation of the effector transcriptome. In the case of powdery mildew, altered expression of certain effector genes was suggested to be involved in adaptation to triticale (Praz *et al.*, 2018). Comparative transcriptomics of different *Z. tritici* strains revealed common expression patterns of a subset of effector genes during host colonization. In contrast, other effector genes displayed differential expression between different strains. It was proposed that differential regulation of effector genes in different fungal genotypes is a major determinant of the infection outcome (Haueisen & Stukenbrock, 2016b; Palma-Guerrero *et al.*, 2016). A further demonstration of the role of differential regulation of effector genes in phenotypic diversity was provided in the oomycete *Phytophthora sojae*, in which gene silencing of an avirulence gene was shown to be involved in host evasion (Qutob *et al.*, 2013; Na & Gijzen, 2016).

Mechanisms of effector gene regulation

During infection, the induction of the infection machinery, including effector gene expression, is tightly regulated and required for the pathogen to complete its life cycle (Lo Presti *et al.*, 2015; Sánchez-Vallet *et al.*, 2018). Effectors have highly specific functions during the infection cycle. Accordingly, in several fungal pathogens it has been shown that different subsets of effector genes have distinct expression patterns, according to their function. For example, in *Colletotrichum higginsianum*, *Leptosphaeria maculans*, *Ustilago maydis* and *Z. tritici,* specific expression of effector genes at the different phases of infection was reported (O'Connell *et al.*, 2012; Haueisen & Stukenbrock, 2016a; Palma-Guerrero *et al.*, 2016; Gervais *et al.*, 2017; Matei *et al.*, 2018; Sánchez-Vallet *et al.*, 2018). How coordinated expression pattern of effector genes is achieved remains to be unveiled (Soyer *et al.*, 2015). Some transcription factors involved in regulation of effector genes have been described, including orthologs of Wor1 and Stu1, which regulate effector genes in several fungal species, while other transcription factors were only identified in a single pathogen species (Zahiri *et al.*, 2010; van der Does *et al.*, 2016; Rybak *et al.*, 2017; van der Does & Rep, 2017; Sánchez-Vallet *et al.*, 2018). For some effector genes the genomic environment has been shown to be involved in their specific expression pattern (Soyer *et al.*, 2015). Effector genes are frequently located in regions of the genome that are rich in transposable elements. These regions are typically heterochromatic as a strategy to defend the genome from deleterious effects of active transposable elements (Slotkin & Martienssen, 2007; Hollister & Gaut, 2009). The heterochromatin is not always restricted to the transposable elements, but can also affect adjacent genes (Hollister & Gaut, 2009; Seidl & Thomma, 2017). Thus, effector genes are frequently in heterochromatic and epigenetically silenced regions

of the genome. In the fungal pathogens *Leptosphaeria maculans* and *Fusarium graminearum* effector genes and secondary metabolite gene clusters are heterochromatic (Connolly *et al.*, 2013; Soyer *et al.*, 2014). In the plant symbiont *Epichloë festucae*, secondary metabolite gene clusters involved in host colonization are located in transposable element-rich subtelomeric regions. In the absence of the host, the clusters are silenced, but the interaction with the host leads to de-repression and induction of the biosynthetic genes (Chujo & Scott, 2014). These data suggest that transposable elements and dynamic changes of chromatin during host colonization are key for the expression of effector genes and for the infection.

The wheat-*Zymoseptoria tritici* pathosystem

Wheat is the most broadly cultivated crop in the world with a total cultivated area of 218 billion ha and an estimated production of 771 million tonnes in 2017 (FAO, 2017). The major wheat species cultivated is *Triticum aestivum* (bread wheat), which is hexaploid and originated from the hybridization of emmer wheat (AABB, *Triticcum dicoccoides*) and *Aegilops tauschii* (DD; Salamini *et al.*, 2002). Due to the large size of its genome (16 Gb) and the high content of repeats (approximately 85%), the genome sequencing of wheat has lagged behind compared to other species. Recently, a total of 21 chromosome-like sequences were assembled, with 107.891 high-confidence annotated genes (Appels *et al.*, 2018). This annotated genome will promote a better understanding of important traits, including resistance to biotic stress. In fact, the high-quality genome sequence, together with high-throughput genotyping platforms, already led to the discovery of several disease resistance genes of wheat (Mago *et al.*, 2015; Keller *et al.*, 2018; Saintenac *et al.*, 2018).

Zymoseptoria tritici (formerly *Mycosphaerella graminicola*) is the most damaging pathogen of wheat in temperate climates and the causal agent of septoria tritici blotch (STB; Fones & Gurr, 2015). *Z. tritici* is an ascomycete fungus that is estimated to cause yield losses of up to 50% under conducive conditions (Torriani *et al.*, 2015). *Z. tritici* originated 10'000-11'000 years ago in the Fertile Crescent (Stukenbrock *et al.*, 2007, 2010). Speciation of *Z. tritici* was associated with its adaptation to wheat. Several closely related species of *Z. tritici* have been isolated from wild grasses in the Middle East, including *Zymoseptoria ardabiliae*, which was isolated from *Dactylis glomerata* and *Lolium perenne* and *Zymoseptoria pseudotritici,* which was isolated from *Agropyron repens* and *Dactylis glomerata* (Stukenbrock *et al.*, 2007, 2012). Remarkably, although the related species were collected from wild grasses growing in the proximity of wheat fields, they have never been identified on wheat. Conversely, *Z. tritici* was only identified on wheat plants, consistent with host specialization (Stukenbrock *et al.*, 2010, 2012). The specialization to wheat by *Z. tritici* was suggested to be associated with the acquisition and fixation of advantageous mutations specialized for the new host (Stukenbrock *et al.*, 2010, 2011). Indeed, three genes with signatures of positive selection were shown to be involved in wheat colonization (Poppe *et al.*, 2015).

Z. tritici is a highly diverse pathogen with large effective population sizes and a high evolutionary potential (Zhan *et al.*, 2003; McDonald & Mundt, 2016). The pathogen is difficult to control because it has evolved resistance against most of the fungicides available on the market (Cools & Fraaije, 2013; Karisto *et al.*, 2018). *Z. tritici* dispersal is mediated by airborne sexual ascospores, which can be disseminated over several kilometres, and by asexual pycnidiospores, which are dispersed more locally by rain splash multiple times within one growing season (McDonald & Mundt,

2016). Full genome sequences are available for 19 strains of *Z. tritici* (Goodwin *et al.*, 2011; Plissonneau *et al.*, 2018; Badet *et al.*, 2019). The genome is 40 Mb in size and consists of 13 core chromosomes and 8 accessory chromosomes (Goodwin *et al.*, 2011). Of approximately 11'000 genes that have been annotated in total, around 300 are predicted effector genes (Plissonneau *et al.*, 2018), but only two of them, the LysM effectors, have a well-characterized function (Marshall *et al.*, 2011). Apart from these two effectors, little is known about the molecular components and mechanisms involved in the colonization of wheat. The life cycle of *Z. tritici* is complex and includes an asymptomatic phase, in which the pathogen penetrates through the stomata and grows in the apoplastic space, followed by the necrotrophic phase, in which the asexual reproduction takes place (Kema *et al.*, 1996; Duncan & Howard, 2000; Steinberg, 2015). *Z. tritici* grows strictly intercellularly, although it has an intimate interaction with the host cells (Kema *et al.*, 1996). The asymptomatic infection phase has frequently been associated with a stealth growth of the pathogen, in which the host does not detect the colonizer. In fact, the LysM effectors are critical to prevent recognition in this phase (Marshall *et al.*, 2011; Rudd *et al.*, 2015). The length of this latent phase is variable and depends on the host and pathogen genotypes and on the environmental conditions, but normally lasts between seven and 36 days (Steinberg, 2015). The mechanisms involving the induction of the host cell death remain unclear, but it is associated with the induction of certain cell wall degrading enzymes, a secreted ribonuclease and necrosis and ethylene-inducing peptide 1 (Nep1)-like proteins (NLPs) (Motteram *et al.*, 2009; Brunner *et al.*, 2013; Rudd *et al.*, 2015; Kettles *et al.*, 2018).

Twenty-one major resistance genes against *Z. tritici* have been identified in wheat and most of them are strain-specific (Brown *et al.*, 2015). Only one of them, *Stb6* has

been cloned so far (Saintenac *et al.*, 2018) and it has been shown to specifically recognize the effector protein AvrStb6 in a gene-for-gene manner (Brading *et al.*, 2002; Zhong *et al.*, 2017; Kema *et al.*, 2018). In contrast to most of the resistance genes against other pathogens, which typically encode intracellular nucleotide binding leucine-rich repeat receptors, *Stb6* encodes a wall-associated receptor kinase (WAK)-like protein, which is most likely located in the plasma membrane (Saintenac *et al.*, 2018).

Thesis outline and research questions

With the identification of several molecular components involved in pathogenicity, advances in our knowledge on the molecular bases of virulence in fungal plant pathogens have been made. However, for many economically relevant fungal pathogens the molecular understanding of virulence lags behind more established model systems. The increasing availability of high-quality genomic and transcriptomic data provides powerful resources for the identification of new components involved in the virulence of fungal plant pathogens. In this thesis, I addressed the following main biological questions:

1. What are the molecular components involved in virulence and host specificity?
2. How do these components relate to phenotypic diversity?
3. How are effector genes regulated?

This thesis is divided into three chapters:

Chapter 1 aimed to identify genes involved in the quantitative virulence difference between two strains of *Z. tritici*. We validated candidate genes in a previously discovered quantitative trait locus (QTL) for virulence. The chapter describes the discovery and the functional characterization of a highly polymorphic fungal avirulence gene involved in strain-specific partial resistance. Using a large collection of *Z. tritici* genomes, an evolutionary analysis of this gene as well as an in-depth investigation of its peculiar genomic environment is also presented.

Chapter 2 aimed to assess the prevalence of host evasion in a natural population of *Z. tritici* and to elucidate how avirulence factor polymorphisms impact host resistance. Different protein isoforms of the avirulence factor described in chapter 1 were

functionally validated and the role of distinct amino acid substitutions was assessed. This chapter also describes the functional analysis of an avirulence gene homologue present in a sister species of *Z. tritici.*

Chapter 3 aimed to study the role of the heterochromatic environment of different effector genes on their tight expression regulation in *Z. tritici* with a focus on the transcriptional induction associated with *in planta* growth. Effector gene induction was monitored *in planta* using cell biological tools to study expression dynamics of effector genes at the cellular level. This chapter further describes the identification of key chromatin-related epigenetic mechanisms involved in effector gene regulation. Chromatin immunoprecipitation allowed to associate the *in planta* upregulation of effector genes with changes in post-translational histone modifications.

References

Appels R, Eversole K, Feuillet C, Keller B, Rogers J, Stein N, Pozniak CJ, Choulet F, Distelfeld A, Poland J, *et al.* 2018. Shifting the limits in wheat research and breeding using a fully annotated reference genome. *Science* **361**.

Ayliffe M, Sørensen CK. 2019. Plant nonhost resistance: paradigms and new environments. *Current Opinion in Plant Biology* **50**: 104–113.

Badet T, Oggenfuss U, Abraham L, Mcdonald BA, Croll D. 2019. A 19-isolate reference-quality global pangenome for the fungal wheat pathogen *Zymoseptoria tritici*.

Bebber DP, Gurr SJ. 2015. Crop-destroying fungal and oomycete pathogens challenge food security. *Fungal Genetics and Biology* **74**: 62–64.

Bent AF, Mackey D. 2007. Elicitors, effectors, and *R* genes: the new paradigm and a lifetime supply of questions. *Annual Review of Phytopathology* **45**: 399–436.

Bettgenhaeuser J, Gardiner M, Spanner R, Green P, Hernández-Pinzón I, Hubbard A, Ayliffe M, Moscou MJ. 2018. The genetic architecture of colonization resistance in *Brachypodium distachyon* to non-adapted stripe rust (*Puccinia striiformis*) isolates. *PLoS Genetics* **14**: 1–26.

Bourras S, Kunz L, Xue M, Praz CR, Müller MC, Kälin C, Schläfli M, Ackermann P, Flückiger S, Parlange F, *et al.* 2019. The *AvrPm3-Pm3* effector-NLR interactions control both race-specific resistance and host-specificity of cereal mildews on wheat. *Nature Communications* **10**: 2292.

Brading PA, Verstappen ECP, Kema GHJ, Brown JKM. 2002. A gene-for-gene relationship between wheat and *Mycosphaerella graminicola*, the Septoria tritici blotch pathogen. *Phytopathology* **92**: 439–445.

Brown JKM, Chartrain L, Lasserre-Zuber P, Saintenac C. 2015. Genetics of resistance to *Zymoseptoria tritici* and applications to wheat breeding. *Fungal Genetics and Biology : FG & B* **79**: 33–41.

Brunner PC, Torriani SFF, Croll D, Stukenbrock EH, McDonald BA. 2013. Coevolution and life cycle specialization of plant cell wall degrading enzymes in a hemibiotrophic pathogen. *Molecular Biology and Evolution* **30**: 1337–1347.

Chen J, Upadhyaya NM, Ortiz D, Sperschneider J, Li F, Bouton C, Breen S, Dong C, Xu B, Zhang X, *et al.* 2017. Loss of *AvrSr50* by somatic exchange in stem rust leads to virulence for *Sr50* resistance in wheat. *Science* **358**: 1607–1610.

Chujo T, Scott B. 2014. Histone H3K9 and H3K27 methylation regulates fungal alkaloid biosynthesis in a fungal endophyte-plant symbiosis. *Molecular Microbiology* **92**: 413–434.

Connolly LR, Smith KM, Freitag M. 2013. The *Fusarium graminearum* histone H3 K27 methyltransferase KMT6 regulates development and expression of secondary metabolite gene clusters. *PLoS Genetics* **9**: e1003916.

Cook DE, Mesarich CH, Thomma BPHJ. 2015. Understanding plant immunity as a surveillance system to detect invasion. *Annual Review of Phytopathology* **53**: 541–563.

Cools HJ, Fraaije BA. 2013. Update on mechanisms of azole resistance in *Mycosphaerella graminicola* and implications for future control. *Pest Management Science* **69**: 150–155.

van der Does HC, Fokkens L, Yang A, Schmidt SM, Langereis L, Lukasiewicz JM, Hughes TR, Rep M. 2016. Transcription factors encoded on core and accessory chromosomes of *Fusarium oxysporum* induce expression of effector genes. *PLoS Genetics* **12**: e1006401.

van der Does HC, Rep M. 2017. Adaptation to the host environment by plant-pathogenic fungi. *Annual Review of Phytopathology* **55**: 427–450.

Dong S, Stam R, Cano LM, Song J, Sklenar J, Yoshida K, Bozkurt TO, Oliva R, Liu Z, Tian M, *et al.* 2014. Effector specialization in a lineage of the Irish potato famine pathogen. *Science* **343**: 552–555.

Duncan KE, Howard RJ. 2000. Cytological analysis of wheat infection by the leaf blotch pathogen *Mycosphaerella graminicola*. *Mycological Research* **104**: 1074–1082.

Duplessis S, Cuomo CA, Lin Y-C, Aerts A, Tisserant E, Veneault-Fourrey C, Joly DL, Hacquard S, Amselem J, Cantarel BL, *et al.* 2011. Obligate biotrophy features unraveled by the genomic analysis of rust fungi. *Proceedings of the National Academy of Sciences* **108**: 9166–9171.

FAO. 2017. FAO statistical database. Food and Agriculture Organization of the United Nations.

Fiorin GL, Sanchéz-Vallet A, Thomazella DP de T, do Prado PFV, do Nascimento LC, Figueira AV de O, Thomma BPHJ, Pereira GAG, Teixeira PJPL. 2018. Suppression of plant immunity by fungal chitinase-like effectors. *Current Biology* **28**: 3023-3030.e5.

Fisher MC, Henk DA, Briggs CJ, Brownstein JS, Madoff LC, McCraw SL, Gurr SJ. 2012. Emerging fungal threats to animal, plant and ecosystem health. *Nature* **484**: 186–194.

Fones H, Gurr S. 2015. The impact of Septoria tritici Blotch disease on wheat: An EU perspective. *Fungal Genetics and Biology* **79**: 3–7.

Friesen TL, Faris JD, Solomon PS, Oliver RP. 2008. Host-specific toxins: effectors of necrotrophic pathogenicity. *Cellular Microbiology* **10**: 1421–1428.

Gervais J, Plissonneau C, Linglin J, Meyer M, Labadie K, Cruaud C, Fudal I, Rouxel T, Balesdent MH. 2017. Different waves of effector genes with contrasted genomic location are expressed by *Leptosphaeria maculans* during cotyledon and stem colonization of oilseed rape. *Molecular Plant Pathology* **18**: 1113–1126.

Gilbert B, Bettgenhaeuser J, Upadhyaya N, Soliveres M, Singh D, Park RF, Moscou MJ, Ayliffe M. 2018. Components of *Brachypodium distachyon* resistance to nonadapted wheat stripe rust pathogens are simply inherited. *PLoS Genetics* **14**: 1–27.

Goodwin SB, Ben M'Barek S, Dhillon B, Wittenberg AHJ, Crane CF, Hane JK, Foster AJ, Van der Lee TAJ, Grimwood J, Aerts A, *et al.* 2011. Finished genome of the fungal wheat pathogen *Mycosphaerella graminicola* reveals dispensome structure, chromosome plasticity, and stealth pathogenesis. *PLoS Genetics* **7**: e1002070.

de Guillen K, Ortiz-Vallejo D, Gracy J, Fournier E, Kroj T, Padilla A. 2015. Structure analysis uncovers a highly diverse but structurally conserved effector family in

phytopathogenic fungi. *PLoS Pathogens* **11**: 1–27.

Haueisen J, Stukenbrock EH. **2016a**. Life cycle specialization of filamentous pathogens - colonization and reproduction in plant tissues. *Current Opinion in Microbiology* **32**: 31–37.

Haueisen J, Stukenbrock EH. **2016b**. Life cycle specialization of filamentous pathogens - colonization and reproduction in plant tissues. *Current Opinion in Microbiology* **32**: 31–37.

Heath MC. **2000**. Nonhost resistance and nonspecific plant defenses. *Current Opinion in Plant Biology* **3**: 315–319.

Hogenhout SA, Van Der Hoorn RAL, Terauchi R, Kamoun S. **2009**. Emerging concepts in effector biology of plant-associated organisms. *Molecular Plant-Microbe Interactions* **22**: 115–122.

Hollister JD, Gaut BS. **2009**. Epigenetic silencing of transposable elements: a trade-off between reduced transposition and deleterious effects on neighboring gene expression. *Genome research* **19**: 1419–1428.

van der Hoorn RA., De Wit PJG., Joosten MHA. 2002. Balancing selection favors guarding resistance proteins. *Trends in Plant Science* **7**: 67–71.

Hörger AC, van der Hoorn RAL. **2013**. The structural basis of specific protease-inhibitor interactions at the plant-pathogen interface. *Current Opinion in Structural Biology* **23**: 842–850.

Inoue Y, Vy TTP, Yoshida K, Asano H, Mitsuoka C, Asuke S, Anh VL, Cumagun CJR, Chuma I, Terauchi R, *et al.* 2017. Evolution of the wheat blast fungus through functional losses in a host specificity determinant. *Science* **357**: 80–83.

Irieda H, Inoue Y, Mori M, Yamada K, Oshikawa Y, Saitoh H, Uemura A, Terauchi R, Kitakura S, Kosaka A, *et al.* 2019. Conserved fungal effector suppresses PAMP-triggered immunity by targeting plant immune kinases. *Proceedings of the National Academy of Sciences of the United States of America* **116**: 496–505.

Jones JDG, Dangl JL. **2006**. The plant immune system. *Nature* **444**: 323–329.

Jonge R De, Esse HP Van, Kombrink A, Shinya T, Desaki Y, Bours R, Krol S Van Der, Shibuya N, Joosten MHAJ, Thomma BPHJ. **2010**. Conserved fungal LysM effector Ecp6 prevents chitin-triggered immunity in plants. **625**: 6–9.

van Kan JA, van den Ackerveken GF, de Wit PJ. **1991**. Cloning and characterization of cDNA of avirulence gene *avr9* of the fungal pathogen *Cladosporium fulvum*, causal agent of tomato leaf mold. *Molecular plant-microbe interactions : MPMI* **4**: 52–59.

Karisto P, Hund A, Yu K, Anderegg J, Walter A, Mascher F, McDonald BA, Mikaberidze A. **2018**. Ranking quantitative resistance to septoria tritici blotch in elite wheat cultivars using automated image analysis. *Phytopathology* **108**: 568–581.

Keller B, Wicker T, Krattinger SG. **2018**. Advances in wheat and pathogen genomics: implications for disease control. *Annual Review of Phytopathology* **56**: 67–87.

Kema GHJ, Mirzadi Gohari A, Aouini L, Gibriel HAY, Ware SB, van den Bosch F, Manning-Smith R, Alonso-Chavez V, Helps J, Ben M'Barek S, *et al.* 2018. Stress

and sexual reproduction affect the dynamics of the wheat pathogen effector AvrStb6 and strobilurin resistance. *Nature Genetics* **50**: 375–380.

Kema GHJ, Yu D, Rijkenberg FHJ, Shaw MW, Baayen RP. **1996**. Histology of the pathogenesis of *Mycosphaerella graminicola* in wheat. *Phytopathology* **86**: 777–786.

Kettles GJ, Bayon C, Sparks CA, Canning G, Kanyuka K, Rudd JJ. **2018**. Characterization of an antimicrobial and phytotoxic ribonuclease secreted by the fungal wheat pathogen *Zymoseptoria tritici*. *New Phytologist* **217**: 320–331.

Kombrink A, Rovenich H, Shi-Kunne X, Rojas-Padilla E, van den Berg GCM, Domazakis E, de Jonge R, Valkenburg D-J, Sánchez-Vallet A, Seidl MF, *et al.* 2017. *Verticillium dahliae* LysM effectors differentially contribute to virulence on plant hosts. *Molecular Plant Pathology* **18**: 596–608.

Mago R, Zhang P, Vautrin S, Šimková H, Bansal U, Luo MC, Rouse M, Karaoglu H, Periyannan S, Kolmer J, *et al.* 2015. The wheat *Sr50* gene reveals rich diversity at a cereal disease resistance locus. *Nature Plants* **1**: 6–8.

Marshall R, Kombrink A, Motteram J, Loza-Reyes E, Lucas J, Hammond-Kosack KE, Thomma BPHJ, Rudd JJ. **2011**. Analysis of two in planta expressed LysM effector homologs from the fungus *Mycosphaerella graminicola* reveals novel functional properties and varying contributions to virulence on wheat. *Plant Physiology* **156**: 756–769.

Matei A, Ernst C, Günl M, Thiele B, Altmüller J, Walbot V, Usadel B, Doehlemann G. **2018**. How to make a tumour: cell type specific dissection of *Ustilago maydis*-induced tumour development in maize leaves. *New Phytologist* **217**: 1681–1695.

McDonald BA, Linde C. **2002**. Pathogen population genetics, evolutionary potential, and durable resistance. *Annual Review of Phytopathology* **40**: 349–379.

McDonald BA, Mundt CC. **2016**. How knowledge of pathogen population biology informs management of Septoria tritici blotch. *Phytopathology* **106**: 948–955.

McDonald MC, Solomon PS. **2018**. Just the surface: advances in the discovery and characterization of necrotrophic wheat effectors. *Current Opinion in Microbiology* **46**: 14–18.

Michelmore R, Coaker G, Bart R, Beattie G, Bent A, Bruce T, Cameron D, Dangl J, Dinesh-Kumar S, Edwards R, *et al.* 2017. Foundational and translational research opportunities to improve plant health. *Molecular Plant-Microbe Interactions* **30**: 515–516.

Misas Villamil JC, Mueller AN, Demir F, Meyer U, Ökmen B, Schulze Hüynck J, Breuer M, Dauben H, Win J, Huesgen PF, *et al.* 2019. A fungal substrate mimicking molecule suppresses plant immunity via an inter-kingdom conserved motif. *Nature Communications* **10**.

Motteram J, Küfner I, Deller S, Brunner F, Hammond-Kosack KE, Nürnberger T, Rudd JJ. **2009**. Molecular characterization and functional analysis of MgNLP, the sole NPP1 domain-containing protein, from the fungal wheat leaf pathogen *Mycosphaerella graminicola*. *Molecular Plant-Microbe Interactions* **22**: 790–799.

Mukhtar MS, Carvunis A, Dreze M, Epple P, Steinbrenner J, Moore J, Tasan M, Galli M, Hao T, Nishimura MT, *et al.* 2011. Independently evolved virulence effectors converge

onto hubs in a plant immune system network. *Science* **333**: 596–601.

Na R, Gijzen M. **2016**. Escaping host immunity: new tricks for plant pathogens. *PLoS Pathogens* **12**: 1–6.

Njau PN, Jin Y, Huerta-Espino J, Keller B, Singh RP. **2010**. Identification and evaluation of sources of resistance to stem rust race Ug99 in wheat. *Plant Disease* **94**: 413–419.

O'Connell RJ, Thon MR, Hacquard S, Amyotte SG, Kleemann J, Torres MF, Damm U, Buiate EA, Epstein L, Alkan N, *et al.* 2012. Lifestyle transitions in plant pathogenic *Colletotrichumy* fungi deciphered by genome and transcriptome analyses. *Nature Genetics* **44**: 1060–1065.

Palma-Guerrero J, Torriani SFF, Zala M, Carter D, Courbot M, Rudd JJ, McDonald BA, Croll D. **2016**. Comparative transcriptomic analyses of *Zymoseptoria tritici* strains show complex lifestyle transitions and intraspecific variability in transcription profiles. *Molecular plant pathology* **17**: 845–859.

Plissonneau C, Hartmann FE, Croll D. **2018**. Pangenome analyses of the wheat pathogen *Zymoseptoria tritici* reveal the structural basis of a highly plastic eukaryotic genome. *BMC Biology* **16**: 5.

Poppe S, Dorsheimer L, Happel P, Stukenbrock EH. **2015**. Rapidly evolving genes are key players in host specialization and virulence of the fungal wheat pathogen *Zymoseptoria tritici* (*Mycosphaerella graminicola*). *PLOS Pathogens* **11**: e1005055.

Praz CR, Menardo F, Robinson MD, Müller MC, Wicker T, Bourras S, Keller B. **2018**. Non-parent of origin expression of numerous effector genes indicates a role of gene regulation in host adaption of the hybrid triticale powdery mildew pathogen. *Frontiers in Plant Science* **9**: 1–19.

Lo Presti L, Lanver D, Schweizer G, Tanaka S, Liang L, Tollot M, Zuccaro A, Reissmann S, Kahmann R. **2015**. Fungal effectors and plant susceptibility. *Annual Review of Plant Biology* **66**: 513–545.

Qutob D, Patrick Chapman B, Gijzen M. **2013**. Transgenerational gene silencing causes gain of virulence in a plant pathogen. *Nature Communications* **4**: 1349.

Rouxel T, Balesdent M-H. **2010**. Avirulence genes. In: Encyclopedia of Life Sciences. Chichester, UK: John Wiley & Sons, Ltd.

Rudd JJ, Kanyuka K, Hassani-Pak K, Derbyshire M, Andongabo A, Devonshire J, Lysenko A, Saqi M, Desai NM, Powers SJ, *et al.* 2015. Transcriptome and metabolite profiling of the infection cycle of *Zymoseptoria tritici* on wheat reveals a biphasic interaction with plant immunity involving differential pathogen chromosomal contributions and a variation on the hemibiotrophic lifestyle definition. *Plant Physiology* **167**: 1158–1185.

Rybak K, See PT, Phan HTT, Syme RA, Moffat CS, Oliver RP, Tan KC. **2017**. A functionally conserved Zn_2Cys_6 binuclear cluster transcription factor class regulates necrotrophic effector gene expression and host-specific virulence of two major *Pleosporales* fungal pathogens of wheat. *Molecular Plant Pathology* **18**: 420–434.

Saintenac C, Lee W-S, Cambon F, Rudd JJ, King RC, Marande W, Powers SJ, Berges H, Phillips AL, Uauy C, *et al.* 2018. Wheat receptor-kinase-like protein Stb6 controls gene-for-gene resistance to fungal pathogen *Zymoseptoria tritici*. *Nature genetics* **50**: 368–374.

Salamini F, Özkan H, Brandolini A, Schäfer-Pregl R, Martin W. **2002**. Genetics and geography of wild cereal domestication in the near east. *Nature Reviews Genetics* **3**: 429–441.

Sánchez-Vallet A, Fouché S, Fudal I, Hartmann FE, Soyer JL, Tellier A, Croll D. 2018. The genome biology of effector gene evolution in filamentous plant pathogens. *Annual Review of Phytopathology* **56**: 21–40.

Sánchez-Vallet A, Mesters JR, Thomma BPHJ. 2015. The battle for chitin recognition in plant-microbe interactions. *FEMS Microbiology Reviews* **39**: 171–183.

Sánchez-Vallet A, Saleem-Batcha R, Kombrink A, Hansen G, Valkenburg D-J, Thomma BPHJ, Mesters JR. 2013. Fungal effector Ecp6 outcompetes host immune receptor for chitin binding through intrachain LysM dimerization. *eLife* **2**: e00790.

Schulze-Lefert P, Panstruga R. 2011. A molecular evolutionary concept connecting nonhost resistance, pathogen host range, and pathogen speciation. *Trends in Plant Science* **16**: 117–125.

Seidl MF, Thomma BPHJ. 2017. Transposable elements direct the coevolution between plants and microbes. *Trends in Genetics* **33**: 842–851.

Singh RP, Hodson DP, Huerta-Espino J, Jin Y, Bhavani S, Njau P, Herrera-Foessel S, Singh PK, Singh S, Govindan V. 2011. The emergence of Ug99 races of the stem rust fungus is a threat to world wheat production. *Annual Review of Phytopathology* **49**: 465–481.

Skamnioti P, Ridout CJ. 2005. Microbial avirulence determinants: Guided missiles or antigenic flak? *Molecular Plant Pathology* **6**: 551–559.

Slotkin RK, Martienssen R. 2007. Transposable elements and the epigenetic regulation of the genome. *Nature reviews. Genetics* **8**: 272–285.

Soyer JL, El Ghalid M, Glaser N, Ollivier B, Linglin J, Grandaubert J, Balesdent M-H, Connolly LR, Freitag M, Rouxel T, *et al.* 2014. Epigenetic control of effector gene expression in the plant pathogenic fungus *Leptosphaeria maculans*. *PLoS Genetics* **10**: e1004227.

Soyer JL, Rouxel T, Fudal I. 2015. Chromatin-based control of effector gene expression in plant-associated fungi. *Current Opinion in Plant Biology* **26**: 51–56.

Steinberg G. 2015. Cell biology of *Zymoseptoria tritici*: Pathogen cell organization and wheat infection. *Fungal Genetics and Biology* **79**: 17–23.

Stukenbrock EH, Banke S, Javan-Nikkhah M, McDonald BA. 2007. Origin and domestication of the fungal wheat pathogen *Mycosphaerella graminicola* via sympatric speciation. *Molecular Biology and Evolution* **24**: 398–411.

Stukenbrock EH, Bataillon T, Dutheil JY, Hansen TT, Li R, Zala M, McDonald BA, Wang J, Schierup MH. 2011. The making of a new pathogen: Insights from comparative population genomics of the domesticated wheat pathogen *Mycosphaerella graminicola* and its wild sister species. *Genome Research* **21**: 2157–2166.

Stukenbrock EH, Jørgensen FG, Zala M, Hansen TT, McDonald BA, Schierup MH. 2010. Whole-genome and chromosome evolution associated with host adaptation and speciation of the wheat pathogen *Mycosphaerella graminicola*. *PLoS Genetics* **6**: 1–13.

Stukenbrock EH, Quaedvlieg W, Javan-Nikhah M, Zala M, Crous PW, McDonald BA. 2012. *Zymoseptoria ardabiliae* and *Z. pseudotritici*, two progenitor species of the septoria tritici leaf blotch fungus *Z. tritici* (synonym: *Mycosphaerella graminicola*). *Mycologia* **104**: 1397–1407.

Thordal-Christensen H. 2003. Fresh insights into processes of nonhost resistance. *Current Opinion in Plant Biology* **6**: 351–357.

Torriani SFF, Melichar JPE, Mills C, Pain N, Sierotzki H, Courbot M. 2015. *Zymoseptoria tritici*: A major threat to wheat production, integrated approaches to control. *Fungal Genetics and*

Biology **79**: 8–12.

Zahiri A, Heimel K, Wahl R, Rath M, Kämper J. **2010**. The *Ustilago maydis* forkhead transcription factor Fox1 is involved in the regulation of genes required for the attenuation of plant defenses during pathogenic development. *Molecular Plant-Microbe Interactions* **23**: 1118–1129.

Zhan J, Pettway RE, McDonald BA. **2003**. The global genetic structure of the wheat pathogen *Mycosphaerella graminicola* is characterized by high nuclear diversity, low mitochondrial diversity, regular recombination, and gene flow. *Fungal Genetics and Biology* **38**: 286–297.

Zhang S, Wang L, Wu W, He L, Yang X, Pan Q. **2015**. Function and evolution of *Magnaporthe oryzae* avirulence gene *AvrPib* responding to the rice blast resistance gene *Pib*. *Scientific Reports* **5**: 11642.

Zhong Z, Marcel TC, Hartmann FE, Ma X, Plissonneau C, Zala M, Ducasse A, Confais J, Compain J, Lapalu N, *et al.* 2017. A small secreted protein in *Zymoseptoria tritici* is responsible for avirulence on wheat cultivars carrying the *Stb6* resistance gene. *New Phytologist* **214**: 619–631.

Chapter 1

A fungal avirulence factor encoded in a highly plastic genomic region triggers partial resistance to septoria tritici blotch

Lukas Meile, Daniel Croll, Patrick C. Brunner, Clémence Plissonneau, Fanny E. Hartmann, Bruce A. McDonald and Andrea Sánchez-Vallet. 2018.

A modified version of this chapter was published in *New Phytologist* **219**: 1048–1061 (2018)

1.1. Abstract

- Host-strain specificity in the wheat-*Zymoseptoria tritici* pathosystem determines the infection outcome and is controlled by resistance genes on the host side, many of which have been identified. On the pathogen side, however, the molecular determinants of specificity remain largely unknown.
- We used genetic mapping, targeted gene disruption and allele swapping to characterize the recognition of the new avirulence factor Avr3D1. We then combined population genetic and comparative genomic analyses to characterize the evolutionary trajectory of *Avr3D1*.
- Avr3D1 is specifically recognized by wheat lines harbouring the *Stb7* resistance gene, triggering a strong defence response without preventing pathogen infection and reproduction. *Avr3D1* resides in a cluster of putative effector genes located in a genome region populated by independent transposable element insertions. The gene was present in all 132 investigated strains and is highly polymorphic, with 30 different protein isoforms identified. We demonstrated that specific amino acid substitutions in Avr3D1 led to evasion of recognition.
- These results demonstrate that quantitative resistance and gene-for-gene interactions are not mutually exclusive. Localizing avirulence genes in highly plastic genomic regions likely facilitates accelerated evolution that enables escape from recognition by resistance proteins.

1.2. Introduction

Regardless of whether they are mutualistic or parasitic, colonizing microbes evolve a high degree of specialization to recognize and infect their hosts and overcome host-inducible defences (van der Does & Rep, 2017). Host manipulation is frequently achieved by the secretion of effectors, which are often small secreted proteins (SSPs) that support growth and development of the microbe by conferring protection against host antimicrobial compounds or by altering host metabolism (Lo Presti *et al.*, 2015). Although effectors are beneficial for host colonization, some are specifically recognized by certain host genotypes, triggering an immune response (Jones & Dangl, 2006; Lo Presti *et al.*, 2015). This interaction typically follows the gene-for-gene model, in which a so-called resistance protein recognizes an effector, which is then called an avirulence factor (Avr, Flor, 1971; Jones & Dangl, 2006). A common assumption is that resistance/avirulence gene interactions confer complete resistance, whereas quantitative resistance, understood here as incomplete or partial resistance that allows some pathogen infection and reproduction, is based on different, race-nonspecific and therefore avirulence-independent mechanisms. This paradigm originated from work on biotrophic pathogens, where avirulence recognition often leads to complete immunity via induction of a hypersensitive response (Cook *et al.*, 2015; Niks *et al.*, 2015). But it is often overlooked that gene-for-gene interactions could also lead to quantitative resistance, as suggested by several studies (Antonovics *et al.*, 2011; Rietman *et al.*, 2012; Chen *et al.*, 2013). Recently, more refined concepts such as the “invasion model” (Cook *et al.*, 2015) or “effector-triggered defence” (Stotz *et al.*, 2014) emphasized a broader perspective for the gene-for-gene model, in which resistance gene-based effector recognition and quantitative resistance are not mutually exclusive (Niks *et al.*, 2015). However,

avirulence factors leading to quantitative resistance have only rarely been described (Schirawski *et al.*, 2010; Rietman *et al.*, 2012).

Host recognition of effectors exerts an evolutionary pressure that favours sequence modification, deletion or acquisition of new effectors to overcome the immune response. Thus, genes encoding effectors are among the most polymorphic found in pathogen genomes (Win *et al.*, 2012). The mechanisms underlying effector diversification remain largely unexplored. Many pathogen genomes are compartmentalized into highly conserved or rapidly evolving regions, often described as the "two-speed genome" (Raffaele & Kamoun, 2012). Effector genes are frequently localized in the highly variable compartments, which are often rich in transposable elements (Ma *et al.*, 2010; Soyer *et al.*, 2014; Plissonneau *et al.*, 2018). Transposable elements are thought to contribute to genome evolution and the diversification of effector genes (Raffaele & Kamoun, 2012). They translocate within a genome, causing gene disruption, duplication or deletion of genomic sequences. In addition, transposable elements contribute to variability by favouring non-homologous recombination or through repeat-induced point mutations (RIP) (Möller & Stukenbrock, 2017; Seidl & Thomma, 2017). Pathogens carrying these highly plastic genome regions are thought to benefit from an increased versatility to adapt to different conditions or to an evolving host (Dong *et al.*, 2015; Faino *et al.*, 2016).

The most damaging pathogen of wheat in Europe is *Zymoseptoria tritici*, an ascomycete fungus that causes septoria tritici blotch (STB, Fones & Gurr, 2015). It is an apoplastic pathogen with a latent necrotrophic lifestyle (Sánchez-Vallet *et al.*,

2015). Fungal hyphae penetrate the stomata and colonize the apoplast during a long asymptomatic phase that lasts between 7 and 14 days, depending on the weather conditions, the host genotype and the pathogen strain. This long latent period is followed by a rapid induction of necrosis that is accompanied by the development of asexual reproductive structures called pycnidia, which contain asexual spores that spread the disease during a growing season (Kema *et al.*, 1996; Duncan & Howard, 2000). The genetic basis of *Z. tritici* virulence is poorly understood as a result of its largely quantitative nature (Hartmann *et al.*, 2017; Stewart *et al.*, 2018). Two highly conserved lysine motif (LysM) effectors, Mg1LysM and Mg3LysM, prevent fungal recognition and shield the fungal cell wall from degradation by host hydrolytic enzymes (Marshall *et al.*, 2011). The other known effectors of *Z. tritici,* Zt80707, AvrStb6 and Zt_8_609, are rapidly evolving small secreted proteins (Poppe *et al.*, 2015; Hartmann *et al.*, 2017; Zhong *et al.*, 2017; Kema *et al.*, 2018). The latter two were identified because they are specifically recognized by certain wheat lines, and they were found to be located in transposable element-rich genomic regions (Brading *et al.*, 2002; Hartmann *et al.*, 2017; Zhong *et al.*, 2017). AvrStb6 is recognized by the resistance protein Stb6 in a gene-for-gene interaction that leads to a strong resistance response, completely blocking the progression of the infection (Kema *et al.*, 2000; Brading *et al.*, 2002; Kema *et al.*, 2018; Saintenac *et al.,* 2018). In addition to *Stb6*, 19 other race-specific *Stb* resistance genes with large effects have been mapped, but their corresponding avirulence factors remain unknown (Brown *et al.*, 2015). We hypothesized that one of these *Stb* genes might be responsible for the differences in resistance of cultivar Runal to two Swiss strains (3D1 and 3D7, Stewart *et al.*, 2018). The more virulent strain 3D7 produced necrotic lesions faster than 3D1. The less virulent strain 3D1 was successful in producing pycnidia, but at a lower density and with a less uniform distribution across the leaf surface than 3D7 (Fig

1a,b). A single, large-effect quantitative trait locus (QTL) encoding differences in lesion size and pycnidia density between 3D1 and 3D7 was mapped to a region on chromosome 7 (Stewart *et al.*, 2018). However, the genes responsible for the differences in virulence were not identified.

Here we aimed to broaden our knowledge of the genetic basis of host-race specificity in *Z. tritici*. First, we showed that *Avr3D1* is the gene responsible for the differences in quantitative virulence between 3D1 and 3D7. We then demonstrated that Avr3D1 is an avirulence factor whose recognition is host-specific, but triggers an incomplete, quantitative resistance. We next studied the evolutionary trajectory of *Avr3D1* by combining population genetic and comparative genomic analyses involving 132 *Z. tritici* strains originating from four field populations on three continents as well as 11 strains of the closest known relatives of *Z. tritici*. We found that *Avr3D1* is a member of an effector gene cluster that is located in a highly dynamic genomic region containing many independent insertions involving different families of transposable elements. Because an intact and presumably functional version of *Avr3D1* was found in all strains of *Z. tritici* and in its closest relatives, we conclude that *Avr3D1* plays an important role in the life history of *Z. tritici*. Maintaining *Avr3D1* in a highly plastic genomic region likely provides an advantage by accelerating evolution that enables an escape from recognition in wheat populations carrying the corresponding resistance gene.

1.3. Materials and methods

1.3.1. Quantitative Trait Locus (QTL) mapping

To generate a genetic map, we used the previously generated restriction site associated DNA sequencing (RADseq) data from the progeny of the cross between 3D7 and 3D1 (Lendenmann *et al.*, 2014). Quality trimmed reads were aligned to the genome of 3D7 (Plissonneau *et al.*, 2016) using bowtie2 with default parameters (Langmead & Salzberg, 2012). Single nucleotide polymorphisms (SNPs) were called in each progeny with the HaplotypeCaller tool from GATK v3.3 (McKenna *et al.*, 2010) and further filtered for their quality using the following parameters: > QUAL 5000, QD > 5, MQ > 20, and ReadPosRankSum, MQRankSum, and BaseQRankSum between -2 and 2. We constructed the linkage map using R/qtl v1.40-8 (Arends *et al.*, 2010). We retained only progenies for which 45% of all SNPs were genotyped, then we removed SNPs genotyped in less than 70% of the progenies. Potential clones (i.e. progenies with more than 90% shared SNPs) were excluded. We removed adjacent nonrecombining markers. QTL mapping was performed with the QTL package in R (R Core Team, 2013), similar to the procedure described by (Lendenmann *et al.*, 2014) using the pycnidia density dataset (Stewart *et al.*, 2018).

1.3.2. *Z. tritici* and bacterial strains

The Swiss strains ST99CH_3D1 (3D1) and ST99CH_3D7 (3D7, described in Linde *et al.*, 2002) or mutant lines derived from them were used in this study. Standard conditions for *Z. tritici* cultivation consisted of yeast-sucrose broth (YSB) medium (10 g/L yeast extract, 10 g/L sucrose, 50 µg/ml kanamycin sulfate) at 18°C or yeast-malt-

sucrose (YMS) medium (4 g/L yeast extract, 4 g/L malt extract, 4g/L sucrose, 12 g/L agar) at 18°C. For molecular cloning and plasmid propagation, *Escherichia coli* strains HST08 (Takara Bio, USA) or NEB® 5-alpha (New England Biolabs) were used. *Agrobacterium tumefaciens*-mediated transformation was performed with *A. tumefaciens* strain AGL1. If not stated otherwise, *E. coli* and *Agrobacterium* lines were grown in Luria Bertani (LB) medium containing kanamycin sulfate (50 µg/mL) at 37°C or in LB medium containing kanamycin sulfate (50 µg/mL), carbenicillin (100 µg/mL) and rifampicin at 28°C (50 µg/mL), respectively.

1.3.3. Generation of plasmid constructs for targeted gene disruption and ectopic gene integration

All PCR reactions for cloning procedures were performed using NEB® Phusion polymerase (New England Biolabs) with primers listed in Table S1. All DNA assembly steps were conducted with the In-Fusion® HD Cloning Kit (Takara Bio, USA) following the manufacturer's instructions. To create constructs for targeted gene disruption, two flanking regions of at least 1 kb in size for homologous recombination were amplified from *Z. tritici* genomic DNA. The hygromycin resistance gene cassette, used as a selectable marker, was amplified from pES6 (Eva H. Stukenbrock, unpublished). The three fragments were assembled into pES1 (Eva H. Stukenbrock, unpublished) and linearized with KpnI and PstI (New England Biolabs), resulting in pES1Δ581_{3D1} and pES1Δ581_{3D7}. To create the construct for ectopic integration of *Avr3D1$_{3D1}$*, a fragment containing *Avr3D1$_{3D1}$* including the 1.3-kb sequence upstream of the start codon and the 1-kb sequence downstream of the stop codon was amplified and cloned into pCGEN (Motteram *et al.*, 2011) that had been linearized with KpnI, resulting in pCGEN-581_{3D1}ect. To exchange the coding sequence (CDS) in pCGEN-581_{3D1}ect, we first digested it with XhoI (New England Biolabs) to linearize it

and remove the *Avr3D1*$_{3D1}$ CDS. In this digestion, the promoter was partially removed from the vector. In a second step a fragment containing the CDS and intron 1 of *Avr3D1*$_{3D7}$ (amplified from 3D7 genomic DNA) and a fragment to reconstitute the promoter sequence of *Avr3D1*$_{3D1}$ (amplified from pCGEN-581$_{3D1}$ect) were assembled into the linearized pCGEN-581$_{3D1}$ect, resulting in pCGEN-581$_{3D7}$ect. Constructs were transformed into *E. coli* by heat shock transformation, mini-prepped and verified by diagnostic digests and Sanger sequencing (MicroSynth, Switzerland). Confirmed plasmids were transformed into *A. tumefaciens* cells by electroporation.

1.3.4. *Agrobacterium tumefaciens*-mediated transformation (ATMT) of *Z. tritici* cells

ATMT of *Z. tritici* was performed according to Zwiers & De Waard, 2001 with the following modifications: *A. tumefaciens* lines were grown as liquid cultures for approx. 24 hrs. Cell concentrations were estimated by measuring the optical density (OD_{600}) and the cultures were diluted to an OD_{600} of 0.15 in induction medium (pH 5.7, 50 µg/mL kanamycin sulfate, 100 µg/mL carbenicillin, 50 µg/mL rifampicin, 10 mM glucose, 200 µM acetosyringone). These cultures were incubated at 28°C until they reached an OD_{600} of 0.25-0.35 and 100 µL were mixed with 100 µL of *Z. tritici* cell suspensions (cells grown on YMS for 4-6 days and washed off with water) and plated on induction medium covered with nitrocellulose membranes. After 3 days of incubation at 18°C, the nitrocellulose membranes were placed on YMS medium containing cefotaxime (200 µg/mL) and either hygromycin B (100 µg/mL) or geneticin (150 µg/mL), depending on the resistance cassette of the construct, and incubated at 18°C until colonies appeared. Colonies were streak-plated on the same selective medium to isolate single colonies before the mutant lines were grown on YMS without selection. For knockout lines, disruption of the target genes was verified using

a PCR-based approach. We determined the copy number of the transgene by quantitative polymerase chain reaction (qPCR) on genomic DNA extracted with DNeasy Plant Mini Kit (Qiagen). The target used was the selection marker and the reference gene was *TFIIIC1* (*Mycgr3G110539*, Table S1). Only single insertion lines were selected for further experiments.

1.3.5. Infection assays

Seeds from wheat (*Triticum aestivum* L.) lines Runal, Titlis, Drifter, Chinese Spring and Arina were purchased from DSP Ltd. (Delley, Switzerland). Seeds were sown in peat substrate Jiffy® GO PP7 (Jiffy Products International) and grown for 17 days in a greenhouse at 18°C (day) and 15°C (night) with a 16-hrs photoperiod and 70% humidity. For all infection experiments, square pots (11x11x12 ME, Lamprecht-Verpackungen GmbH, Germany) containing 16-18 seedlings or 2x3 pot arrays (7x7 cm and 200 mL each, Bachmann Plantec AG, Switzerland) containing two seedlings per unit were used. The infection procedure for the two pot types was identical. *Z. tritici* inoculum was prepared as follows: 50 mL of YSB medium were inoculated in 100-mL Erlenmeyer flasks from *Z. tritici* glycerol stocks stored at -80°C. After 4-6 days of incubation (18°C, shaking at 120 rpm), liquid cultures were filtered through sterile cheesecloth and pelleted (3273 g, 15 min, 4°C). The supernatant was discarded and the cells were resuspended in sterile deionized water and stored on ice until infection (0-2 days). The concentrations of the spore suspensions were determined using KOVA® Glasstic® counting chambers (Hycor Biomedical, Inc., USA) and adjusted to 10^6 spores/mL in 0.1% (v/v) Tween® 20. Spore viability and concentration was analysed by performing a developmental assay on YMS medium as described below. Plants were sprayed until run-off with 15 mL spore suspension per pot/array. Square pots were placed in plastic bags (PE-LD, 380x240 mm) to

support the leaves and stems. Subsequently, they were placed in a second plastic bag (PE-LD 650x400 mm, two pots each), which was sealed to keep humidity at 100%. Pot arrays were placed directly into the sealing bags. After three days, the sealing bags were trimmed to a height of around 27 cm and then opened, in the case of the 2x3 pot arrays, or completely removed in the case of the square pots, leaving the supporting bags intact in the latter case. For symptom quantification, second or third leaves were mounted on paper sheets, scanned with a flatbed scanner (CanoScan LiDE 220) and analysed using automated image analysis (Stewart *et al*., 2016). Data analysis and plotting was performed using RStudio Version 1.0.143. Confidence intervals of the medians were determined using the "boot" package and Kolmogorov-Smirnov (KS) tests for statistical significance with the "Matching" package.

1.3.6. RNA isolation and quantitative reverse transcription PCR (qRT-PCR)

Second leaves from cv. Runal were infected with 3D1 or 3D7, harvested and scanned as described. Immediately after scanning, the tip 2 cm of the leaves were excised and discarded and the adjacent 8.5 cm sections were frozen in N_2. Three biological replicates were harvested. Leaf tissue was homogenized using a Bead Ruptor with a cooling unit (Omni International) and zirconium oxide beads (1.4 mm). RNA was isolated using the GENEzol reagent (Geneaid Biotech) and purified with the RNeasy Mini kit (Quiagen) including an on-column DNase treatment with the RNase-Free DNase Set (Qiagen) according to the manufacturer's instructions. cDNA was produced with the RevertAid First Strand cDNA Synthesis Kit (Invitrogen), using up to 900 ng RNA (estimated with NanoDrop) per reaction. To determine expression of *Avr3D1* relative to the *18S* reference gene, qRT-PCR was performed with a LightCycler® 480 (Roche) using white 384-well plates. Each reaction consisted of 250

nM of each primer, template cDNA generated from 11-30 ng of RNA and 1x HOT FIREPol® EvaGreen® qPCR Mix Plus mastermix (Solis BioDyne) in a total volume of 10 µL. Amplification was performed with a 10-min step of initial denaturation and enzyme activation and 40 cycles of 95°C (15 s) and 60°C (60 s). Each sample was run in technical triplicates. Relative expression was calculated with LightCycler® 480 software using the "advanced relative quantification" tool. The mean and confidence interval of the mean was calculated with RStudio Version 1.0.143.

1.3.7. Stress and development assay

The obtained *Z. tritici* mutant lines were tested for an altered, plant-unrelated phenotype under various conditions including stress by growing them on PDA, YMS and YMS supplemented with H_2O_2 (2 mM for 3D1 lines and 1 mM for 3D7 lines) or 1 M NaCl at 18°C. All media contained kanamycin sulfate (50 µg/mL). An additional stress condition consisted of growth at 28°C on YMS. Inoculum preparation and quantification were the same as for the infection assays. 2.5-µL drops of spore suspensions of 10^7, 10^6, 10^5 and 10^4 spores/mL were plated on the media described above. Plates were assessed after 6 days of upside-down incubation. Mutant lines exhibiting abnormal development or growth deficiencies were excluded from further experiments.

1.3.8. Manual annotation of three small secreted proteins in the QTL for virulence

We used RNA sequencing (RNA-seq) raw data of IPO323 infecting wheat seedlings (Rudd *et al.*, 2015) to manually annotate the gene *Zt09_7_00581*. To annotate the other genes in the cluster, we used RNA-seq raw data of 3D7 from two different experiments and at 6 different time points (Palma-Guerrero *et al.*, 2016). The data

were previously deposited in NCBI with the experiment numbers SRP061444 and ERP009837. RNA-seq reads were analysed as described in Hartmann & Croll (2017). Possible reading frames were manually examined using Integrative Genomics Viewer (IGV, Broad Institute, Robinson *et al.*, 2011). Signal peptides were predicted using Signal P 4.1 (CBS, Petersen *et al.*, 2011).

1.3.9. *Zymoseptoria tritici* strain collections

We used 132 strains collected in four different countries (Switzerland, Israel, US and Australia; Zhan *et al.*, 2005). Whole-genome Illumina sequencing data of the 132 strains were previously deposited on the NCBI Short Read Archive under the BioProject ID numbers PRJNA178194 and PRJNA327615 (Torriani *et al.*, 2011; Croll *et al.*, 2013; Hartmann & Croll, 2017; Hartmann *et al.*, 2017). We used complete genome assemblies of IPO323, ST99CH_3D1 (3D1), ST99CH_3D7 (3D7), ST99CH_1E4 (1E4) and ST99CH_1A5 (1A5) previously described by Goodwin *et al.*, (2011) and Plissonneau *et al.*, (2016; 2018). BLAST searches were performed using the blastn command of the ncbi-blast-2.2.30+ software (Camacho *et al.*, 2009). Synteny of the QTL between IPO323, 3D1, 3D7, 1E4 and 1A5 was analysed using blastn and visualized using the R package genoPlotR v. 0.8.4 (Guy *et al.*, 2010). Homologues of *Avr3D1* were identified by blastn using CLC Genomic Workbench 9 (Qiagen) in the strains 3D1, 3D7, 1E4 and 1A5.

We searched for homologues of *Avr3D1* using the blast algorithm implemented in CLC Genomics Workbench 9 (Qiagen) in one strain of *Zymoseptoria passerinii* [NCBI genome accession no. AFIY01 (fungal strain SP63)], four strains of *Z. ardabiliae* [STIR04 1.1.1 (accession no. AFIU01), STIR04 1.1.2 (AFIV01), STIR04 3.13.1 (AFIW01), STIR04 3.3.2 (AFIX01)], one strain of *Z. brevis* Zb18110 (LAFY01), and

five strains of the sister species *Z. pseudotritici* [STIR04 2.2.1 (AFIQ01), STIR04 3.11.1 (AFIO01), STIR04 4.3.1 (AFIR01), STIR04 5.3 (AFIS01), STIR04 5.9.1 (AFIT01)]. The genomes were downloaded from NCBI under the accession numbers PRJNA63035, PRJNA277173, PRJNA63037, PRJNA63039, PRJNA343335, PRJNA343334, PRJNA343333, PRJNA343332, PRJNA63049, PRJNA273516 and PRJNA46489.

1.3.10. Presence/absence polymorphism of transposable elements and annotation

Repetitive DNA was identified for the 132 strains. For 3D1, 3D7, 1E4 and 1A5 full genome annotations were already available (Plissonneau *et al.*, 2016; Plissonneau *et al.*, 2018). We annotated and masked repetitive elements in the genomes of the remaining 128 strains using RepeatModeler version 1.0.8, as described before (Plissonneau *et al.*, 2016) and we masked the genomes using RepeatMasker version 4.0.5 with the library previously obtained for *Z. tritici* strain IPO323 (Grandaubert *et al.*, 2015) according to transposable element nomenclature defined by Wicker *et al*., (2007).

1.3.11. DNA and protein alignments and phylogenetic tree

DNA and protein sequence alignments of Avr3D1 and the other SSPs from different strains were obtained using CLC Genomics Workbench 9 (Qiagen). For the phylogenetic analysis, amino acid sequences of Avr3D1 were aligned using Muscle. The Maximum Likelihood Phylogeny Reconstruction was performed applying WAG model, with the software Mega6 (Tamura *et al.*, 2013).

1.3.12. Population genetic analysis

DnaSP v5 (Librado & Rozas, 2009) was used to calculate summary statistics of population genetic parameters associated with *Avr3D1*. Sliding window analyses of π were conducted using DnaSP with a window length set to 20 bp and a step size of 5 bp. The haplotype alignment of the coding region was used to generate a parsimony haplotype network using the TCS method (Clement *et al.*, 2000) as implemented in the PopART package v. 1.7 (Leigh & Bryant, 2015). TCS utilizes statistical parsimony methods to infer unrooted cladograms based on Templeton's 95% parsimony connection limit. Mutational steps resulting in nonsynonymous changes were identified with DnaSP. The degree of selection was estimated by comparing dN (the number of nonsynonymous changes per nonsynonymous site) with dS (the number of synonymous changes per synonymous site) for all pairwise sequence comparisons using DnaSP. A dN/dS ratio of 1 ($\omega = 1$) indicates neutrality, while $\omega < 1$ suggests purifying, and $\omega > 1$ suggests diversifying selection. Since diversifying selection is unlikely to affect all nucleotides in a gene, ω averaged over all sites is rarely > 1. We focused on detecting positive selection that affects only specific codons in *Avr3D1* by applying the maximum likelihood method CodeML implemented in the PAML software (Phylogenetic Analysis by Maximum Likelihood, Yang, 1997; Yang, 2007).

1.4. Results

1.4.1. Differences in virulence map to an effector gene cluster on chromosome 7

To identify the gene(s) responsible for the differences in virulence between 3D1 and 3D7, we generated a new linkage map based on the completely assembled genome of the parental strain 3D7 (Plissonneau *et al.*, 2016). Mapping onto the new genome sequence provided twice as many SNP markers and enabled the identification of additional crossovers that allowed us to reduce the number of candidate genes in the previously identified virulence QTL on chromosome 7 (Stewart *et al.*, 2018). The new map yielded a narrower QTL interval (logarithm of the odds, LOD=41.5, $p<10^{-15}$) located within the original QTL interval. The 95% confidence interval for the new QTL in 3D7 spanned 75 kb and contained only 4 of the 35 genes identified in the original QTL, including *Mycgr3T105313*, *Zt09_7_00581*, *Mycgr3T94659* (*Zt09_7_00582*) and the predicted SSP-encoding gene *QTL7_5*. A manual RNA-seq-supported reannotation in 3D7 of the confidence interval revealed two additional genes predicted to encode SSPs, which were named *SSP_3* and *SSP_4* (Fig S1, Table S2). *Zt09_7_00581* was reannotated as also encoding a predicted SSP after identifying an upstream start codon (Fig S1, Table S2). The four genes predicted to encode SSPs in 3D7 formed a cluster of putative effectors.

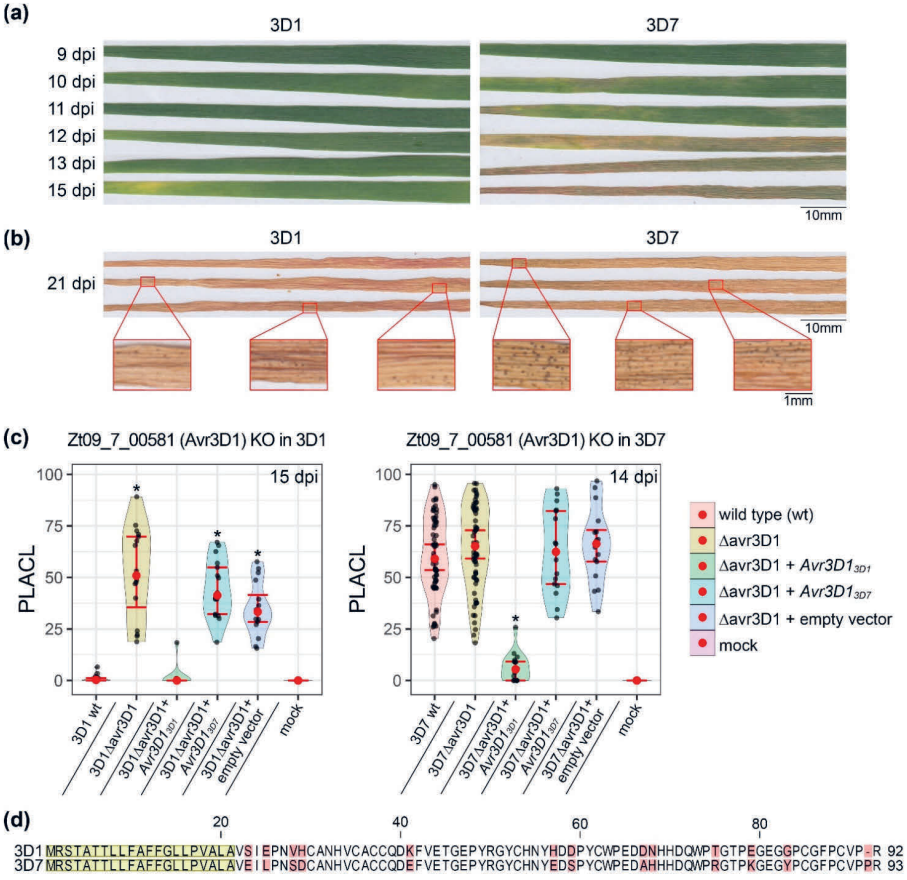

Figure 1. *Z09_7_00581* encodes the avirulence factor Avr3D1. (a) The second true leaves of the wheat cultivar Runal spray-infected with *Z. tritici* strains 3D1 and 3D7 and harvested at different days post inoculation (dpi). **(b)** Fully necrotized leaves with pycnidia of cv. Runal infected by 3D1 and 3D7 at 21 dpi. The leaves shown in panel a are from a different experiment than the leaves shown in panel b. Experiments were repeated twice with similar results. **(c)** Percentage of leaf area covered by lesions (PLACL) produced by the wild type (wt), the Avr3D1 knockout (KO, Δavr3D1) and the ectopic mutants expressing the *Avr3D1* allele of either 3D1 (*Avr3D1*$_{3D1}$) or 3D7 (*Avr3D1*$_{3D7}$) in the knockout background. Left panel: Mutants in the 3D1 background at 15 dpi. Right panel: Mutants in the 3D7 background at 14 dpi. Red dots represent the median of at least 15 leaves (except for the mock treatment, for which at least 8 leaves were used), error bars represent 95% confidence intervals of the medians and black dots represent individual data points. Asterisks indicate statistical differences between wild type and knockout (p-value < 0.01, Kolmogorov-Smirnov test). (d) Amino acid sequence alignment of Avr3D1 isoforms of 3D1 and 3D7. The signal peptide sequence is highlighted in yellow and sequence polymorphisms between both alleles are shown in red.

1.4.2. Avr3D1 recognition contributes to quantitative resistance

In contrast to *SSP_3* and *SSP_4*, the genes *Zt09_7_00581* and *QTL7_5* are highly expressed during infection (Stewart *et al.*, 2018, Fig S1b). Therefore, we considered them as the best candidate genes to explain the virulence QTL and they were selected for functional validation. Knockout mutants in both parental strains were generated by targeted gene disruption and used for virulence assessments in cv. Runal. Mutants in *QTL7_5* in the 3D7 and 3D1 backgrounds (3D7∆qtl7_5 and 3D1∆qtl7_5) did not show an altered phenotype when they were scored for host damage (Fig S2), suggesting that *QTL7_5* is not involved in virulence on cv. Runal. Similarly, the virulence phenotype of the *Zt09_7_00581* mutant in the 3D7 background (3D7∆avr3D1) was unaltered compared to the wild type (Fig 1c, S3), but disrupting *Zt09_7_00581* in 3D1 (3D1∆avr3D1) led to faster development of necrotic lesions and to the production of more pycnidia compared to the wild type 3D1 (Fig 1c, S3, S4). Phenotypic alterations of the knockout lines in 3D1 were specific to *in planta* conditions, as no developmental alterations were observed when the mutants were grown on solid media used for stress assays (Fig S5). The facts that *Zt09_7_00581* negatively affects virulence in 3D1 but not in 3D7 and that *in vitro* growth is unaffected by gene deletion suggests that this gene encodes an avirulence factor, so we renamed this gene *Avr3D1*. Even though Avr3D1 hinders the progression of the infection by 3D1, the avirulent strain is able to infect and produce pycnidia. Thus, Avr3D1 triggers a quantitative resistance response.

To find out if 3D7 modulates the expression of *Avr3D1* to escape recognition, we quantified expression levels during infection for both strains. The expression pattern of *Avr3D1* in the virulent 3D7 strain was similar to 3D1, demonstrating that 3D7 is able to infect despite highly expressing *Avr3D1*. *Avr3D1* expression was high during

the entire asymptomatic phase, peaking before the switch to the necrotrophic phase but dropping rapidly after the first symptoms appeared (Fig S6), indicating a role for this SSP in host colonization, possibly during the asymptomatic phase, the switch to necrotrophy, or both.

1.4.3. Avr3D1 is recognized by different wheat lines harbouring *Stb7*

To determine if recognition of $Avr3D1_{3D1}$ is mediated by a specific resistance protein, a set of 16 additional wheat lines was assessed for resistance against 3D1 and 3D1Δavr3D1. Three (Estanzuela Federal, Kavkaz-K4500 L.6.A.4 and TE-9111) out of 16 wheat lines exhibited a significantly lower level of resistance against 3D1Δavr3D1 compared to 3D1 (Fig 2, S7), suggesting the presence of a host-specific factor contributing to resistance against 3D1, possibly a resistance protein. In none of these three wheat lines did the presence of Avr3D1 completely abolish lesion development and pycnidia production, demonstrating that the quantitative nature of $Avr3D1_{3D1}$-induced resistance is a general phenomenon and not restricted to cv. Runal. All three lines that exhibited $Avr3D1_{3D1}$-triggered resistance were reported to carry the resistance gene *Stb7* (Brown *et al.*, 2015) and are also likely to carry the linked resistance gene *Stb12* (Chartrain *et al.*, 2005), leading us to propose Stb7 and Stb12 as putative candidate resistance proteins recognizing $Avr3D1_{3D1}$.

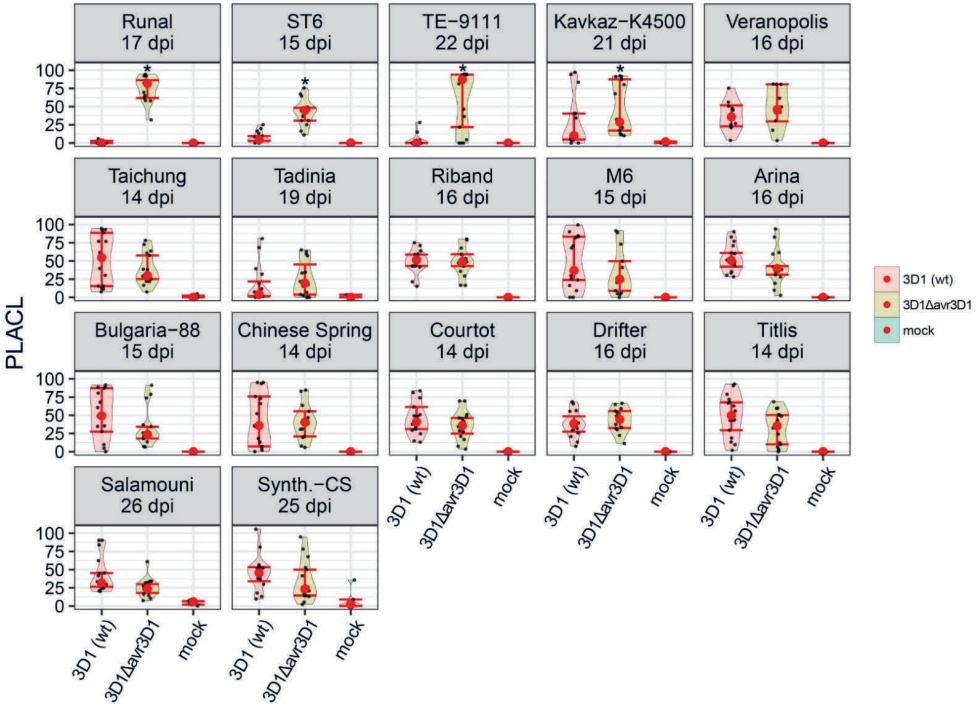

Figure 2. Avr3D1 is specifically recognized by four wheat lines. Violin plots showing the percentage of leaf area covered by lesions (PLACL) produced by *Z. tritici* wild type (wt) 3D1, the Avr3D1 knockout (3D1Δavr3D1) and the mock control in seventeen wheat lines. Harvesting time points varied because of host-specific infection dynamics. Red dots represent the median of at least 10 leaves (except for the mock treatments, for which at least 4 leaves were used), error bars represent 95% confidence intervals of the medians and black dots represent individual data points. Asterisks indicate statistical differences between wild type and knockout (p-value < 0.01, Kolmogorov-Smirnov test). Synth. CS = Synthetic Chinese Spring; ST6 = Estanzuela Federal; M6 = M6 synthetic (W-7984), Kavkaz-K4500= Kavkaz-K4500 L.6.A.4, dpi = days post inoculation. This experiment was repeated with the wheat lines Runal, Kavkaz-K4500 L.6.A.4, ST6, TE-9111, Arina, Titlis, M6 and Bulgaria-88 and similar results were obtained.

1.4.4. The effector cluster resides in a highly dynamic region of the genome

Effector genes are located in plastic, transposable element-rich regions of the genome in many fungal pathogens (Soyer *et al.*, 2014; Dong *et al.*, 2015; Faino *et al.*, 2016). We explored the plasticity of the genomic region harbouring the effector gene cluster in order to understand the evolution of *Avr3D1*. With this aim, we performed alignments of the QTL of the 3D7 genome to the genomes of 3D1, the reference strain IPO323 and Swiss strains 1E4 and 1A5. These alignments revealed the absence of *SSP_3* and *SSP_4* in 3D1, IPO323 and 1E4 and the absence of *SSP_3* in 1A5 (Fig 3a, S8). In order to gain further insight into the plasticity of this effector cluster, we extended our analysis using Illumina genome sequences of 128 *Z. tritici* strains obtained from four different field populations located on three continents (Hartmann & Croll, 2017; Hartmann *et al.*, 2017). *SSP_3* and *SSP_4* were absent in 65% and 42% of the strains, respectively, whereas *Avr3D1* and *QTL7_5* were present in all or 95% of the strains, respectively (Fig 3b). The presence/absence polymorphisms exhibited by several SSP-encoding genes in this cluster highlight the dynamic nature of the genomic region harbouring the virulence QTL.

To investigate whether *Avr3D1*, *SSP3*, *SSP4* and *QTL7_5* originated after speciation, we analyzed *Z. tritici* sister species to determine if they contained homologs of the genes. A homolog of *Avr3D1* was identified in all examined strains of *Zymoseptoria pseudotritici* and *Zymoseptoria ardabiliae*, but not in *Zymoseptoria brevis* or *Zymoseptoria passerinii*, suggesting that *Avr3D1* originated before *Z. tritici* speciation. Homologs of *QTL7_5* and *SSP_3* were found in only 2 out of 4 strains of *Z. ardabiliae* but not in *Z. pseudotritici* (Fig 3b). Homologs of *SSP_4* were not identified in the other *Zymoseptoria* species, indicating that this gene may have originated after *Z. tritici* speciation.

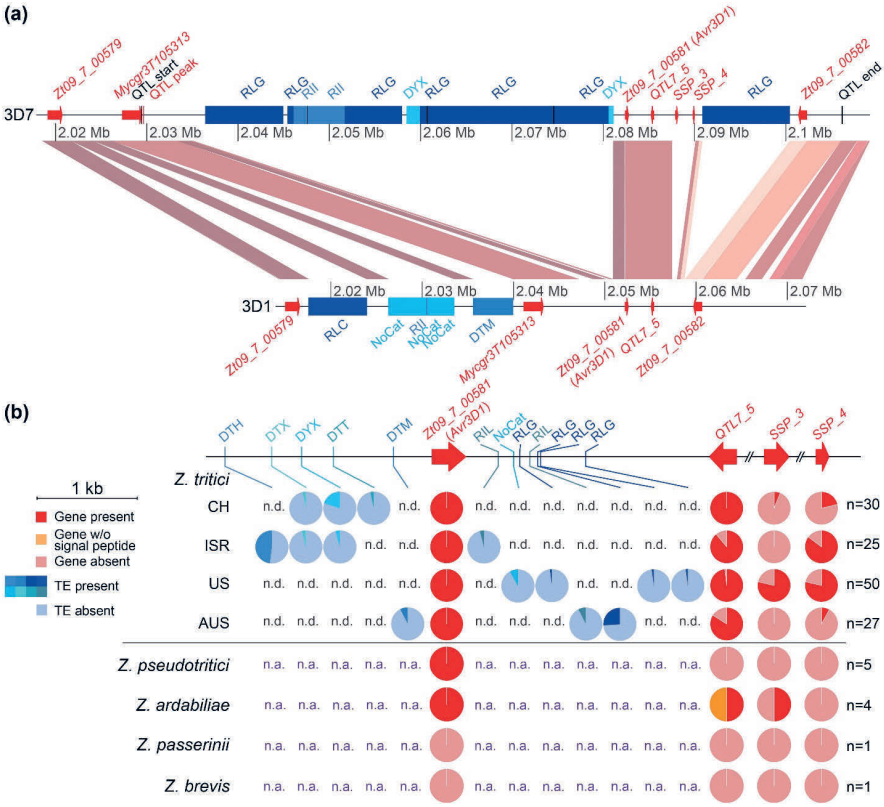

Figure 3. A dynamic and effector-rich region on chromosome 7 is associated with quantitative virulence. (a) Synteny plot comparing the quantitative trait locus (QTL) for virulence between *Z. tritici* strains 3D7 and 3D1. The borders of the 95% confidence interval of the QTL in 3D7 are marked by black vertical lines. Genes are represented by red arrows and transposable elements are represented by blue blocks. Collinear sequences between the two strains are shown in different shades of brown indicating sequence identity. **(b)** Presence/absence polymorphisms of genes predicted to encode small secreted proteins (SSPs) and transposable elements (TEs) in different populations of *Z. tritici* and in four closely related species. The pie charts in red shades show the presence/absence polymorphisms of genes encoding SSPs. The blue pie charts display the presence/absence polymorphisms of transposable elements in *Z. tritici* strains up- and downstream of the gene *Zt09_7_00581*. The transposable elements were classified according to the three-letter code described in Wicker *et al*. (2016): The first letter indicates the class (R = RNA class and D = DNA class); the second letter indicates the order (L = LTR, I = Line, T= TIR, Y= Crypton); and the third letter indicates the superfamily (C = *Copia*, G = *Gypsy*, L = *L1*, I = *I*, H= *PIF-Harbinger*, M = *Mutator*, T = *Tc1-Mariner*, X = unknown). n.d.= not detected, n.a.= not analyzed, n = number of strains, NoCat = no category, CH = Switzerland, ISR = Israel, AUS = Australia.

We extended our investigation on the genomic plasticity of the effector gene cluster to consider the presence of repetitive elements and transposable elements. Two insertions of transposable elements (of 44.5 kb and 9.5 kb, respectively) flanked the four SSP-encoding genes in 3D7, but not in 3D1, where a different transposable element insertion was present upstream of the QTL (Fig 3a). The insertion upstream of the SSP genes in 3D7 consisted of an island of 10 different transposable elements, located 1.3 kb upstream of the start codon of *Avr3D1*. The closest transposable element to *Avr3D1* is a DNA transposable element from the Crypton superfamily, which is relatively rare in *Z. tritici*. Upstream of the Crypton element, three different long terminal repeats (LTRs) from the superfamily Gypsy, the most frequent retrotransposons in *Z. tritici* (Grandaubert *et al.*, 2015), were inserted. A Gypsy LTR was also inserted only in 3D7 1 kb downstream of the effector cluster. No transposable element insertions occurred in the QTL region of the reference strain IPO323 or the Swiss strains 1E4 and 1A5 (Fig S8). Like in 3D1, transposable element insertions upstream of the QTL were identified in 1E4 and 1A5 (Fig S8). Although all the insertions were upstream of the gene *Zt09_7_00580*, they were located at different positions and classified as different superfamilies (Copia in 3D1 and Mutator in 1E4 and 1A5). We extended the analysis of chromosomal rearrangements to the 132 global strains. Remarkably, we observed that 18% of these strains contained at least one transposable element within 6.5 kb upstream of the cluster. Furthermore, seven different insertions were identified between *Avr3D1* and *QTL7_5*. The inserted transposable elements belonged to different superfamilies and were located at various positions (Fig 3b), suggesting that several different insertion events occurred independently. Thus, the effector cluster resides in a highly dynamic region of the genome, in accordance with what has been previously

described for other pathogenic fungi in which effectors reside in fast-evolving regions of their two-speed genome (Raffaele & Kamoun, 2012).

1.4.5. *Avr3D1* is highly polymorphic in four global *Z. tritici* field populations

Escape from recognition is often mediated by modifications in avirulence gene sequences. Therefore, we explored sequence polymorphisms of the avirulence gene *Avr3D1*. In the strain 3D1, the avirulent allele of *Avr3D1* (*Avr3D1*$_{3D1}$) encodes a protein of 92 amino acids with a predicted signal peptide of 21 amino acids and a high number of cysteines (8 residues, 11.3%). *Avr3D1* has three exons, of which only exon 1 and exon 2 contain coding DNA. The sequence polymorphism of *Avr3D1* was analysed in the same four global *Z. tritici* populations used for transposable element presence/absence analyses. Among these 132 strains, 31 different alleles were identified, encoding 30 different protein isoforms, all of which were population-specific (Fig 4a).

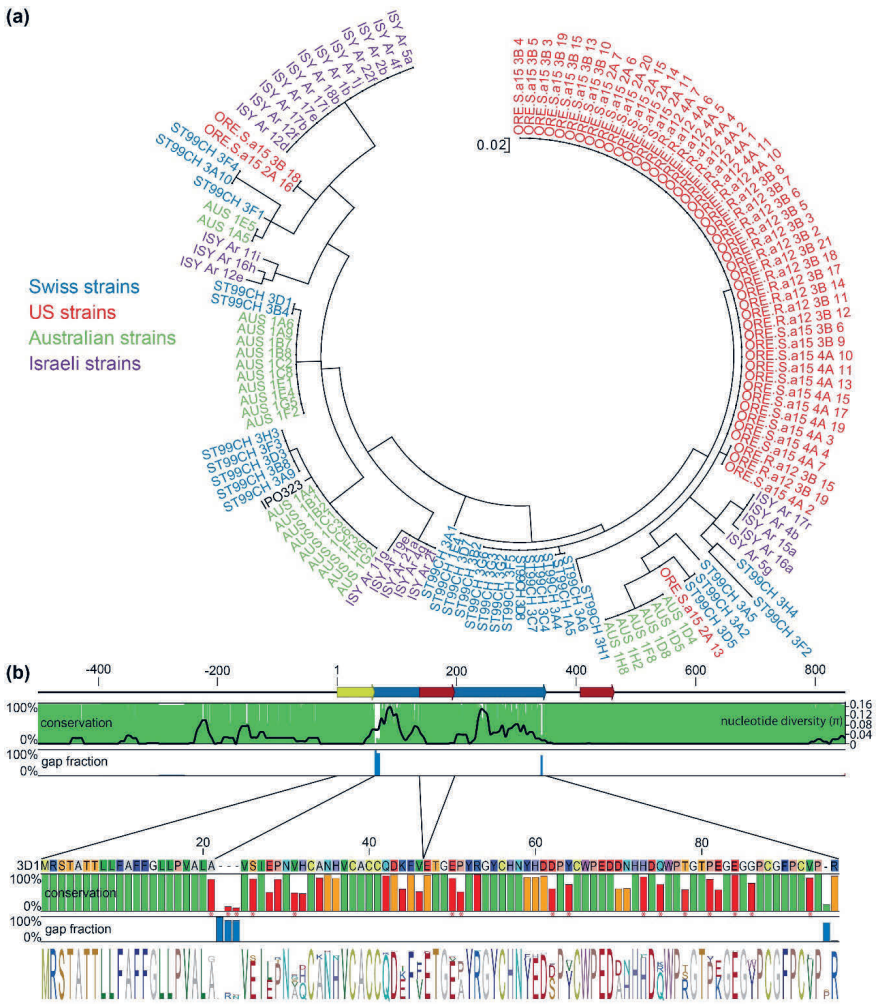

Figure 4. Avr3D1 is highly polymorphic and exhibits the signature of diversifying selection. **(a)** Phylogenetic tree of the protein sequence of Avr3D1 generated from 132 *Z. tritici* strains from four populations and the reference strain IPO323. (b) Upper panel: Representation of the *Avr3D1* gene including two introns (red arrows), the coding DNA sequence (CDS) of the mature protein (blue arrow) and the signal peptide (yellow arrow). Conservation and gap fractions of each nucleotide in 132 global *Z. tritici* strains is shown for each nucleotide as green and blue vertical bars, respectively. Nucleotide diversity (π) of *Avr3D1* is represented with a black line. Lower panel: Protein sequence encoded by the avirulent allele $Avr3D1_{3D1}$. Conservation is shown as vertical bars in green, orange and red, representing purifying, neutral or diversifying selection, respectively, as determined by analysis of dN/dS ratios. Residues under significant ($p<0.01$) diversifying selection are labelled with red asterisks. Gap fractions are shown as blue vertical bars. The consensus sequence and sequence diversity are depicted as sequence logos.

Strikingly, the 500 bp upstream of the start codon and the 500 bp following the stop codon showed lower diversity ($\pi_{Up\ flanking}$ = 0.0179; $\pi_{Down\ flanking}$ = 0.0023) than the coding DNA sequence (CDS; π_{CDS} = 0.067). In addition, nucleotide diversity was much lower in the first intron ($\pi_{intron1}$ = 0.0003) and the signal peptide sequence (π_{sp} = 0.0112) compared to the sequence encoding the mature protein ($\pi_{mature\ protein}$ = 0.068, Fig 4). This pattern is consistent with accelerated diversification of the CDS, as confirmed by the high ratio between nonsynonymous and synonymous mutations (dN/dS) in the populations (Notes S1, Fig S9). According to the codon-based maximum likelihood approach, 58 out of 96 codon sites were estimated to be under purifying selection, 3 were neutral, and 35 were under diversifying selection (Fig 4b, Notes S1, Table S3), suggesting that strong diversifying selection has led to high sequence polymorphism of *Avr3D1*. We hypothesize that numerous adaptive mutations have occurred in this avirulence gene, most probably to counteract recognition by a resistance protein.

Despite the high protein diversity, the amino acid substitutions did not affect the signal peptide and did not occur in any of the eight cysteine residues, indicating that the overall backbone structure of Avr3D1 is conserved. Remarkably, in the homologues in *Z. pseudotritici* and *Z. ardabiliae* (with 60.2% and 53.5% protein identity, respectively) all the cysteine residues were also conserved (Fig 4, S10, S11). This conservation of the overall protein structure may indicate a general role for Avr3D1 in host colonization that was preserved after speciation.

1.4.6. Substitutions in *Avr3D1* lead to evasion of recognition

The Avr3D1 isoforms in the avirulent strain 3D1 and in the virulent strain 3D7 share 86% sequence identity as a consequence of 12 amino acid substitutions and one gap

in 3D7 (Fig 1d). To determine the impact of these differences on recognition, we ectopically expressed the 3D1 (*Avr3D1*$_{3D1}$) and the 3D7 (*Avr3D1*$_{3D7}$) alleles of *Avr3D1* under the control of the promoter from 3D1 in the knockout background and tested the ability to complement the phenotype of 3D1Δavr3D1. *Avr3D1*$_{3D1}$ fully complemented the virulence phenotype of 3D1Δavr3D1 with respect to both lesion development and pycnidia production. However, *Avr3D1*$_{3D7}$ did not alter the phenotype of 3D1Δavr3D1, indicating that Avr3D1$_{3D1}$ but not Avr3D1$_{3D7}$ triggers an immune response in cv. Runal (Fig 1c). Moreover, expression of *Avr3D1*$_{3D1}$ under the control of the promoter from 3D1 in the 3D7Δavr3D1 background led to a significant reduction in disease (avirulence), whereas expression of *Avr3D1*$_{3D7}$ did not alter the phenotype in the same genetic background (Fig 1c). Therefore, Avr3D1$_{3D1}$, but not Avr3D1$_{3D7}$, is recognized in both genetic backgrounds, demonstrating that substitutions in Avr3D1 led to evasion of recognition in the virulent strain 3D7.

1.5. Discussion

In numerous plant pathosystems, a key determinant of host specificity is the resistance protein-mediated recognition of avirulence factors, which are often SSPs. Though 20 race-specific large-effect resistance genes against *Z. tritici* have been mapped in the wheat genome, their fungal interactors remain unknown with the exception of the resistance gene *Stb6*. Here, we report the discovery of a new *Z. tritici* gene, *Avr3D1*, encoding a cysteine-rich small secreted protein that triggers quantitative resistance in wheat lines harbouring the *Stb7* locus.

1.5.1. Avr3D1 recognition induces quantitative resistance

Avr3D1 is a candidate effector that is expressed during the latent phase but downregulated upon the onset of the necrotrophic phase, suggesting a function in host colonization during the latent phase or in the transition to the necrotrophic phase. The recognition of the avirulent allele leads to a dramatic reduction in the amount of infection and pycnidia formation. This demonstrates that Avr3D1 is an avirulence factor that is likely to be specifically recognized by an *Stb* gene. The fact that only certain wheat lines recognize Avr3D1 suggests that recognition follows the gene-for-gene model. In contrast to what has been shown for most other avirulence factors, Avr3D1 recognition does not lead to full resistance, but instead to quantitative resistance in which the pathogen is impaired in its ability to infect, but eventually completes its life cycle. The mechanisms through which *Z. tritici* eventually circumvents the resistance response remain unknown. We hypothesize that the magnitude of the defence response is not strong enough to prevent the progression of the infection and/or that the downregulation of *Avr3D1* during the necrotrophic phase substantially decreases the defence response. The induction of this type of partial resistance might be a shared characteristic among non-obligate pathogens that grow in the apoplast and normally do not trigger a hypersensitive response (Stotz et al. 2014). The strength of this partial or incomplete resistance response may still be sufficient to limit propagation of the pathogen under field conditions, in which case the underlying resistance gene could be a valuable source of resistance for breeding programs. Pyramiding of *Stb* resistance genes is an objective in several breeding programs because this approach is thought to be an effective and durable strategy to control septoria tritici blotch in the field (Chartrain *et al.*, 2004; Kettles & Kanyuka, 2016). In fact, TE-9111 and Kavkaz-K4500 L6.A.4, two of the lines that

specifically recognized Avr3D1, contain at least three *Stb* genes and are major sources of resistance to *Z. tritici* (Chartrain *et al.*, 2004). Our work might contribute to the identification of the corresponding *Stb* gene in the future.

In this work, we show that asexual reproduction can occur even upon induction of effector-triggered defence. In the case of AvrStb6 recognition, Stb6 strongly hinders the progression of infection, abolishing the induction of necrosis (Kema *et al.*, 2000; Ware, 2006; Zhong *et al.*, 2017). In contrast, recognition of Avr3D1 triggers a weaker form of resistance that prolongs the asymptomatic phase, while allowing necrotic lesions to develop and pycnidia to form. Though we cannot rule out the possibility that other protein isoforms of Avr3D1 might trigger a stronger resistance that completely blocks the progression of infection, these findings highlight the continuum between qualitative and quantitative resistance in gene-for-gene interactions. Although we identified an avirulence gene that has a large effect on some wheat lines, additional factors must contribute to the differences in virulence between the two strains, because the density of pycnidia formed by the Avr3D1 knockout in the avirulent strain was still lower than the pycnidia density produced by the virulent strain. The provided data further highlight the quantitative nature of wheat-*Z. tritici* interactions.

1.5.2. Chromosome rearrangements contribute to diversification of the effector gene cluster

Avr3D1 and the three other genes in the effector gene cluster are located on the right arm of chromosome 7, which is distinctive because of its low overall expression levels (Rudd *et al.*, 2015) and its enrichment in heterochromatin (Schotanus *et al.*, 2015). In fact, it was postulated that this region originated from a fusion between an

accessory chromosome and a core chromosome (Schotanus *et al.*, 2015). Numerous independent insertions of transposable elements surrounding *Avr3D1* were identified in 132 global strains of *Z. tritici*. Transposable elements are frequently described as an evolutionary force shaping adjacent regions by contributing to diversification through non-homologous recombination or RIP (Faino *et al.*, 2016; Wicker *et al.*, 2016). Given that four putative effector genes are clustered in this region, transposable elements could play a similar role in facilitating rapid evolution of these effectors, but may also enable concerted expression of effector genes during infection by chromatin remodelling (Soyer *et al.*, 2014; Schotanus *et al.*, 2015). In the case of this effector gene cluster, transposable elements might have contributed to the high diversity of the avirulence gene *Avr3D1* and the presence/absence polymorphisms shown for the other effector genes. Sequence diversification is particularly relevant for pathogen effectors, as they are key players in the coevolution with their hosts. Indeed, sequence modifications of Avr3D1 in the virulent strain allowed an escape from recognition by the corresponding resistance protein.

1.5.3. Avr3D1 sequence variation to evade recognition

A common evolutionary strategy for evading recognition is the loss of an entire avirulence gene (Schürch *et al.*, 2004; Mackey & McFall, 2006; de Jonge *et al.*, 2012; Hartmann *et al.*, 2017). However, loss of *Avr3D1* was not observed in any of the 132 global strains, despite its location in a highly plastic genomic region, as shown by presence/absence polymorphisms for neighbouring genes and transposable elements. Other deleterious mutations such as frameshifts, premature stop codons and non-functional splice sites were not found. Despite the high overall diversity, all the cysteine residues and the signal peptide, two core features of effector proteins, were completely conserved. The absence of any high-impact mutations suggests that

loss of *Avr3D1* may impose a significant fitness cost. We therefore hypothesize that Avr3D1 plays a crucial role in the life history of *Z. tritici*, though we could not demonstrate a contribution of Avr3D1 to lesion or pycnidia formation in susceptible wheat lines during the seedling stage under greenhouse conditions. It is possible that the role of Avr3D1 is more pronounced under field conditions or at different developmental stages, e.g. in adult plants. An additional hypothesis to explain the apparent dispensability of Avr3D1 is that functional redundancy masks phenotypic effects in the knockout mutants (Marshall *et al.*, 2011; Win *et al.*, 2012; Mirzadi Gohari *et al.*, 2015; Rudd *et al.*, 2015).

1.5.4. Conclusion

We identified a new major avirulence factor of *Z. tritici* (Avr3D1) that we postulate to be recognized by Stb7 or Stb12, though further analysis will be required to validate this hypothesis. Unlike what has been described for most described avirulence factors, recognition of Avr3D1 does not prevent lesion formation or pathogen reproduction, demonstrating that race-specific resistance is not always qualitative. Our comprehensive comparative genomic analysis suggests that effectors in *Z. tritici* are located in dynamic genomic compartments favouring rapid evolution, which may facilitate adaptation to the evolving wheat host.

1.6. Acknowledgments

We thank Zacharie Ngamenie, Susanne Meile, Anna Spescha and Barryette Oberholzer for their help in various experiments. Eva Stukenbrock and Jason Rudd provided the vectors pES1, pES6 and pCGEN. We thank Marc-Henri Lebrun and Thierry Marcel who provided us with wheat seeds. qPCR was performed in collaboration with the Genetic Diversity Centre (GDC), ETH Zurich. This research was supported by the Swiss National Science Foundation (Grants 31003A_155955, 31003A_173265), ETH Zurich Research Commission Grant 12-03 and an INRA Young Scientist grant.

1.7. References

Antonovics J, Thrall PH, Burdon JJ, Laine AL. 2011. Partial resistance in the *Linum-Melampsora* host-pathogen system: does partial resistance make the red queen run slower? *Evolution* **65**(2): 512-522.

Arends D, Prins P, Jansen RC, Broman KW. 2010. R/qtl: high-throughput multiple QTL mapping. *Bioinformatics* **26**(23): 2990-2992.

Brading PA, Verstappen ECP, Kema GHJ, Brown JKM. 2002. A gene-for-gene relationship between wheat and *Mycosphaerella graminicola*, the septoria tritici blotch pathogen. *Phytopathology* **92**(4): 439-445.

Brown JKM, Chartrain L, Lasserre-Zuber P, Saintenac C. 2015. Genetics of resistance to *Zymoseptoria tritici* and applications to wheat breeding. *Fungal Genetics and Biology* **79**(Supplement C): 33-41.

Camacho C, Coulouris G, Avagyan V, Ma N, Papadopoulos J, Bealer K, Madden TL. 2009. BLAST+: architecture and applications. *BMC Bioinformatics* 10(1): 421.

Chartrain L, Berry ST, Brown JKM. 2005. Resistance of wheat line Kavkaz-K4500 L.6.A.4 to septoria tritici blotch controlled by isolate-specific resistance genes. *Phytopathology* **95**(6): 664-671.

Chartrain L, Brading PA, Makepeace JC, Brown JKM. 2004. Sources of resistance to septoria tritici blotch and implications for wheat breeding. *Plant Pathology* **53**(4): 454-460.

Chen J, Jing J, Zhan Z, Zhang T, Zhang C, Piao Z. 2013. Identification of novel QTLs for isolate-specific partial resistance to *Plasmodiophora brassicae* in *Brassica rapa*. *PloS one* **8**(12): e85307.

Clement M, Posada D, Crandall KA. 2000. TCS: a computer program to estimate gene genealogies. *Molecular Ecology* **9**(10): 1657-1659.

Cook DE, Mesarich CH, Thomma BP. 2015. Understanding plant immunity as a surveillance system to detect invasion. *Annual Review of Phytopathology* **53**(1): 541-563.

Croll D, Zala M, McDonald BA. 2013. Breakage-fusion-bridge cycles and large insertions contribute to the rapid evolution of accessory chromosomes in a fungal pathogen. *PLoS Genetics* **9**(6): e1003567.

de Jonge R, Peter van Esse H, Maruthachalam K, Bolton MD, Santhanam P, Saber MK, Zhang Z, Usami T, Lievens B, Subbarao KV, et al. 2012. Tomato immune receptor Ve1 recognizes effector of multiple fungal pathogens uncovered by genome and RNA sequencing. *Proceedings of the National Academy of Sciences, USA* 109(13): 5110-5115.

Dong S, Raffaele S, Kamoun S. 2015. The two-speed genomes of filamentous pathogens: waltz with plants. *Current Opinion in Genetics & Development* **35**(Supplement C): 57-65.

Duncan KE, Howard RJ. 2000. Cytological analysis of wheat infection by the leaf blotch pathogen *Mycosphaerella graminicola*. *Mycological Research* **104**(9): 1074-1082.

Faino L, Seidl MF, Shi-Kunne X, Pauper M, van den Berg GCM, Wittenberg AHJ, Thomma BPHJ. 2016. Transposons passively and actively contribute to evolution of the two-speed genome of a fungal pathogen. *Genome Research* **26**(8): 1091-1100.

Flor HH. 1971. Current status of the gene-for-gene concept. *Annual Review of Phytopathology* **9**(1): 275-296.

Fones H, Gurr S. 2015. The impact of Septoria tritici Blotch disease on wheat: An EU perspective. *Fungal Genetics and Biology* **79**(Supplement C): 3-7.

Goodwin SB, Ben M'Barek S, Dhillon B, Wittenberg AHJ, Crane CF, Hane JK, Foster AJ, Van der Lee TAJ, Grimwood J, Aerts A, et al. 2011. Finished genome of the fungal wheat pathogen *Mycosphaerella graminicola* reveals dispensome structure, chromosome plasticity, and stealth pathogenesis. *PLoS Genetics* 7(6): e1002070.

Grandaubert J, Bhattacharyya A, Stukenbrock EH. 2015. RNA-seq-based gene annotation and comparative genomics of four fungal grass pathogens in the genus *Zymoseptoria* identify novel orphan genes and species-specific invasions of transposable elements. *G3 : genes - genomes - genetics* **5**(7): 1323-1333.

Guy L, Roat Kultima J, Andersson SGE. 2010. genoPlotR: comparative gene and genome visualization in R. *Bioinformatics* **26**(18): 2334-2335.

Hartmann FE, Croll D. 2017. Distinct trajectories of massive recent gene gains and losses in populations of a microbial eukaryotic pathogen. *Molecular Biology and Evolution* **34**(11): 2808-2822.

Hartmann FE, Sánchez-Vallet A, McDonald BA, Croll D. 2017. A fungal wheat pathogen evolved host specialization by extensive chromosomal rearrangements. *The ISME journal* **11**: 1189.

Jones JDG, Dangl JL. 2006. The plant immune system. *Nature* **444**: 323.

Kema GHJ, Verstappen EC, Waalwijk C. 2000. Avirulence in the wheat Septoria tritici leaf blotch fungus *Mycosphaerella graminicola* is controlled by a single locus. *Molecular Plant-Microbe Interactions* **13**(12): 1375-1379.

Kema GHJ, Yu D, Rijkenberg FH, Shaw MW, Baayen RP. 1996. Histology of the pathogenesis of *Mycosphaerella graminicola* in wheat. *Phytopathology* **86**(7): 777-786.

Kema GHJ, Verstappen ECP, Waalwijk C. 2000. Avirulence in the wheat septoria tritici leaf blotch fungus *Mycosphaerella graminicola* is controlled by a single locus. *Molecular Plant-Microbe Interactions* **13**(12): 1375-1379.

Kema GHJ, Mirzadi Gohari A, Aouini L, Gibriel HAY, Ware SB, van den Bosch F, Manning-Smith R, Alonso-Chavez V, Helps J, Ben M'Barek S, et al. 2018. Stress and sexual reproduction affect the dynamics of the wheat pathogen effector AvrStb6 and strobilurin resistance. *Nature Genetics*. doi: 10.1038/s41588-018-0052-9

Kettles GJ, Kanyuka K. 2016. Dissecting the molecular interactions between wheat and the fungal pathogen *Zymoseptoria tritici*. *Frontiers in plant science* **7**: 508.

Langmead B, Salzberg SL. 2012. Fast gapped-read alignment with Bowtie 2. *Nature Methods* **9**: 357.

Leigh JW, Bryant D. 2015. popart: full-feature software for haplotype network construction. *Methods in ecology and evolution / British Ecological Society* **6**(9): 1110-1116.

Lendenmann MH, Croll D, Stewart EL, McDonald BA. 2014. Quantitative trait locus mapping of melanization in the plant pathogenic fungus *Zymoseptoria tritici*. *G3 : genes - genomes - genetics* **4**(12): 2519-2533.

Librado P, Rozas J. 2009. DnaSP v5: a software for comprehensive analysis of DNA polymorphism data. *Bioinformatics* **25**(11): 1451-1452.

Linde CC, Zhan J, McDonald BA. 2002. Population structure of *Mycosphaerella graminicola*: from lesions to continents. *Phytopathology* **92**(9): 946-955.

Lo Presti L, Lanver D, Schweizer G, Tanaka S, Liang L, Tollot M, Zuccaro A, Reissmann S, Kahmann R. 2015. Fungal effectors and plant susceptibility. *Annual Review of Plant Biology* 66: 513-545.

Ma L-J, van der Does HC, Borkovich KA, Coleman JJ, Daboussi M-J, Di Pietro A, Dufresne M, Freitag M, Grabherr M, Henrissat B, et al. 2010. Comparative genomics reveals mobile pathogenicity chromosomes in *Fusarium*. *Nature* 464: 367.

Mackey D, McFall AJ. 2006. MAMPs and MIMPs: proposed classifications for inducers of innate immunity. *Molecular Microbiology* **61**(6): 1365-1371.

Marshall R, Kombrink A, Motteram J, Loza-Reyes E, Lucas J, Hammond-Kosack KE, Thomma BPHJ, Rudd JJ. 2011. Analysis of two in planta expressed LysM effector homologs from the fungus *Mycosphaerella graminicola* reveals novel functional

properties and varying contributions to virulence on wheat. *Plant Physiology* **156**(2): 756-769.

McKenna A, Hanna M, Banks E, Sivachenko A, Cibulskis K, Kernytsky A, Garimella K, Altshuler D, Gabriel S, Daly M, et al. 2010. The Genome Analysis Toolkit: A MapReduce framework for analyzing next-generation DNA sequencing data. *Genome Research* 20(9): 1297-1303.

Mirzadi Gohari A, Ware SB, Wittenberg AH, Mehrabi R, Ben M'Barek S, Verstappen EC, van der Lee TA, Robert O, Schouten HJ, de Wit PP, et al. 2015. Effector discovery in the fungal wheat pathogen *Zymoseptoria tritici*. *Molecular Plant Pathology* 16(9): 931-945.

Möller M, Stukenbrock EH. 2017. Evolution and genome architecture in fungal plant pathogens. *Nature Reviews Microbiology* **15**: 756.

Motteram J, Lovegrove A, Pirie E, Marsh J, Devonshire J, van de Meene A, Hammond-Kosack K, Rudd JJ. 2011. Aberrant protein N-glycosylation impacts upon infection-related growth transitions of the haploid plant-pathogenic fungus *Mycosphaerella graminicola*. *Molecular Microbiology* **81**(2): 415-433.

Niks RE, Qi X, Marcel TC. 2015. Quantitative resistance to biotrophic filamentous plant pathogens: concepts, misconceptions, and mechanisms. *Annual Review of Phytopathology* **53**(1): 445-470.

Palma-Guerrero J, Torriani SFF, Zala M, Carter D, Courbot M, Rudd JJ, McDonald BA, Croll D. 2016. Comparative transcriptomic analyses of *Zymoseptoria tritici* strains show complex lifestyle transitions and intraspecific variability in transcription profiles. *Molecular Plant Pathology* **17**(6): 845-859.

Petersen TN, Brunak S, von Heijne G, Nielsen H. 2011. SignalP 4.0: discriminating signal peptides from transmembrane regions. *Nature Methods* **8**: 785.

Plissonneau C, Hartmann FE, Croll D. 2018. Pangenome analyses of the wheat pathogen *Zymoseptoria tritici* reveal the structural basis of a highly plastic eukaryotic genome. *BMC Biology* **16**(1): 5.

Plissonneau C, Stürchler A, Croll D. 2016. The evolution of orphan regions in genomes of a fungal pathogen of wheat. *mBio* **7**(5): e01231-16.

Poppe S, Dorsheimer L, Happel P, Stukenbrock EH. 2015. Rapidly evolving genes are key players in host specialization and virulence of the fungal wheat pathogen *Zymoseptoria tritici* (*Mycosphaerella graminicola*). *PLoS Pathogens* **11**(7): e1005055.

Raffaele S, Kamoun S. 2012. Genome evolution in filamentous plant pathogens: why bigger can be better. *Nature Reviews. Microbiology* **10**: 417.

Rietman H, Bijsterbosch G, Cano LM, Lee H-R, Vossen JH, Jacobsen E, Visser RGF, Kamoun S, Vleeshouwers VGAA. 2012. Qualitative and quantitative late blight resistance in the potato cultivar Sarpo Mira is determined by the perception of five distinct RXLR effectors. *Molecular Plant-Microbe Interactions* **25**(7): 910-919.

Robinson JT, Thorvaldsdóttir H, Winckler W, Guttman M, Lander ES, Getz G, Mesirov JP. 2011. Integrative genomics viewer. *Nature Biotechnology* 29: 24.

Rudd JJ, Kanyuka K, Hassani-Pak K, Derbyshire M, Andongabo A, Devonshire J, Lysenko A, Saqi M, Desai NM, Powers SJ, et al. 2015. Transcriptome and metabolite profiling of the infection cycle of *Zymoseptoria tritici* on wheat reveals a biphasic interaction with plant immunity involving differential pathogen chromosomal contributions and a variation on the hemibiotrophic lifestyle definition. *Plant Physiology* 167(3): 1158-1185.

Saintenac C, Lee W-S, Cambon F, Rudd JJ, King RC, Marande W, Powers SJ, Bergès H, Phillips AL, Uauy C, et al. 2018. Wheat receptor-kinase-like protein Stb6 controls gene-for-gene resistance to fungal pathogen *Zymoseptoria tritici*. *Nature Genetics*. doi: 10.1038/s41588-018-0051-x

Sánchez-Vallet A, McDonald MC, Solomon PS, McDonald BA. 2015. Is *Zymoseptoria tritici* a hemibiotroph? *Fungal Genetics and Biology* **79**: 29-32.

Schirawski J, Mannhaupt G, Münch K, Brefort T, Schipper K, Doehlemann G, Di Stasio M, Rössel N, Mendoza-Mendoza A, Pester D, et al. 2010. Pathogenicity determinants in smut fungi revealed by genome comparison. *Science* 330(6010): 1546-1548.

Schotanus K, Soyer JL, Connolly LR, Grandaubert J, Happel P, Smith KM, Freitag M, Stukenbrock EH. 2015. Histone modifications rather than the novel regional centromeres of *Zymoseptoria tritici* distinguish core and accessory chromosomes. *Epigenetics & chromatin* **8**(1): 41.

Schürch S, Linde CC, Knogge W, Jackson LF, McDonald BA. 2004. Molecular population genetic analysis differentiates two virulence mechanisms of the fungal avirulence gene *NIP1*. *Molecular Plant-Microbe Interactions* **17**(10): 1114-1125.

Seidl MF, Thomma BPHJ. 2017. Transposable elements direct the coevolution between plants and microbes. *Trends in Genetics* **33**(11): 842-851.

Soyer JL, El Ghalid M, Glaser N, Ollivier B, Linglin J, Grandaubert J, Balesdent M-H, Connolly LR, Freitag M, Rouxel T, et al. 2014. Epigenetic control of effector gene expression in the plant pathogenic fungus *Leptosphaeria maculans*. *PLoS Genetics* 10(3): e1004227.

Stewart EI, Croll D, Lendenmann MH, Sanchez-Vallet A, Hartmann FE, Palma-Guerrero J, Ma X, McDonald BA. 2018. Quantitative trait locus mapping reveals complex genetic architecture of quantitative virulence in the wheat pathogen *Zymoseptoria tritici*. *Molecular Plant Pathology* **19**(1): 201-216.

Stewart EL, Hagerty CH, Mikaberidze A, Mundt CC, Zhong Z, McDonald BA. 2016. An improved method for measuring quantitative resistance to the wheat pathogen *Zymoseptoria tritici* using high-throughput automated image analysis. *Phytopathology* **106**(7): 782-788.

Stotz HU, Mitrousia GK, de Wit PJGM, Fitt BDL. 2014. Effector-triggered defence against apoplastic fungal pathogens. *Trends in Plant Science* **19**(8): 491-500.

Tamura K, Stecher G, Peterson D, Filipski A, Kumar S. 2013. MEGA6: molecular evolutionary genetics analysis version 6.0. *Molecular Biology and Evolution* **30**(12): 2725-2729.

Torriani SFF, Stukenbrock EH, Brunner PC, McDonald BA, Croll D. 2011. Evidence for extensive recent intron transposition in closely related fungi. *Current Biology* **21**(23): 2017-2022.

van der Does HC, Rep M. 2017. Adaptation to the host environment by plant-pathogenic fungi. *Annual Review of Phytopathology* **55**(1): 427-450.

Ware SB. 2006. Aspects of sexual reproduction in Mycosphaerella species on wheat and barley: genetic studies on specificity, mapping, and fungicide resistance. PhD thesis, Wageningen Universiteit, Wageningen, The Netherlands.

Wicker T, Sabot F, Hua-Van A, Bennetzen JL, Capy P, Chalhoub B, Flavell A, Leroy P, Morgante M, Panaud O, et al. 2007. A unified classification system for eukaryotic transposable elements. *Nature Reviews. Genetics* 8: 973.

Wicker T, Yu Y, Haberer G, Mayer KFX, Marri PR, Rounsley S, Chen M, Zuccolo A, Panaud O, Wing RA, et al. 2016. DNA transposon activity is associated with increased mutation rates in genes of rice and other grasses. *Nature Communications* **7**: 12790.

Win J, Chaparro-Garcia A, Belhaj K, Saunders DGO, Yoshida K, Dong S, Schornack S, Zipfel C, Robatzek S, Hogenhout SA, et al. 2012. Effector biology of plant-associated organisms: concepts and perspectives. *Cold Spring Harbor Symposia on Quantitative Biology* 77: 235-247.

Yang Z. 1997. PAML: a program package for phylogenetic analysis by maximum likelihood. *Bioinformatics* **13**(5): 555-556.

Yang Z. 2007. PAML 4: phylogenetic analysis by maximum likelihood. *Molecular Biology and Evolution* **24**(8): 1586-1591.

Zhan J, Linde CC, Jürgens T, Merz U, Steinebrunner F, McDonald BA. 2005. Variation for neutral markers is correlated with variation for quantitative traits in the plant pathogenic fungus *Mycosphaerella graminicola*. *Molecular Ecology* **14**(9): 2683-2693.

Zhong Z, Marcel TC, Hartmann FE, Ma X, Plissonneau C, Zala M, Ducasse A, Confais J, Compain J, Lapalu N, et al. 2017. A small secreted protein in *Zymoseptoria tritici* is responsible for avirulence on wheat cultivars carrying the *Stb6* resistance gene. *New Phytologist* **214**(2): 619-631.

Zwiers L-H, De Waard MA. 2001. Efficient *Agrobacterium tumefaciens*-mediated gene disruption in the phytopathogen *Mycosphaerella graminicola*. *Current Genetics* **39**(5): 388-393.

1.8. Supporting Information

Figure S1. Manual annotation of putative effector genes in the QTL for virulence.

Figure S2. The gene *QTL7_5* does not contribute to virulence.

Figure S3. *Z09_7_00581* encodes the avirulence factor Avr3D1 and sequence modifications lead to evasion of recognition**.**

Figure S4. *Avr3D1* does not explain all the differences in virulence between 3D1 and 3D7.

Figure S5. *In vitro* growth of the mutant lines was unaltered under several stress conditions.

Figure S6. *Avr3D1* expression peaks at the end of the latent phase.

Figure S7. Specific recognition of Avr3D1 by certain wheat lines leads to a reduction in pycnidia formation.

Figure S8. Synteny plot of the QTL between five *Zymoseptoria tritici* strains.

Figure S9. Frequency distribution of dN : dS ratios for all pairwise *Avr3D1* haplotype comparisons**.**

Figure S10. Homologous sequences of *Avr3D1* identified in five strains of *Zymoseptoria pseudotritici*.

Figure S11. Homologous sequences of *Avr3D1* identified in four strains of *Zymoseptoria ardabiliae*.

Table S1. Primers used in this study.

Table S2. Effector gene cluster annotation. gff file of the manually reannotated effector genes identified in the QTL.

Table S3. Model test and parameter estimates of diversifying selection with PAML based on the total *Avr3D1* data set.

Notes S1. Population genetic analysis

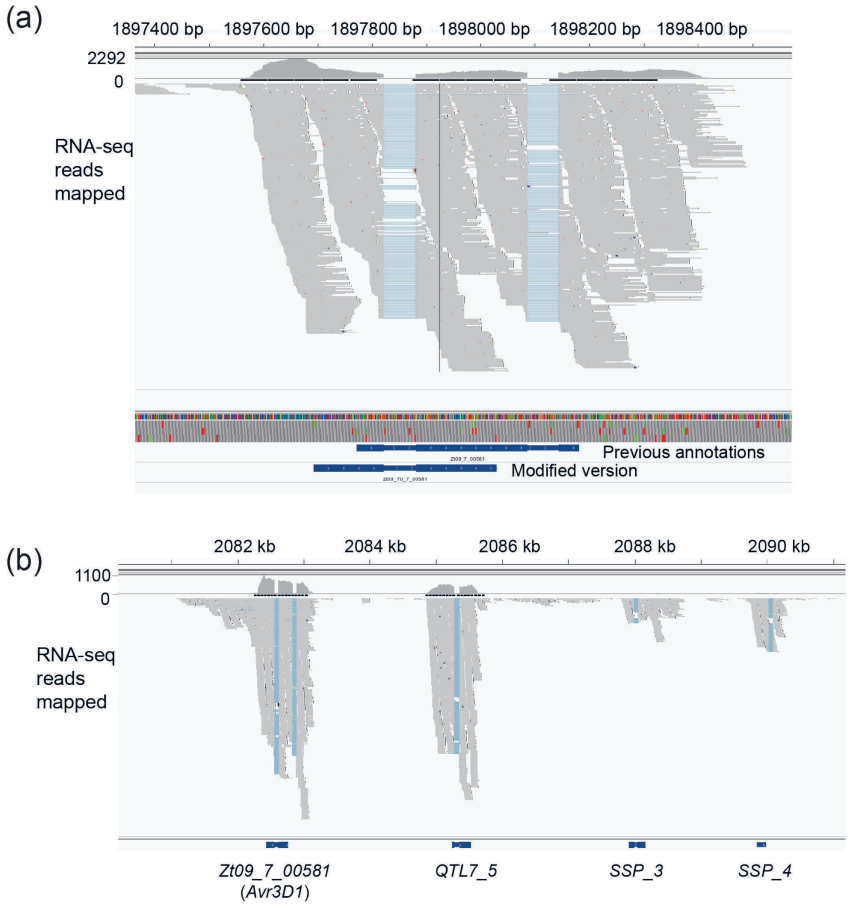

Figure S1. Manual annotation of putative effector genes in the QTL for virulence.

(a) RNA reads from the *Z. tritici* reference genome IPO323 mapped to gene *Z09_7_00581* (Rudd *et al.*, 2015). Possible start and stop codons are shown in green and red, respectively, for all forward reading frames. The previous model of *Z09_7_00581* (Grandaubert *et al.*, 2015, equivalent to JGI model) and the manually curated model are represented by blue boxes. (b) RNA reads of 3D7 genome (Palma-Guerrero *et al.*, 2016) mapped against the region containing the cluster of four genes predicted to encode SSPs.

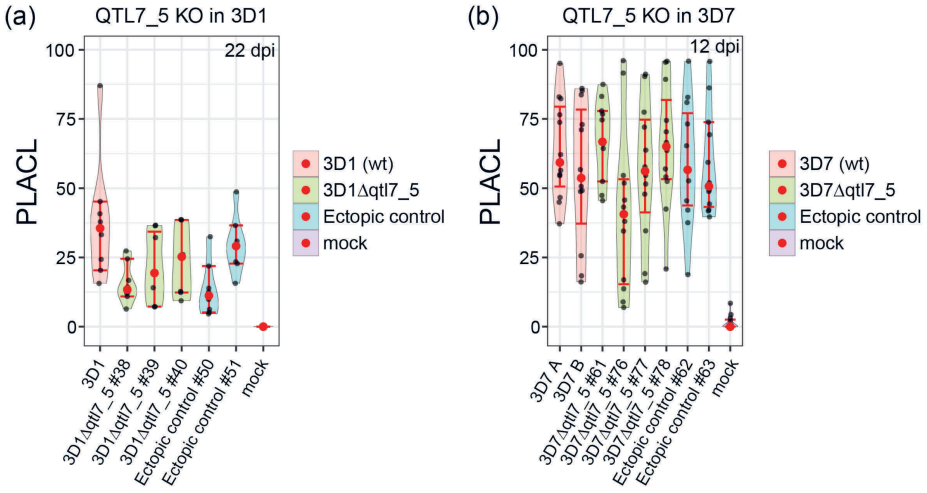

Figure S2. The gene *QTL7_5* does not contribute to virulence.

Percentage of leaf area covered by lesions (PLACL, upper panel) produced on the wheat cultivar Runal by the *Z. tritici* wild type (wt, red), three or four independent knockout (KO) lines of the gene *QTL7_5* (Δqtl7_5, green), two ectopic controls lines of the transformation (blue) and mock treatment (purple). (a) Mutants obtained in the 3D1 background. (b) Mutants in the 3D7 background. Red dots represent the median of at least seven leaves (panel A) or twelve leaves (panel B; except for the mock treatment, for which eight leaves were used), error bars represent 95% confidence intervals of the medians and black dots represent individual data points. dpi = days post inoculation. Note that plants used for panel A were regularly trimmed to the second true leaf. No statistical differences between knockout mutants and control lines was observed (α=0.01, Kolmogorov-Smirnov test).

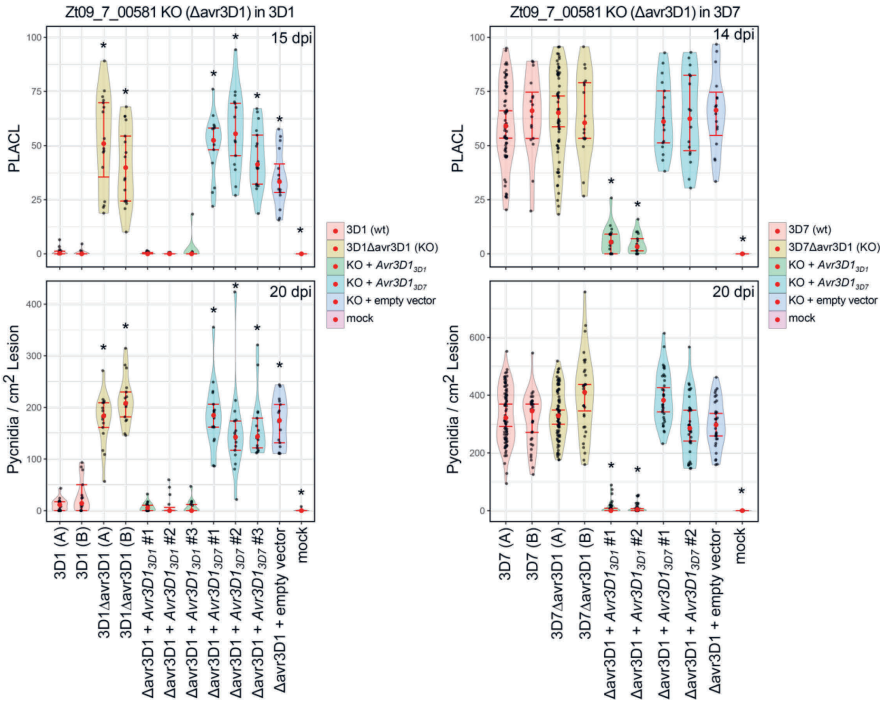

Figure S3. *Z09_7_00581* encodes the avirulence factor Avr3D1 and sequence modifications lead to evasion of recognition.

Percentage of leaf area covered by lesions (PLACL, upper panels) and pycnidia/cm^2 lesion (lower panels) produced on wheat cultivar Runal by the *Z. tritici* wild type (wt, red), the knockout (KO) in *Avr3D1* (Δavr3D1, yellow), three or two independent mutant lines expressing the 3D1 allele (*Avr3D1$_{3D1}$*, green) or the 3D7 allele (*Avr3D1$_{3D7}$*, blue), the transformation control (transformed with the empty pCGEN vector, purple) and the mock treatment (pink). Mutants were obtained in the 3D1 background (left) and in the 3D7 background (right). Two independent cultures of the wild type and the knockouts (A and B) were used for infection. Red dots represent the median of at least fourteen leaves (except for the mock treatment, for which at least eight leaves were used), error bars represent the 95% confidence intervals of the medians and black dots represent individual data points. Asterisks represent statistical differences between wild types (3D1 or 3D7 culture A, respectively, p-value < 0.01, Kolmogorov-Smirnov test) and mutants. dpi = days post inoculation. The experiments were repeated twice with similar results.

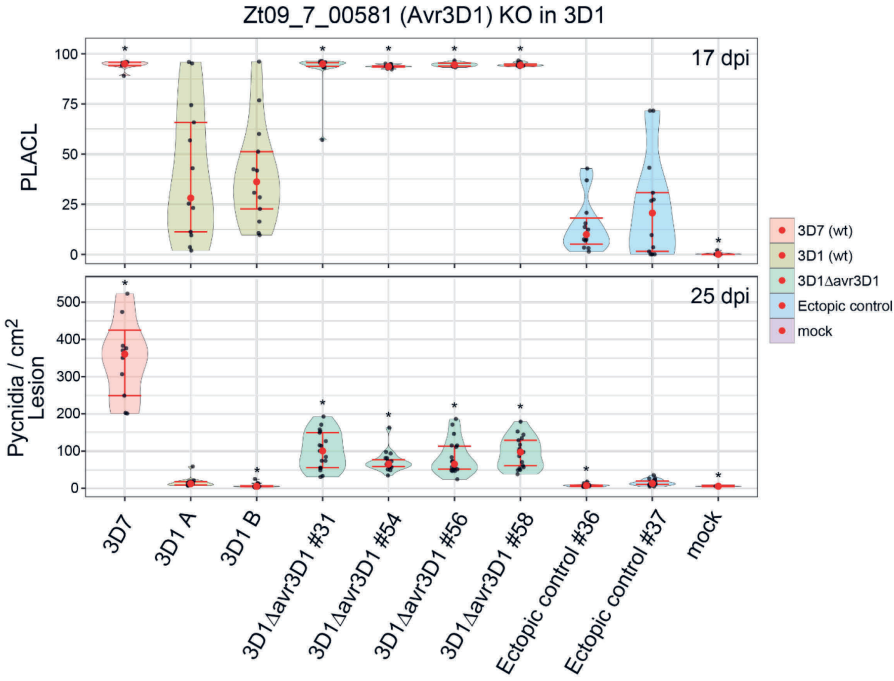

Figure S4. *Avr3D1* does not explain all the differences in virulence between 3D1 and 3D7.

Percentage of leaf area covered by lesions (PLACL) at 17 dpi (2nd true leaf, upper panel) and pycnidia density (pycnidia / cm^2 lesion) at 25 dpi (3rd true leaf, lower panel) produced on wheat cultivar Runal by *Z. tritici* 3D7, the wild type (wt) 3D1 (two independent inocula, A and B), four independent Avr3D1 knockout lines (KO, 3D1Δavr3D1) and two independent ectopic control lines of the transformation. Red dots represent the median of at least ten leaves (except for the mock treatment, for which at least four leaves were used), error bars represent 95% confidence intervals of the medians and black dots represent individual data points. dpi = days post inoculation. Asterisks indicate statistical differences between 3D1 wild type (A) and mutants (p-value < 0.01, Kolmogorov-Smirnov test).

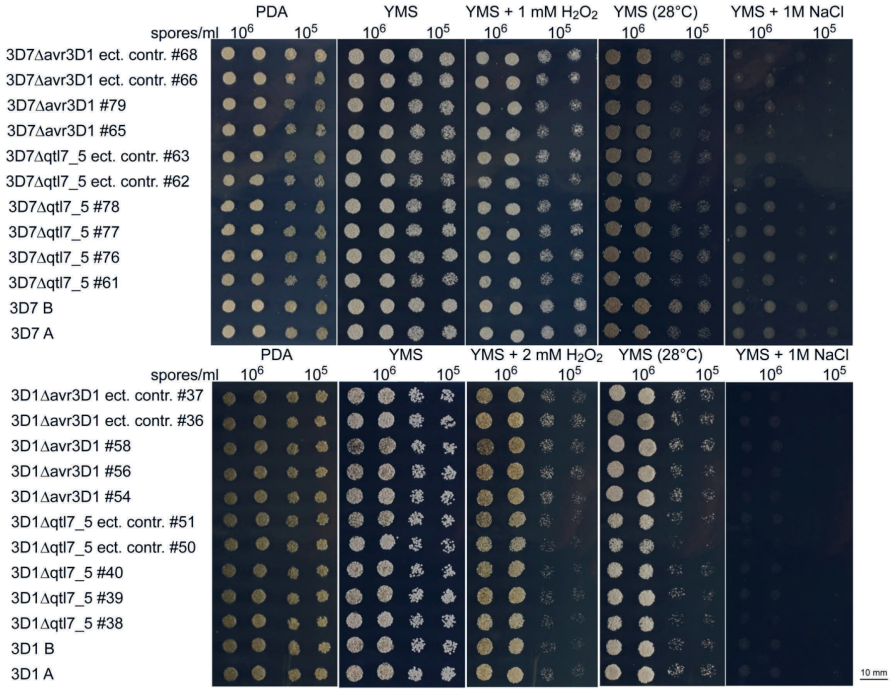

Figure S5. *In vitro* growth of the mutant lines was unaltered under several stress conditions.

Phenotypes of the *Z. tritici* wild types and the mutants in solid media. For each mutant and condition two drops of 2.5 µl at two different spore concentrations (10^6 and 10^5 spores/ml) are shown. All the plates were incubated at 18°C, unless indicated otherwise.

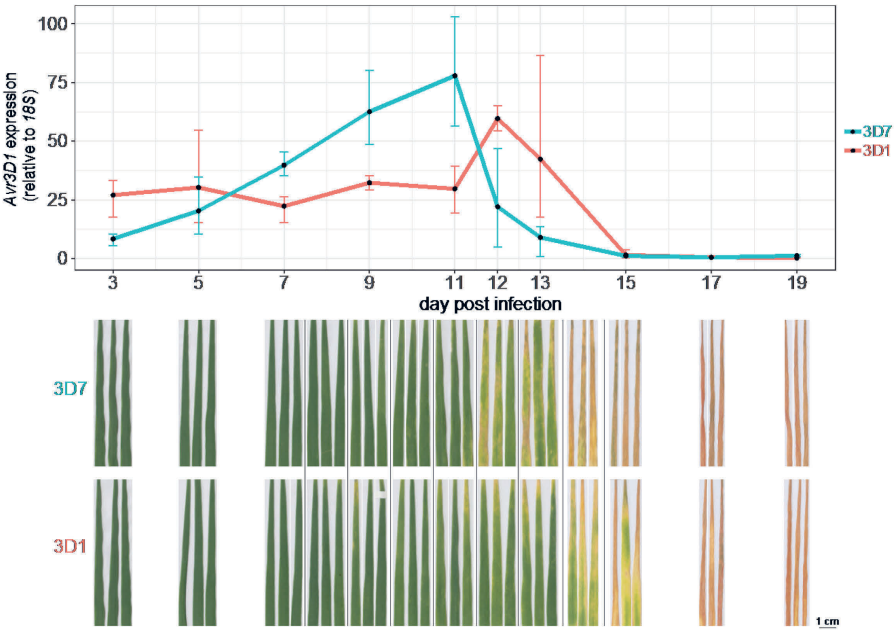

Figure S6. *Avr3D1* expression peaks at the end of the latent phase.

Expression profile of *Avr3D1* in *Z. tritici* 3D1 (red) and 3D7 (blue) during infection of the wheat cultivar Runal. The values shown are the average of three biological replicates of the relative expression levels of *Avr3D1* with respect to the reference *18S* rRNA gene. Error bars represent the 95% confidence intervals of the averages. Pictures show phenotypes of the infected leaves at each time point.

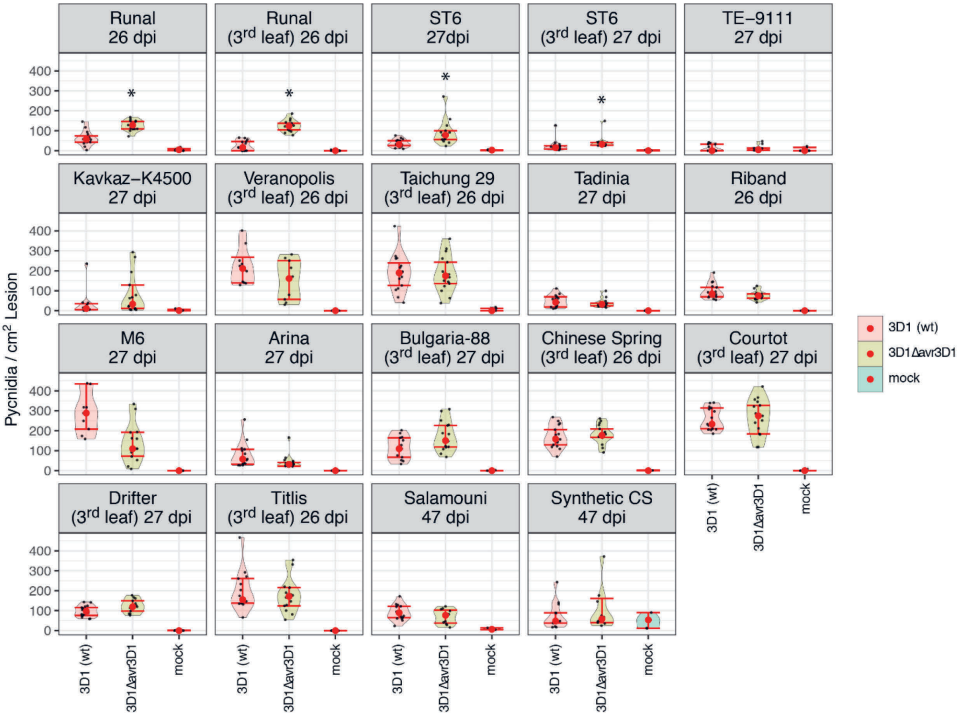

Figure S7. Specific recognition of Avr3D1 by certain wheat lines leads to a reduction in pycnidia formation.

Violin plots showing pycnidia density (pycnidia/cm^2 lesion) produced by the *Z. tritici* wild type (wt) 3D1, the Avr3D1 knockout (3D1Δavr3D1) and the mock control in seventeen wheat lines. Harvesting time points varied because of host-specific infection dynamics. Either second or third leaves were harvested depending on where more pycnidia were observed, except for the cultivars Runal and ST6, in which leaves from both positions were analysed. Red dots represent the median of at least ten leaves (except for the mock treatment, for which at least four leaves were used), error bars represent 95% confidence intervals of the medians and black dots represent individual data points. Asterisks indicate statistical differences between wild type and knockout (p-value < 0.01, Kolmogorov-Smirnov test). Synthetic CS = Synthetic Chinese Spring; ST6= Estanzuela Federal; M6= M6 synthetic (W-7984), Kavkaz-K4500 = Kavkaz-K4500 L.6.A.4, dpi = days post inoculation. This experiment was repeated with the wheat lines Runal, Kavkaz-K4500 L.6.A.4, ST6, TE-9111, Arina, Titlis, M6 and Bulgaria 88 and similar results were obtained.

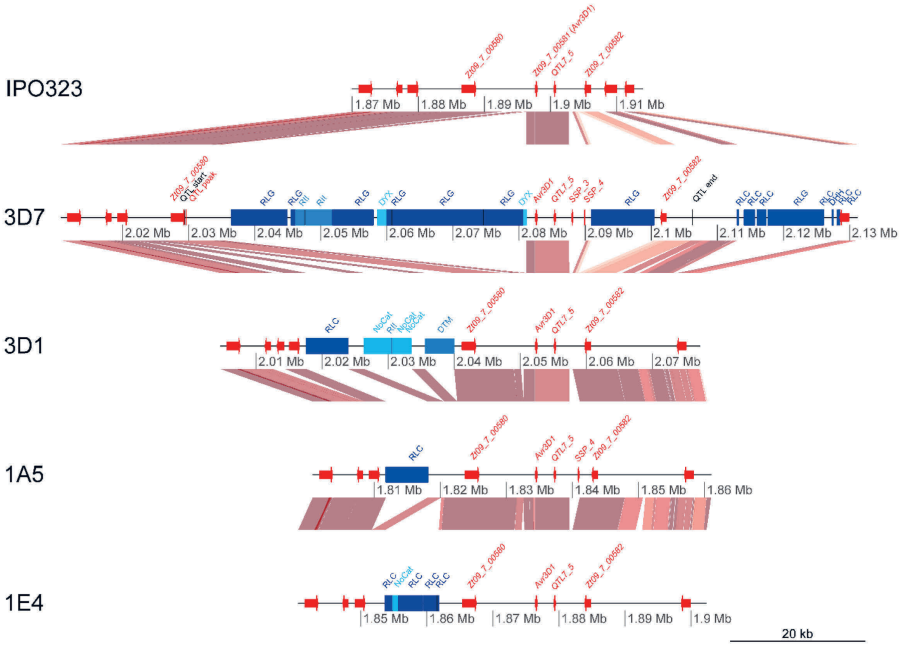

Figure S8. Synteny plot of the QTL between five *Zymoseptoria tritici* strains.

Synteny plot comparing the QTL region for virulence between strains IPO323, 3D7, 3D1, 1E4 and 1A5. The borders of the 95% confidence interval of the QTL in 3D7 are marked by black vertical lines. Genes are represented by red arrows and transposable elements are represented by blue blocks. Collinear sequences between the two strains are shown in different shades of brown according to their sequence identity. Gene annotation used for all the strains correspond to Grandaubert *et al*., (2015) for simplicity. The transposable elements were classified according to the three-letter code described in Wicker *et al*. (2016): The first letter indicates the class (R = RNA class and D = DNA class); the second letter indicates the order (L = LTR, I = Line, T= TIR, Y= Crypton, H = Helitron); and the third letter indicates the superfamily (C = *Copia*, G = *Gypsy*, I = *I*, H= *PIF-Harbinger*, M = *Mutator*, X = unknown).

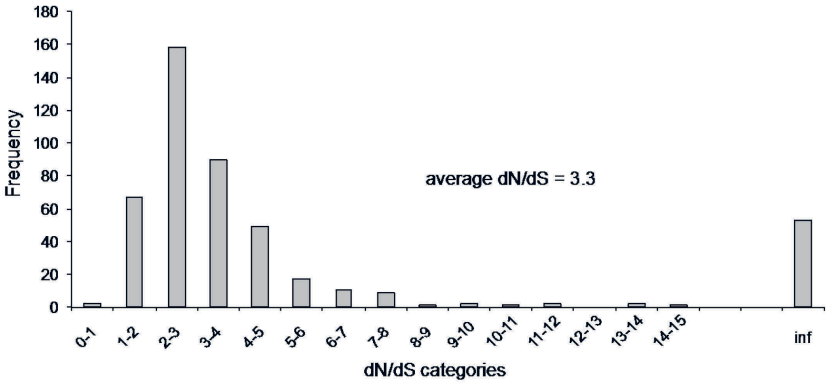

Figure S9. Frequency distribution of dN : dS ratios for all pairwise *Avr3D1* haplotype comparisons.

"inf" indicates infinite values due to comparisons among sequence pairs containing only nonsynonymous changes. Values above 1 indicate diversifying selection.

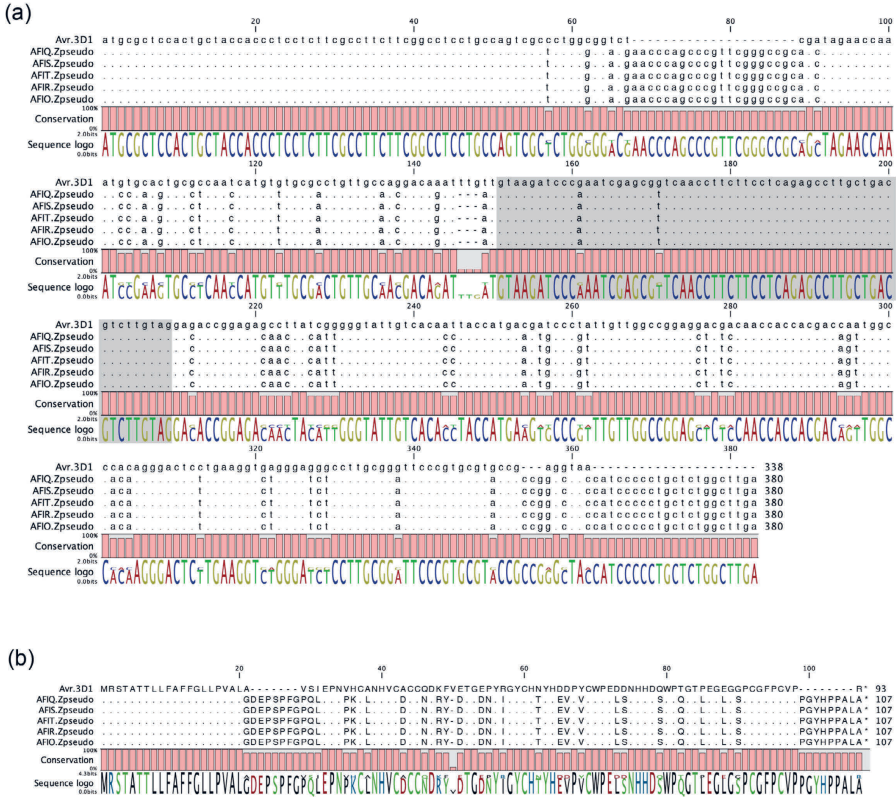

Figure S10. Homologous sequences of *Avr3D1* identified in five strains of *Zymoseptoria pseudotritici*.

(a) Nucleotide variations of Iranian *Z. pseudotritici* strains STIR04 2.2.1 (AFIQ01), STIR04 3.11.1 (AFIO01), STIR04 4.3.1 (AFIR01), STIR04 5.3 (AFIS01), STIR04 5.9.1 (AFIT01) are shown with respect to Swiss *Z. tritici* reference strain 3D1. Dots indicate identical nucleotides, the grey region highlights the intron sequence. (b) Amino acid variations are shown with respect to Swiss *Z. tritici* reference strain 3D1. Dots indicate identical amino acids.

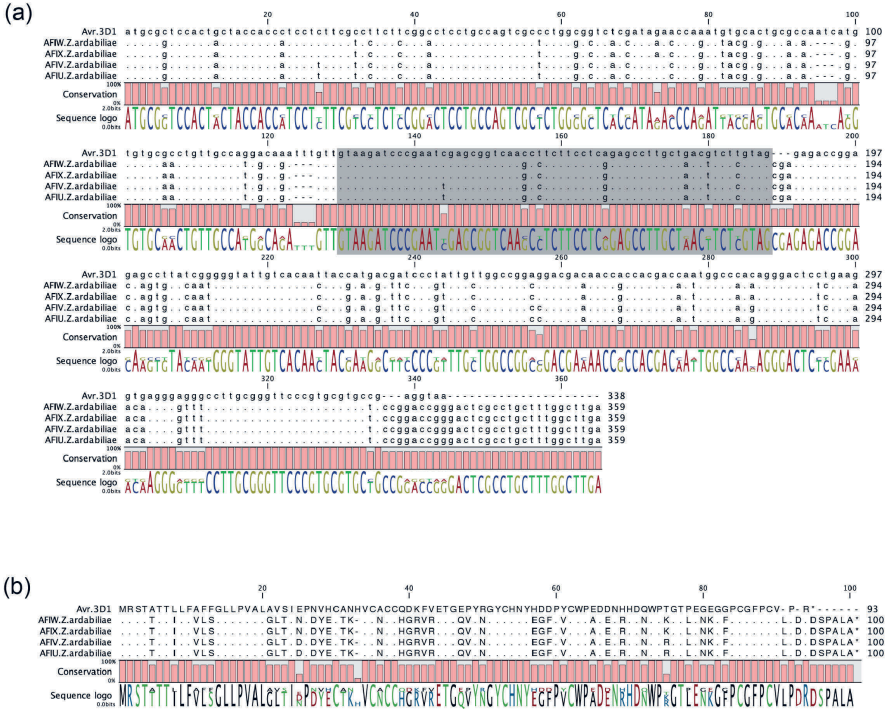

Figure S11. Homologous sequences of *Avr3D1* identified in four strains of *Zymoseptoria ardabiliae*.

(a) Nucleotide variations of Iranian *Z. ardabiliae* strains STIR04 1.1.1 (AFIU01), STIR04 1.1.2 (AFIV01), STIR04 3.13.1 (AFIW01), STIR04 3.3.2 (AFIX01) are shown with respect to Swiss *Z. tritici* reference strain 3D1. Dots indicate identical nucleotides and the grey region denotes the intron sequence. (b) Amino acid variations are shown with respect to the Swiss *Z. tritici* reference strain 3D1. Dots indicate identical amino acids.

Table S1. Primers used in this study.

Number	Name	Sequence (5'-3')	Application
LMp_36	I-F_UF-00581KO_F	TAATTAAGATATCGAGCTCGGACTTCTTCCGACGACTTCC	Avr3D1 deletion (upstream flanking region; with LMp_37)
LMp_37	I-F_UF-00581KO_R	CTCCTTCAATATCAAAGCCGCATTGTGTCGAGGCTGGTG	Avr3D1 deletion (upstream flanking region; with LMp_36)
LMp_38	I-F_DF-00581KO_F	ATAGAGATCTGCTAGCCATCCTCCTCTTCGCCTTCTTCGG	Avr3D1 deletion (downstream flanking region; with LMp_39)
LMp_39	I-F_DF-00581KO_R	CAGTGCCAAGCTTGCATGCCAATAATCCCATCCTACCTCGCC	Avr3D1 deletion (downstream flanking region; with LMp_38)
LMp_40	I-F_UF-3D7_5KO_F	CAGTGCCAAGCTTGCATGCCACTGCCAGATGTGTTCCTCAG	QTL7_5 deletion (upstream flanking region; with LMp_41)
LMp_41	I-F_UF-3D7_5KO_R	ATAGAGATCTGCTAGCCATCCATTGTTGTGGATGGGTTGC	QTL7_5 deletion (upstream flanking region; with LMp_40)
LMp_42	I-F_DF-3D7_5KO_F	CTCCTTCAATATCAAAGCCGGTTTCGCCATCTTCGCTGC	QTL7_5 deletion (downstream flanking region; with LMp_43)
LMp_43	I-F_DF-3D7_5KO_R	TAATTAAGATATCGAGCTCGGGCTTTCGTTCAGTCAACTCG	QTL7_5 deletion (downstream flanking region; with LMp_42)
LMp_26	Hyg_univ_F	CGGCTTTGATATTGAAGGAGC	Gene deletion (Hygromycin resistance gene; with LMp_27)
LMp_27	Hyg_univ_R	GATGGCTAGCAGATCTCTATTCC	Gene deletion (Hygromycin resistance gene; with LMp_26)
LMp_95	IF-581ect_F2	GCCGAATTCGAGCTCGCTACCTTGAGTGGACATGAGGA	Ectopic integration of $Avr3D1_{3D1}$ (with LMp_96)
LMp_96	IF-581ect_R2	CATGGTGGAGTGAGGGGTACCAATAATCCCATCCTACCTCGC	Ectopic integration of $Avr3D1_{3D1}$ (with LMp_95)
LMp_97	IF-XhoI-581prom_F	TCGCCGTGCCTGGGCT	Ectopic integration of $Avr3D1_{3D7}$ (with LMp_98)
LMp_98	IF-581prom_R	GCTGGTGTCGTGGTGTTGTG	Ectopic integration of $Avr3D1_{3D7}$ (with LMp_97)
LMp_99	IF-581CDS_F	CACAACACCACGACACCAGC	Ectopic integration of $Avr3D1_{3D7}$ (with LMp_100)
LMp_100	IF-XhoI-581CDS_R	TGGACTCCTTCTCGCTCTCG	Ectopic integration of $Avr3D1_{3D7}$ (with LMp_99)

ASVp_1	100846.UP_F	CACTCTCGGAGCACTCCTCGATT	Verification of Δ581 lines (with LMp_4)
LMp_4	d3_100846	AGTCAATGGACCTGGCTCAAC	Verification of Δ581 lines (with ASVp_1)
LMp_16	3D7_5KO_scr_R	CCCAAAGAATCAAAGGTGTG	Verification of ΔQTL7_5 lines (with LMp_19 or LMp_76)
LMp_19	u1_3D7_5	GCACCATTGAACGTCCTGAG	Verification of Δ QTL7_5 lines (with LMp_16)
LMp_66	581_wt_F	ATGCGCTCCACTGCTACCAC	Verification of Δ581 lines (with ASVp_2)
ASVp_2	100846.Down_R	AGCGCACTTGAATACGACTACATG	Verification of Δ581 lines (LMp_66)
LMp_76	3D7_5_wt_F	TCCACAACAATGCGTTTCG	Verification of Δ QTL7_5 lines (with LMp_16)
LMp_77	581_q_F	GAAGGAGTCCATTGCGTTTC	qRT-PCR (with LMp_78)
LMp_78	581_q_R	TGAAACATCCTTCTTCCCACG	qRT-PCR (with LMp_77)
ASVp_3	Zt18S_F	CCAGCAAATCCTTCGATCTC	qRT-PCR reference gene (with Zt18S_R)
ASVp_4	Zt18S_R	CCACTTTGACATTTCCACACC	qRT-PCR reference gene (with Zt18S_F)
ASVp_5	FL_TFC1_F	TGCTCAGATTGTGCGAAGAC	qPCR reference gene (with FL_TFC1_R)
ASVp_6	FL_TFC1_R	TCGTAGTCCGATACCATGAGG	qPCR reference gene (with FL_TFC1_F)
ASVp_7	GenR_q_F	CTGTGCTCGACGTTGTCACT	qPCR for copy number detection (with GenR_q_R)
ASVp_8	GenR_q_R	ATACTTTCTCGGCAGGAGCA	qPCR for copy number detection (with GenR_q_F)
ASVp_9	HygR_q_F	CGTCTGCTGCTCCATACAAG	qPCR for copy number detection (with HygR_q_R)
ASVp_10	HygR_q_R	CTCGATGAGCTGATGCTTTG	qPCR for copy number detection (with HygR_q_F)

Table S2. Effector gene cluster annotation.

gff file of the manually reannotated effector genes identified in the QTL.

# start gene Avr3D1								
3D7.chr_7	AUGUSTUS	gene	2082428	2082768	1	+	.	Avr3D1
3D7.chr_7	AUGUSTUS	transcript	2082428	2082768	1	+	.	Avr3D1.t1
3D7.chr_7	AUGUSTUS	start_codon	2082428	2082430	.	+	0	transcript_id "Avr3D1.t1"; gene_id "Avr3D1";
3D7.chr_7	AUGUSTUS	intron	2082557	2082615	1	+	.	transcript_id "Avr3D1.t1"; gene_id "Avr3D1";
3D7.chr_7	AUGUSTUS	CDS	2082428	2082556	1	+	0	transcript_id "Avr3D1.t1"; gene_id "Avr3D1";
3D7.chr_7	AUGUSTUS	CDS	2082616	2082768	1	+	1	transcript_id "Avr3D1.t1"; gene_id "Avr3D1";
3D7.chr_7	AUGUSTUS	stop_codon	2082766	2082768	.	+	0	transcript_id "Avr3D1.t1"; gene_id "Avr3D1";
# protein sequence = [MRSTATTLLFAFFGLLPVALAVEILPNSDCANHVCACCQDEFVETGEPYRGYCHNYEDSPYCWPEDAHHHDQWPRGTPKGEGYPCGFPCVPPR]								
# end gene Avr3D1								
# start gene QTL7_5								
3D7.chr_7	AUGUSTUS	gene	2085251	2085526	1	-	.	QTL7_5
3D7.chr_7	AUGUSTUS	transcript	2085251	2085526	1	-	.	QTL7_5.t1
3D7.chr_7	AUGUSTUS	stop_codon	2085249	2085251	.	-	0	transcript_id "QTL7_5.t1"; gene_id "QTL7_5";
3D7.chr_7	AUGUSTUS	intron	2085279	2085356	1	-	.	transcript_id "QTL7_5.t1"; gene_id "QTL7_5";
3D7.chr_7	AUGUSTUS	CDS	2085357	2085526	1	-	0	transcript_id "QTL7_5.t1"; gene_id "QTL7_5";
3D7.chr_7	AUGUSTUS	CDS	2085251	2085278	1	-	1	transcript_id "QTL7_5.t1"; gene_id "QTL7_5";
3D7.chr_7	AUGUSTUS	start_codon	2085524	2085526	.	-	0	transcript_id "QTL7_5.t1"; gene_id "QTL7_5";
# protein sequence = [MRFAIFAAIAIWAGQAAADTCGDLACSVHGGPCFYGCMDEYGGLIPSTVKYKGRCRHGSHGSYCK]								
# end gene QTL7_5								
# start gene SSP_3								
3D7.chr_7	AUGUSTUS	gene	2087916	2088164	1	+	.	SSP_3
3D7.chr_7	AUGUSTUS	transcript	2087916	2088164	1	+	.	SSP_3.t1
3D7.chr_7	AUGUSTUS	start_codon	2087916	2087918	.	+	0	transcript_id "SSP_3.t1"; gene_id "SSP_3";
3D7.chr_7	AUGUSTUS	intron	2087991	2088050	1	+	.	transcript_id "SSP_3.t1"; gene_id "SSP_3";
3D7.chr_7	AUGUSTUS	CDS	2087916	2087990	1	+	0	transcript_id "SSP_3.t1"; gene_id "SSP_3";
3D7.chr_7	AUGUSTUS	CDS	2088051	2088164	1	+	1	transcript_id "SSP_3.t1"; gene_id "SSP_3";
3D7.chr_7	AUGUSTUS	stop_codon	2088162	2088164	.	+	0	transcript_id "SSP_3.t1"; gene_id "SSP_3";
# protein sequence = [MKLSALVALMVAAMTSSVLADYADYVRVYPHDPIDGLPLTHIPRQNKCYQAAITQCGAEAANCSPLTRVSKGHTTHWYVDCRY]								
# end gene SSP_3								
# start gene SSP_4								
3D7.chr_7	AUGUSTUS	gene	2089853	2089984	1	+	.	SSP_4
3D7.chr_7	AUGUSTUS	transcript	2089853	2089984	1	+	.	SSP_4.t1
3D7.chr_7	AUGUSTUS	start_codon	2089853	2089855	.	+	0	transcript_id "SSP_4.t1"; gene_id "SSP_4";
D7.chr_7	AUGUSTUS	CDS	2089853	2089984	1	+	1	transcript_id "SSP_4.t1"; gene_id "SSP_4";
3D7.chr_7	AUGUSTUS	stop_codon	2089984	2089986	.	+	0	transcript_id "SSP_4.t1"; gene_id "SSP_4";
# protein sequence = [MQLFALATLIAAVLAVAVPDPEARGRGAVCSQQHCPFWCTICD]								
# end gene SSP_4								

Table S3. Model test and parameter estimates of diversifying selection with PAML based on the total *Avr3D1* data set.

Model	parameter estimates			L	PSS
M0: one ratio	ω = 4.24			-1385	none
M1: neutral	p0 = 0.57	p1 = 0.43		-1350	na
	ω0 = 0	ω1 = 1			
M2: selection	p0 = 0.43	p1 = 0.30	p2 = 0.27	-1295	18
	ω0 = 0	ω1 = 1	ω2 = 10.9		
M7: beta	p = 0.01	q = 0.01		-1361	na
M8: beta & ω	p = 0.01	q = 0.01		-1295	20
	p0 = 0.74	p1 = 0.26	ω = 10.8		

p0, p1, p2 = proportion of codon sites having the ω ratios of the respective site class

p, q = parameters of the beta distribution for ω

L = likelihood estimate

PSS = number of positively selected sites with probability p > 0.99

ω, omega = dN/dS

na = not applicable

Notes S1. Population genetic analysis. Strong evidence for non-neutral evolution in *Avr3D1*.

Thirty-one different alleles were identified for the gene *Avr3D1* in *Z. tritici*. There were 65 polymorphic sites with a total of 78 substitutions. The distribution of dN/dS estimates averaged over the entire gene was calculated (Fig S9) for all pairwise sequence comparisons. Fifty-three comparisons resulted in “infinite” values of dN/dS, indicating that only nonsynonymous changes were detected between those sequence pairs. Excluding these values, the average dN/dS ratio over all codon haplotypes was 3.3, which is significantly larger than the ratio of 1.0 expected for a neutral gene.

We also conducted codon-based selection analyses using PAML (Table S3). The maximum likelihood approach indicated that evolutionary models with variable dN/dS among codon sites (models M7 and M8) fitted the data significantly better than the one ratio model M0 ($p < 0.001$ for both comparisons). Furthermore, the neutral model M7 (ln -1361) fitted the data less well than the selection model M8 (ln -1295, $p < 0.001$), suggesting that diversifying selection is acting on the *Avr3D1* gene. Out of 96 codon sites, 58 were estimated to be under purifying selection, 3 were neutral, and 35 were in the category of diversifying selection, with an estimated dN/dS of 10.79, suggesting that strong diversifying selection is operating at these sites. These inferred selection categories for each site are color-coded in Fig 4b.

References

Grandaubert J, Bhattacharyya A, Stukenbrock EH. 2015. RNA-seq-based gene annotation and comparative genomics of four fungal grass pathogens in the genus *Zymoseptoria* identify novel orphan genes and species-specific invasions of transposable elements. *G3 : genes - genomes - genetics* **5**(7): 1323-1333.

Palma-Guerrero J, Torriani SFF, Zala M, Carter D, Courbot M, Rudd JJ, McDonald BA, Croll D. 2016. Comparative transcriptomic analyses of *Zymoseptoria tritici* strains show complex lifestyle transitions and intraspecific variability in transcription profiles. *Molecular Plant Pathology* **17**(6): 845-859.

Rudd JJ, Kanyuka K, Hassani-Pak K, Derbyshire M, Andongabo A, Devonshire J, Lysenko A, Saqi M, Desai NM, Powers SJ, et al. 2015. Transcriptome and metabolite profiling of the infection cycle of *Zymoseptoria tritici* on wheat reveals a biphasic interaction with plant immunity involving differential pathogen chromosomal contributions and a variation on the hemibiotrophic lifestyle definition. *Plant Physiology* **167**(3): 1158-1185.

Chapter 2

Various mutations in a fungal *Avr* gene circumvent host defences in an additive manner

Lukas Meile, Zoe Bernasconi*, Jules Peter*, Bruce McDonald and Andrea Sánchez-Vallet

* These authors contributed equally to this work

2.1. Abstract

The ability of a pathogen to infect a given host depends on its capacity to escape and suppress host defences. A key component of these defences is the detection of secreted pathogen proteins that act as avirulence factors by triggering host resistance. Altering the sequence of avirulence factors is a common strategy of many pathogens to gain virulence, but the contribution of avirulence factor polymorphism to phenotypic diversity in natural pathogen populations remains largely unknown. In this work, we studied how sequence polymorphisms of the avirulence factor Avr3D1 in the fungal wheat pathogen *Zymoseptoria tritici* are functionally linked to host evasion. By using a panel of naturally occurring strains that encode different isoforms of Avr3D1, we demonstrated that host evasion in a Swiss population of *Z. tritici* is common. We showed additive effects of various mutations on recognition by a resistant wheat cultivar and we pinpointed candidate protein residues critical for recognition. We further revealed that Avr3D1 potentially contributes to nonhost resistance against a closely related *Zymoseptoria* species, suggesting that escape from recognition of avirulence factors might have contributed to the adaptation of *Z. tritici* to wheat. Our results connect avirulence factor diversity to a highly quantitative resistance phenotype, raising the possibility that the high virulence diversity observed in *Z. tritici* populations is considerably shaped by avirulence factors.

2.2. Introduction

The success of a pathogen is strongly determined by its capacity to surmount or avoid the immune response of the host (Schulze-Lefert & Panstruga, 2011; Ayliffe & Sørensen, 2019). Plants and pathogens are engaged in a molecular arms-race, characterized by the co-evolution of a multi-layered host immune system and of diverse pathogen adaptation strategies to prevent the induction of immune responses (Jones & Dangl, 2006; Cook *et al.*, 2015; Toruño *et al.*, 2016). Plants, including the most important crops in the world, have evolved mechanisms to detect invading pathogens (Cook *et al.*, 2015; Michelmore *et al.*, 2017). This specific recognition triggers an immune response that hinders the progression of the invading microorganism (Zipfel, 2014; Cook *et al.*, 2015). The ability to overcome this immune response depends mainly on pathogen effectors, which are compounds, including proteins, that are produced by the pathogen and enable host colonization by interfering with plant defences, signalling and development (Hogenhout *et al.*, 2009; Lo Presti *et al.*, 2015; Toruño *et al.*, 2016). Although effectors normally provide an advantage to the pathogen, they are frequently recognized by resistance (R) proteins present in certain host genotypes, triggering a defence response (Flor, 1971; Stergiopoulos & de Wit, 2009). This recognition can be direct if triggered by effector-R protein binding or indirect if an altered effector target rather than the effector itself is detected (Van der Hoorn *et al.*, 2002; Jones & Dangl, 2006). In both cases, the recognized effectors are known as avirulence factors (Avrs), and the pathogens' survival depends on their ability to escape recognition of these Avrs or circumvent the immune response. Although Avr recognition has been traditionally investigated in the context of resistance against adapted pathogens, increasing evidence indicates that Avr recognition is also involved in nonhost resistance (Schulze-Lefert & Panstruga,

2011; Bettgenhaeuser *et al.*, 2018; Gilbert *et al.*, 2018; Ayliffe & Sørensen, 2019). Effectors are determinants of host specialization because of two main reasons: first, their functions can be highly specialized to certain hosts (Walton, 1996; Dong *et al.*, 2014), and second, they are recognized by resistance proteins encoded only in certain host genotypes (Flor, 1971). Hence, the repertioire of effectors present in a microorganism largely defines the compatibility with a host genotype or even with a host species (Ayliffe & Sørensen, 2019). Successful pathogens evolved towards both functional optimization of their effectors and evasion of host recognition (Sánchez-Vallet *et al.*, 2018; Frantzeskakis *et al.*, 2019). Direct recognition by resistance proteins is generally specific for certain isoforms of the avirulence factor. Thus, escape from recognition can be mediated by sequence modifications (Fudal *et al.*, 2009; Kanzaki *et al.*, 2012; Zhong *et al.*, 2017; Meile *et al.*, 2018) and by the secretion of fungal suppressors of the activity of the resistance proteins (Houterman *et al.*, 2008; Bourras *et al.*, 2016). Other mechanisms like gene deletion (Rouxel *et al.*, 2003; Gilroy *et al.*, 2011; De Jonge *et al.*, 2012; Hartmann *et al.*, 2017) and changes in effector gene expression (Qutob *et al.*, 2013; Wu *et al.*, 2015) also exist, but they come with the drawback of losing the benefits of the effector function. Thus, effector proteins with major virulence functions frequently escape recognition through modifications in the sequence (Van der Hoorn *et al.*, 2002). However, the mutations that avoid recognition by the host might also lead to reduction of the functionality of the effector and, hence, pathogen fitness. In such cases, compensatory mutations might arise to reduce the cost of escaping from recognition (Brunner & McDonald, 2018). Hence, fungal effector genes, especially avirulence genes, are frequently highly polymorphic and under diversifying selection.

Zymoseptoria tritici is the causal agent of septoria tritici blotch (STB), the major disease of wheat in Europe (Fones & Gurr, 2015). *Z. tritici* is a fast evolving latent necrotroph and has overcome most of the genetic resistance that is currently used in breeding programs. Resistance to STB is a highly quantitative trait involving 21 major and mostly strain-specific *Stb* resistance genes, of which only one has been cloned, and many quantitative trait loci and marker-trait associations (Kollers *et al.*, 2013; Brown *et al.*, 2015; Yates *et al.*, 2019). Despite the great efforts to characterize resistance to STB, the mechanisms of escape from recognition are not fully understood. A putative Avr (Zt_8_609) was shown to be under presence/absence polymorphism in *Z. tritici* populations (Hartmann *et al.*, 2017). In contrast, the only two *Avrs* that have been cloned (*Avr3D1* and *AvrStb6*) are present in all or nearly all the strains investigated so far, respectively, highly polymorphic and under diversifying selection (Zhong *et al.*, 2017; Brunner & McDonald, 2018; Meile *et al.*, 2018). Avr3D1 is specifically recognized by certain wheat lines and this recognition triggers a partial resistance, hindering pathogen progression but nonetheless allowing a certain level of asexual reproduction. *Avr3D1* is highly polymorphic and 30 different protein isoforms of Avr3D1 were identified in 132 strains collected from four different populations. All of these isoforms have a predicted signal peptide and all cysteine residues are conserved, suggesting that protein function is preserved. Remarkably, 16 out of 96 codons are under significant diversifying selection and were postulated to be involved in escape from recognition (Meile *et al.*, 2018). However, only two Avr3D1 isoforms have been assessed in detail for their avirulence activity. The isoform of the strain ST99CH_3D1 (3D1) triggers partial resistance, while the isoform of the strain ST99CH_3D7 (3D7) completely lacks avirulence activity. These two isoforms share only 86% sequence identity and amino acid differences are

distributed across the full mature protein sequence (Meile *et al.*, 2018). Therefore, the molecular bases of recognition specificity of Avr3D1 remain largely unknown.

Z. tritici originated in the Fertile Crescent 10'000 -11'000 years ago and its speciation involved a host jump during wheat domestication (Stukenbrock *et al.*, 2007). *Z. tritici* is highly specialized to wheat. On the other hand, the closely related *Zymoseptoria* species *Z. pseudotritici* and *Z. ardabiliae* are not able to infect wheat, but are pathogenic on wild grasses (Stukenbrock *et al.*, 2012). Remarkably, the genomes of these three species are highly similar and several effector genes of *Z. tritici* are also present in the genomes of *Z. pseudotritici* and *Z. ardabiliae* (Stukenbrock *et al.*, 2012). The molecular components involved in adaptation of *Z. tritici* to wheat remain largely unknown, although some genes under positive selection were shown to be involved (Poppe *et al.*, 2015).

Here, we explored the natural diversity of *Avr3D1* in the context of host evasion. We identified several protein residues of Avr3D1 that are critical for recognition and that contribute to host evasion in an additive way. We show that a homologue of Avr3D1 from the sister species *Z. ardabiliae* is recognized in wheat and we therefore speculate that accumulation of Avrs might contribute to nonhost resistance of wheat against this species.

2.3. Materials and Methods

2.3.1. *Z. tritici* strains and genome resources

For the infection assays described below, we used a selection of previously described *Z. tritici* strains collected in four different countries [Switzerland (CH), Israel

(ISY_Ar), USA (ORE) and Australia (AUS); (Zhan *et al.*, 2005)] as well as the Dutch reference strain IPO323 (Goodwin *et al.*, 2011).

The *Avr3D1* DNA and protein sequences used here had been obtained from 132 strains [described in (Zhan *et al.*, 2005) and sequenced in {Formatting Citation}; BioProject accession numbers PRJNA178194 and PRJNA327615) in a previous study (Meile *et al.*, 2018]. To determine the *Avr3D1* sequence of strain IPO87019 (Kema *et al.*, 1996), filtered raw reads were downloaded from the JGI Genome Portal (Project ID: 1090932), assembled and subjected to BLAST search using the De Novo Assembly tool, the Extract Consensus Sequence tool and the BLAST tool implemented in CLC Genomics Workbench 9.5.4; (Qiagen, Redwood city, CA, USA). The same software was used to identify a homologue of *Avr3D1* on chromosome 5 in strain 3D1. The *Avr3D1* sequences of strains ISR398 and ISR8036 (Yechilevich-Auster *et al.*, 1983) were determined by Sanger sequencing (Microsynth AG, Balgach, Switzerland) using amplicons generated with the Phusion polymerase (NEB, Ipswich, MA, USA) and primers depicted in Table S1 from genomic DNA in technical duplicates.

2.3.2. Identification of *Avr3D1* homologues in related *Zymoseptoria* species

We searched for homologues of *Avr3D1* using the BLAST tool implemented in CLC Genomics Workbench 11.0 in four strains of *Z. ardabiliae* (STIR04 1.1.1, STIR04 1.1.2, STIR04 3.13.1 and STIR04 3.3.2), five strains of *Z. pseudotritici* (STIR04 2.2.1, STIR04 3.11.1, STIR04 4.3.1, STIR04 5.3, STIR04 5.9.1), one strain of *Z. passerinii* (SP63) and one strain of *Z. brevis* (Zb18110) using the blastn program (Match cost: 2; mismatch cost: 3; gap existence cost: 5; gap extension cost: 2; word size: 11; filtered for low complexity). To determine the protein sequence of the homologues,

their DNA sequences were aligned to the sequence of *Avr3D1*$_{3D1}$ using CLC Genomics Genomics Workbench 11.0 and the start codon, the stop codon and intron 1 were identified (Figure S2). Signal peptide and effector predictions were performed using SignalP 3.0 (Dyrløv Bendtsen *et al.*, 2004) and EffectorP 1.0 (Sperschneider *et al.*, 2016), respectively. A maximum likelihood tree of protein sequences was obtained in CLC Genomics Workbench 11.0 using the Jukes-Cantor distance measure. The genome sequences were downloaded from NCBI (BioProject accession numbers PRJNA343332, PRJNA343333, PRJNA343334, PRJNA343335, PRJNA277173, PRJNA46489, PRJNA63035, PRJNA63037, PRJNA63039, PRJNA63049 and PRJNA273516 (Stukenbrock *et al.*, 2011; Grandaubert *et al.*, 2015).

2.3.3. Generation of plasmid constructs and transformation of *Z. tritici*

To generate plasmid constructs for the ectopic expression of various alleles of *Avr3D1* in *Z. tritici*, we exchanged the coding DNA sequence (CDS) and intron 1 of *Avr3D1* in the plasmid pCGEN-*Avr3D1*$_{3D1}$ect, which had been generated in a previous study (Meile *et al.*, 2018) under the name pCGEN-581$_{3D1}$ect. pCGEN-*Avr3D1*$_{3D1}$ect harbours the *Avr3D1* allele from strain 3D1 and is based on pCGEN, a plasmid designed for *Agrobacterium tumefaciens*-mediated transformation of fungi (Motteram *et al.*, 2011). To replace the CDS, pCGEN-*Avr3D1*$_{3D1}$ect was first digested with XhoI, removing the CDS and part of the promoter sequence. The resulting linearized plasmid, the amplified CDS of a different strain or species and a fragment to reconstitute the original promoter sequence were then assembled using the In-Fusion HD Cloning Kit (Takara Bio Inc., Shiga, Japan), resulting in pCGEN-*Avr3D1*$_{strain_of_interest}$ect. The primers used for cloning are depicted in Table S1 and the cloning procedure is illustrated in Figure S1. *Z. tritici* was transformed by

Agrobacterium tumefaciens-mediated transformation as described before (Zwiers & De Waard, 2001; Meile *et al.*, 2018), using the *A. tumefaciens* strain AGL-1. For the obtained mutants, the copy number of the inserted T-DNA was determined by qPCR on genomic DNA. Transformant lines with more than one T-DNA copy were excluded from further experiments.

2.3.4. Infection assays

Wheat seeds (*Triticum aestivum* L.) of cultivars Runal, Titlis and Drifter were purchased from DSP Ltd. (Delley, Switzerland). Seeds of the cultivar Estanzuela Federal (ST6) and the breeding line TE 9111 were a gift from Thierry Marcel and Marc-Henri Lebrun. Seedlings were grown prior to infection similarly as previously described (Meile *et al.*, 2018). Briefly, the peat substrate Jiffy GO PP7 (Jiffy Products International, Moerdijk, the Netherlands) and square pots (11 x 11 x 12 cm) were used to grown seedlings for 15-18 d in a glasshouse at 18°C (day) and 15°C (night) with a 16-h photoperiod and 75% humidity.

To prepare *Z. tritici* inoculum, a dense blastospore suspension grown in yeast sucrose broth (YSB; 10 g/L yeast extract, 10 g/L sucrose, 50 µg/mL kanamycin sulphate) for 4-6 days (18°C, 120 rpm) was filtered through cheese cloth. Blastospores were then harvested by centrifugation (3273 g, 4°C, 15 min), resuspended in water and stored on ice until infection (0–1 d). Their concentration was determined using KOVA Glasstic counting chambers (Hycor Biomedical, Inc., Garden Grove, CA, USA) and adjusted to 10^6 or $5x10^6$ spores/mL in 0.1% Tween 20. Thirty mL of this suspension was used to spray-inoculate two pots containing 16-20 seedlings each.

Pots containing inoculated plants were then placed in plastic bags for 3 days as previously described (Meile *et al.*, 2018) to increase humidity. Inoculated plants were kept under the same conditions as before inoculation in the case of experiments that included only Swiss strains or mutant strains derived from the Swiss strain 3D1. Whenever strains from Israel, Australia and the USA were used, the inoculated plants were kept in a closed growth chamber (16-h photoperiod, 18°C (day), 15°C (night), 80% humidity).

2.3.5. Phenotyping and data analysis

Symptoms were quantified by mounting the second leaves on paper sheets with the adaxial side facing up, scanning them using a flatbed scanner (CanoScan LiDE 220; 1200 dpi resolution) and analysing them with an ImageJ-based automated image analysis tool (Schneider *et al.*, 2012; Stewart *et al.*, 2016). The obtained phenotype data were analysed and plotted using the "ggplot2" package in RStudio v.1.2.1335. Confidence intervals of the medians were estimated using the "boot" package and Kolmogorov–Smirnov tests for statistical significance were performed using the "Matching" package.

2.4. Results

2.4.1. Different *Z. tritici* strains carrying different alleles of *Avr3D1* escape recognition in cultivar Runal

To explore whether host evasion is prevalent in the context of the avirulence gene *Avr3D1* and to identify mutations that likely contribute to host evasion, we assessed virulence of a set of 22 *Z. tritici* strains carrying a total of 18 different *Avr3D1* alleles in wheat lines of contrasting ability to recognize the Avr3D1 isoform of strain 3D1 ($Avr3D1_{3D1}$). The wheat lines Runal, TE-9111 and Estanzuela Federal (ST6) had been shown to recognize $Avr3D1_{3D1}$ and are therefore here referred to as resistant hosts, while the wheat lines Titlis and Drifter do not carry the corresponding resistance gene (Meile *et al.*, 2018) and are therefore here referred to as susceptible hosts. Each strain was phenotyped on at least two resistant hosts and on at least one susceptible host. A strain was considered avirulent on resistant hosts if it produced fewer symptoms than the virulent control strain 3D7 and considered virulent if symptoms were comparable to 3D7. On susceptible hosts, strains were considered avirulent if they produced fewer symptoms than both the control strains 3D7 and 3D1, which are both virulent on susceptible hosts and considered virulent if symptoms were similar or more abundant compared to at least one of the control strains. Fifteen (68%) strains were virulent on at least one resistant host (Table 1), suggesting that they are able to escape Avr3D1-triggered defence and carry candidate virulent *Avr3D1* alleles. The remaining seven (32%) strains were avirulent on all tested resistant hosts; however, three (14%) of them were also avirulent on the susceptible hosts (Table 1), suggesting that their virulence is generally low, regardless of a possible Avr3D1-triggered defence. Four (18%) strains were avirulent on all resistant

hosts but virulent on susceptible hosts (Table 1), suggesting that they carry candidate avirulent *Avr3D1* alleles. The strains ST99CH_3A10 (3A10) and ST99CH_3F4 (3F4) had the same allele, but gave opposite phenotypes. While 3A10 displayed behaviour typical of an avirulent strain, 3F4 fully colonized the resistant cultivar Runal.

Table 1. The majority of *Z. tritici* strains harbouring different alleles of *Avr3D1* evade host recognition.

Twenty-four strains from different populations (ST99CH strains were collected from Switzerland; ISY_Ar from Israel; ORE from Oregon; AUS from Australia; IPO323 from The Netherlands) were assessed for cultivar-specific virulence using wheat lines either with (Runal, ST6 and TE-9111) or without (Titlis and Drifter) specific resistance triggered by the avirulence factor Avr3D1. Different background colours of the strain names indicate the presence of different isoforms of Avr3D1. In resistant lines, strains were considered avirulent ("a", green background) if the percentage of leaf area covered by lesions (PLACL) was lower than for the virulent strain 3D7 and strains were considered virulent ("v", brown background) if lesions developed similarly or faster than in 3D7. In susceptible cultivars, strains were considered avirulent if the PLACL was lower compared to both 3D1 and 3D7 and considered virulent in any other case. Predictions on whether the strains are likely to harbour a virulent or an avirulent isoform of Avr3D1 are indicated. Strains that were avirulent in all tested resistant and susceptible cultivars were not considered for predictions about Avr3D1 recognition. The PLACL was determined using automated image analysis and compared between strains using the Kolmogorov-Smirnov test (α=0.01) n.d.= not determined.

Strain	Resistant hosts			Susceptible hosts		Prediction
	Runal	ST6	TE-9111	Titlis	Drifter	
ST99CH_3D1	a	a	a	v	v	-
ST99CH_3B4	a	a	n.d.	a	n.d.	not possible
ST99CH_3D7	v	v	v	v	v	
ST99CH_3A1	v	v	n.d.	v	a	virulent
ST99CH_3A10	a	a	a	a	v	not possible
ST99CH_3F4	v	n.d.	a	n.d.	v	
ST99CH_3A2	v	v	n.d.	a	n.d.	virulent
ST99CH_3A5	v	v	n.d.	v	n.d.	virulent
ST99CH_3A6	v	a	n.d.	v	n.d.	virulent
ST99CH_3F1	v	a	v	v	v	virulent
ST99CH_3F2	v	v	n.d.	v	n.d.	virulent
ST99CH_3F3	a	a	v	a	v	virulent
ST99CH_3D3	v	n.d.	v	n.d.	v	
ST99CH_3G6	v	v	n.d.	a	n.d.	virulent
ST99CH_3H1	v	a	n.d.	v	n.d.	virulent
ST99CH_3H4	v	v	n.d.	v	n.d.	virulent
ISY_Ar_12d	a	a	n.d.	n.d.	a	not possible
ISY_Ar_19e	a	a	n.d.	n.d.	a	avirulent
ISY_Ar_21a	a	a	n.d.	n.d.	v	
ISY_Ar_16h	a	a	a	n.d.	v	avirulent
ORE.S.a15 2A16	a	a	n.d.	n.d.	v	avirulent
ORE.R.a12.3B3	a	v	n.d.	n.d.	v	virulent
IPO323	v	v	n.d.	n.d.	v	virulent
AUS_1E5	a	v	n.d.	n.d.	a	virulent

2.4.2. Different isoforms trigger different magnitudes of defence

To further determine whether mutations in the coding region of *Avr3D1* caused escape from recognition, we sought to eliminate *Avr3D1*-unrelated strain-to-strain differences by using isogenic mutant lines. We further examined the isoforms of strains for which we got unclear results like avirulence on susceptible hosts or different outcomes on different resistant hosts. In addition, we also investigated the Avr3D1 isoform present in the two Swiss strains 3A10 and 3F4 because infections with these wild type strains led to contrasting predictions about the recognition of the corresponding isoforms (Table 1). Expression of different alleles of *Avr3D1* in the

Table 2. Several isoforms of Avr3D1 trigger defence responses.

Pairwise comparison of virulence phenotypes, measured as percentage of leaf area covered by lesions (PLACL), of isogenic *Zymoseptoria tritici* lines expressing different alleles of *Avr3D1*. The PLACL was determined using automated image analysis and compared with the control lacking *Avr3D1* (3D1Δ*avr3D1*) gene or expressing the avirulent allele of *Avr3D1* (*Avr3D1*$_{3D1}$) using the Kolmogorov-Smirnov test (α=0.01). Predictions are based on the phenotype of wild type strains (Table 1). n.d.= not determined. Asterisks indicate that virulence differences could not be consistently observed at different time points or in different experiments.

isoform	prediction	virulence vs. 3D1Δ*avr3D1*	virulence vs. 3D1Δ*avr3D1* +*Avr3D1* $_{3D1}$
ST99CH_3D1	-	lower	-
ST99CH_3D7	-	equal	higher
ST99CH_3F4	not possible	lower	higher/equal*
ISY_Ar_19e	a	lower	lower
AUS_1A6	n.d.	lower	higher/equal*
AUS_1B1	n.d.	equal	higher
AUS_1E5	v	equal/higher*	higher
ISY_Ar_16h	a	lower	lower
ORE.R.a12.3B3	v	lower	higher
IPO87019	n.d.	lower	lower
ISR398	n.d.	lower	lower

virulent genetic background of strain 3D1 lacking the *Avr3D1* gene (3D1Δ*avr3D1*) was pursued. This way, nine different Avr3D1 isoforms were evaluated for their capacity to induce defences in cultivar Runal, using transformant lines expressing *Avr3D1*$_{3D1}$, *Avr3D1*$_{3D7}$, and the line 3D1Δ*avr3D1* as controls. Two isoforms (from the strains AUS_1E5 and AUS_1B1), in addition to the one from strain 3D7, did not result in changes in virulence compared to 3D1Δ*avr3D1*, suggesting that they are not recognized and are therefore considered virulent isoforms. Seven isoforms, including Avr3D1$_{3F4}$, led to a reduction of symptoms compared to 3D1Δ*avr3D1* (Table 2) and, thus, were considered to be recognized by the resistant cultivar and therefore to be avirulent isoforms. Interestingly, the reduction of virulence was not the same for all the tested isoforms. Isoforms from the strain 3F4 (Avr3D1$_{3F4}$), the strain AUS_1A6 (Avr3D1$_{AUS_1A6}$) and the strain ORE_3B3 led to a smaller reduction of symptoms than Avr3D1$_{3D1}$, while the isoforms of the strains ISY_Ar_19e, IPO87019, ISY_Ar_16h and ISR398 (Avr3D1$_{IPO87019}$, Avr3D1$_{ISY_Ar_16h}$ and Avr3D1$_{ISR398}$, respectively) reduced symptoms even more than Avr3D1$_{3D1}$ (Table 2, Fig 1). Remarkably, no tested isoform completely abolished symptom development (Fig 1, lower panel), suggesting that the quantitative nature of Avr3D1-triggered resistance is a general feature of *Z.tritici.*

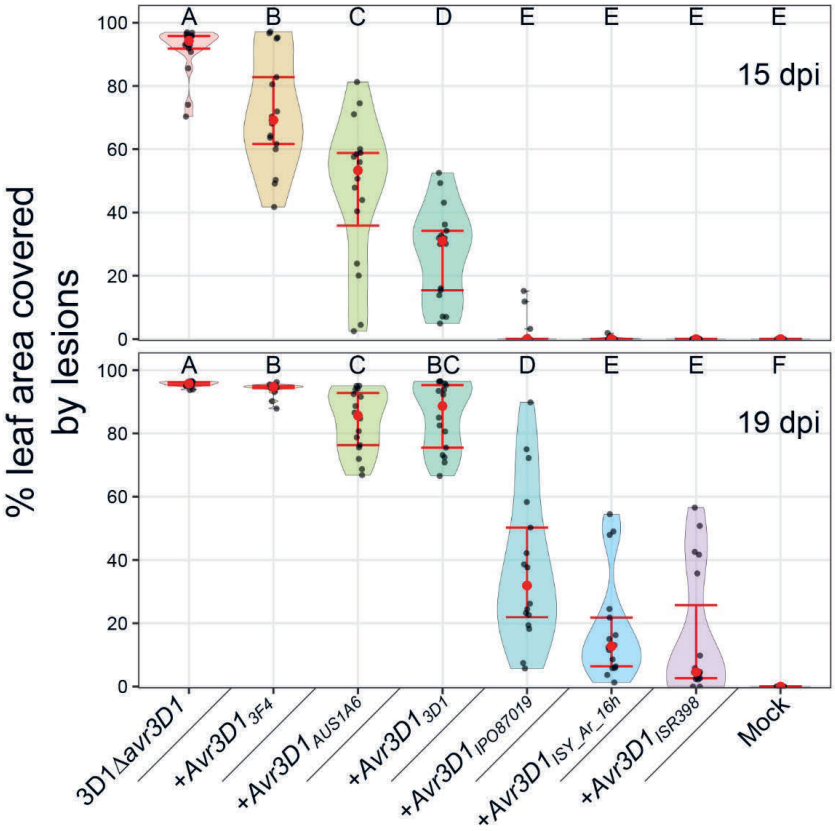

Figure 1. Different isoforms of Avr3D1 trigger different magnitudes of defence responses.

Violin plots showing the percentage of leaf area covered by lesions of wheat leaves (cultivar Runal) infected with *Z. tritici* strain 3D1 lacking *Avr3D1* (3D1Δ*avr3D1*) and the same strain harbouring an ectopic copy of different alleles of *Avr3D1* (+*Avr3D1*$_{strain\ name}$). Plants were phenotyped at 15 (upper panel) and 19 (lower panel) days post infection (dpi) using automated image analysis. Red dots represent the median, error bars represent the 95% confidence interval of the median and grey dots represent the individual data points. Letters indicate statistical groups according to the Kolmogorov-Smirnov test ($p<0.01$).

2.4.3. Several mutations in Avr3D1 can explain host evasion

To identify candidate residues in Avr3D1 which could be causative for host evasion, we aligned 33 different isoform sequences identified in 135 strains isolated from 5 different countries. We identified 31 amino acid substitutions that occurred in avirulent and candidate avirulent isoforms (Table 3, highlighted in deep or light green, respectively). These mutations were considered as probably not involved in fully preventing recognition by the host. Additionally, we identified 20 amino acid substitutions that uniquely occurred in candidate virulent isoforms (Table 3, highlighted in light red) and eight substitutions that uniquely occurred in isoforms that completely escaped recognition in infection assays using isogenic lines. These eight substitutions therefore represent high-priority candidate mutations for host evasion (Table 3; 24insV, V31S, H32D, A34K, H36N, K44T, Q75K, 95insP; highlighted in deep red). Virulent isoforms or candidate virulent isoforms harboured between one and three of these high-priority candidate mutations.

The three highly avirulent isoforms Avr3D1$_{IPO87019}$, Avr3D1$_{ISY_Ar_16h}$ and Avr3D1$_{ISR389}$ all shared a tyrosine residue at position 81 while the isoforms that partially escape recognition, Avr3D1$_{3D1}$, Avr3D1$_{AUS_1A6}$, Avr3D1$_{ISY_Ar_19e}$ and Avr3D1$_{ORE3B3}$ carried a proline residue at the same position (Table 3), suggesting that this residue is critical for partial escape from recognition.. Similarly, Avr3D1$_{3D1}$ and Avr3D1$_{AUS_1A6}$ exhibited a slight difference in triggering defence and the only amino acid difference between them is G86W, which likely explains their quantitative phenotypic difference (Table 3).

Table 3. Several amino acid substitutions in Avr3D1 are associated with host evasion (next page).

Alignment of 33 Avr3D1 isoforms found in 135 *Zymoseptoria tritici* strains. Fully conserved residues are not shown and residues that are identical to the isoform of strain 3D1 are represented as a dot. In the left column, a deep green or deep red background indicates (partially) avirulent or virulent isoforms, respectively, based on the virulence phenotype of isogenic lines expressing these isoforms. A light green or light red background indicates putatively (partially) avirulent or putatively virulent isoforms, respectively, based on the virulence phenotypes of the corresponding wild type strains. Deep green amino acid substitutions occurred in at least one avirulent isoform and light green substitutions occurred in at least one putatively avirulent isoform. Deep red or light red substitutions occurred in at least one virulent or putatively virulent isoform, respectively, but in none of the (putatively) avirulent isoforms. Numbers indicate the position of the alignment and asterisks in the top row indicate residues that had previously been shown to be under significant diversifying selection (Meile *et al*., 2018).

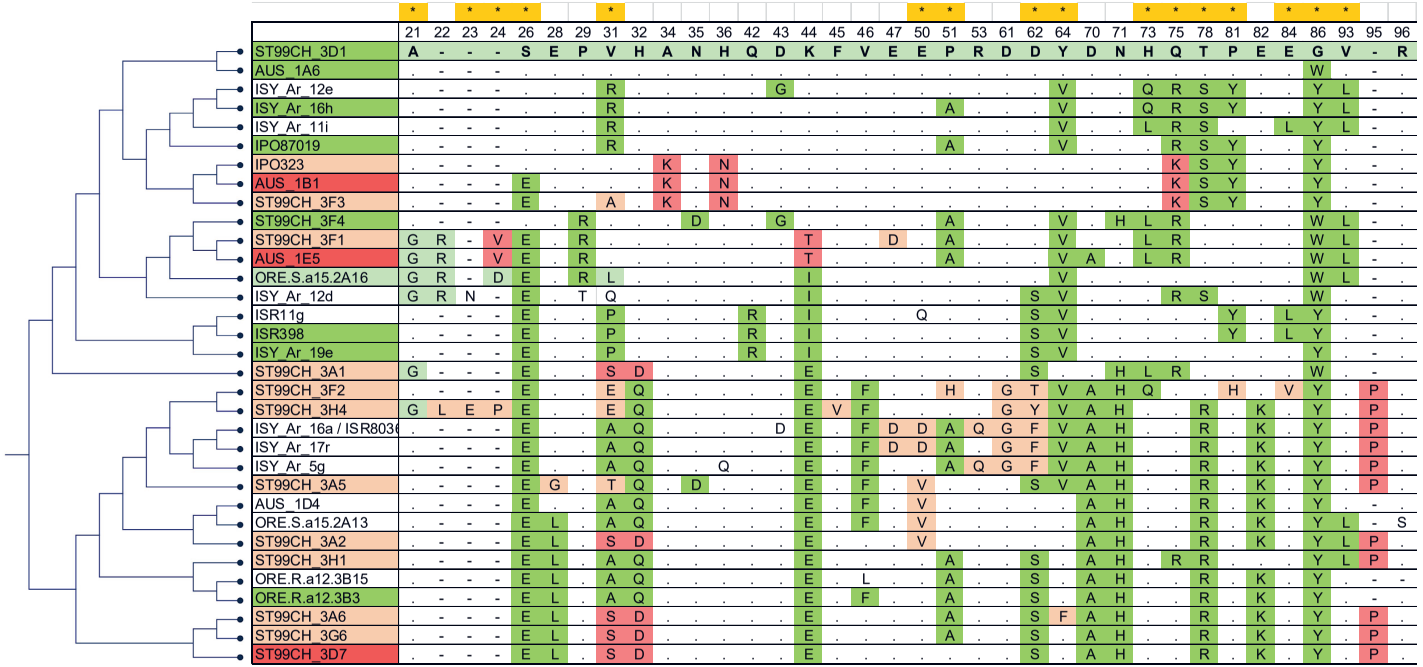
21 22 23 24 26 28 29 31 32 34 35 36 42 43 44 45 46 47 50 51 53 61 62 64 70 71 73 75 78 81 82 84 86 93 95 96
ST99CH_3D1 A - - - S E P V H A N H Q D K F V E E P R D D Y D N H Q T P E E G V - R
AUS_1A6 W
ISY_Ar_12e R G V Q R S Y Y L
ISY_Ar_16h R A V Q R S Y Y L
ISY_Ar_11i R V L R S L Y L
IPO87019 R A V R S Y Y
IPO323 K N K S Y Y
AUS_1B1 E K N K S Y Y
ST99CH_3F3 E A K N K S Y Y
ST99CH_3F4 R D G A V H L R W L
ST99CH_3F1 G R - V E R T D A V L R W L
AUS_1E5 G R - V E R T A V A L R W L
ORE.S.a15.2A16 G R - D E R L I V W L
ISY_Ar_12d G R N - E T Q I S V R S W
ISR11g E P R I Q S V Y L Y
ISR398 E P R I S V Y L Y
ISY_Ar_19e E P R I S V Y
ST99CH_3A1 G E S D E S H L R W
ST99CH_3F2 E E Q E F H G T V A H Q H V Y P
ST99CH_3H4 G L E P E E Q E V F G Y V A H R K Y P
ISY_Ar_16a / ISR803 E A Q D E F D D A Q G F V A H R K Y P
ISY_Ar_17r E A Q E F D D A G F V A H R K Y P
ISY_Ar_5g E A Q Q E F A Q G F V A H R K Y P
ST99CH_3A5 E G T Q D E F V S V A H R K Y P
AUS_1D4 E A Q E F V A H R K Y
ORE.S.a15.2A13 E L A Q E F V A H R K Y L S
ST99CH_3A2 E L S D E V A H R K Y L P
ST99CH_3H1 E L A Q E A S A H R R Y L P
ORE.R.a12.3B15 E L A Q E L A S A H R K Y
ORE.R.a12.3B3 E L A Q E F A S A H R K Y
ST99CH_3A6 E L S D E A S F A H R K Y P
ST99CH_3G6 E L A Q E A S A H R K Y P
ST99CH_3D7 E L S D E S A H R K Y P

2.4.4. A homologue of Avr3D1 from a different *Zymoseptoria* species triggers resistance in wheat

To study a possible role of Avr3D1 in nonhost resistance, we sought to test whether a homologue of Avr3D1 found in a related *Zymoseptoria* species can trigger defence in cultivar Runal. Using BLAST, we identified two homologues of Avr3D1 each in *Zymoseptoria ardabiliae* and *Zymoseptoria pseudotritici* but none in *Zymoseptoria brevis* and *Zymoseptoria passerinii*. One homologue was also identified in *Z. tritici* on chromosome 5 (Figures S2 & S3). The closest homologues of *Z. ardabiliae* and *Z. pseudotritici* shared 53.4% and 60.2% protein sequence identity with $Avr3D1_{3D1}$, respectively. In *Z. pseudotritici*, the closest homologue (ZpAvr3D1) was found in all five investigated strains and its protein sequence is fully conserved among them. The closest homologue in *Z. ardabiliae* (ZaAvr3D1) was also found in all investigated strains, present as two different isoforms with a sequence identity of 98% and a frequency of 50% each (Meile *et al.*, 2018). Despite the relatively low sequence identity shared with Avr3D1, all cysteine residues were conserved in ZpAvr3D1 and ZaAvr3D1 (Figure S3). In addition, *in silico* signal peptide and effector predictions revealed that both homologues are likely to be secreted and to act as effectors. To test whether it also triggers defence in wheat, *ZaAvr3D1* was expressed in the virulent *Z. tritici* line 3D1Δ*avr3D1*. The homologue triggered a defence response, which led to an even higher reduction in symptoms than $Avr3D1_{3D1}$ (Figures 2 & S4), suggesting that defence in wheat can be triggered by effectors of the non-pathogen *Z. ardabiliae*.

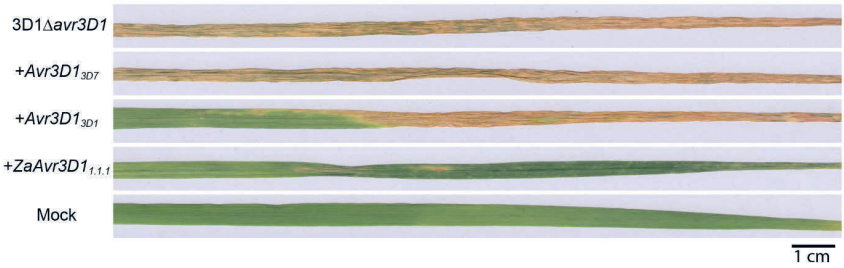

Figure 2. A homologous candidate effector of a sister species of *Zymoseptoria tritici* triggers defence in wheat.

Adaxial side of representative second wheat leaves of cultivar Runal infected with *Z. tritici* mutant lines that express different alleles of *Avr3D1* or its homologue cloned from *Zymoseptoria ardabiliae*. All mutant lines were obtained in an isogenic background (3D1Δ*avr3D1)*. Leaves were harvested 20 days post infection.

2.5. Discussion

To successfully establish an infection, plant pathogens need to overcome host defences. Various mechanisms have evolved in pathogens to evade recognition by the host, including changes in the protein sequence of avirulence factors. However, how Avr sequence mutations that occur in natural populations contribute to virulence is not always well understood. In this work, we characterize the mechanistic bases of host evasion by exploring the natural diversity of the avirulence factor Avr3D1 in the fast-evolving fungal plant pathogen *Zymoseptoria tritici*. We identified several natural isoforms of Avr3D1 that are recognized. We additionally demonstrated that several alterations of the Avr protein sequence are linked to host evasion and that Avr sequence polymorphism is a key determinant of the quantitative nature of Avr3D1-triggered defence. Remarkably, we found evidences for the contribution of this avirulence factor to nonhost resistance against a different *Zymoseptoria* species.

In a previous work, we showed that *Avr3D1* is highly polymorphic in natural populations of *Z. tritici* (Meile *et al.*, 2018). We now demonstrated the prevalence of host evasion and showed that at least three virulent isoforms arose independently. The identified residues involved in recognition are located in different positions of the primary structure of the protein. Although we cannot exclude that they are nearby in the tertiary structure, our analysis of natural isoforms of Avr3D1 indicate that, most probably, different regions of the protein are recognized by the corresponding resistance protein. Similar scenarios were described for the avirulence factors AvrL567 in flax rust and ATR1 in *Hyaloperonospora arabidopsidis*, in which mutations associated with differential recognition were located in different positions of the proteins (Wang *et al.*, 2007; Chou *et al.*, 2011; Ravensdale *et al.*, 2012). This is in

accordance with the fact that a full spectrum of quantitative avirulence activity was identified for the different isoforms of Avr3D1. The substitution G86W had a small contribution to loss of recognition. Thus, multiple sites of recognition of the avirulence factor might have additive effects on the strength of the interaction between the resistance protein and the avirulence factor. Interestingly, we identified isoforms that triggered a stronger immune response than the isoform originally identified as avirulent ($Avr3D1_{3D1}$, Meile *et al.*, 2018), suggesting that $Avr3D1_{3D1}$ is not an original isoform but partially escaped recognition. In line with this observation, quantitative gene-for-gene interactions have been suggested to be based on defeated *R* genes (Li *et al.*, 1999; Poland *et al.*, 2009). Here, we propose that several mutations led to a gradual loss of recognition of Avr3D1 and, consequently, to the quantitative phenotype.

Although we show here that indeed many isoforms at least partially escape recognition, several residues under diversifying selection were not identified as candidate residues for host evasion in our phenotype-based analysis. For example, the S26E substitution occurs in both virulent and avirulent isoforms (Table 3) and the question arises why such a substitution was selected for. However, selection is probably not only based on escape from recognition, but also on effector function optimization. Similarly, in *Blumeria graminis* f.sp. *graminis*, several residues of the effector AvrPm3 under positive selection were also postulated to be part of the functional domain (McNally *et al.*, 2018). In addition, in cases in which the effector function is disturbed by the alteration of residues critical for recognition, compensatory mutations might emerge to preserve the effector function. Furthermore, like *Avr* genes, host resistance genes are often highly diverse and different resistance gene alleles show specificity for certain *Avr* alleles (Ellis *et al.*,

1999; Rose *et al.*, 2004; Kanzaki *et al.*, 2012; Bourras *et al.*, 2015). Therefore, different wheat lines carrying different isoforms of the unknown resistance protein recognizing Avr3D1 could have exerted evolutionary pressure on Avr3D1 as well and thereby contributed to diversity.

We tested different wheat lines carrying the unknown resistance gene against $Avr3D1_{3D1}$ for resistance against a panel of *Z. tritici* strains with different alleles of *Avr3D1*. The majority of the strains overcame resistance in at least one of the wheat lines. Specifically, out of the 16 investigated Swiss strains, only two were shown to be avirulent on wheat lines harbouring the resistance gene. The two virulent strains ORE.R.a12.3B3 and 3F4 escaped recognition in spite of carrying inherently avirulent isoforms (i.e. isoforms which can potentially be recognized in the right context). However, the highly quantitative nature of both the *Z. tritici*-wheat pathosystem and the Avr-triggered defence response complicates the picture of Avr3D1-triggered defence: Avr3D1 may still contribute to partial resistance in apparently virulent strains, especially if the magnitude of Avr-triggered defence is on the low side of the spectrum. The strains ORE.R.a12.3B3 and 3F4 are possible examples for this scenario, since their virulence is comparable to the virulent reference strain 3D7 and their isoform is only partially recognized. Ultimately, the outcome of a specific strain-host interaction is likely determined by a combination of the genetic background of the strain, the magnitude of defence triggered by the specific Avr isoform and possibly also by the timing and the level of *Avr* expression. Interestingly, the observation that Avr-triggered defence can underlie minor differences in the virulence phenotype raises the possibility that the quantitative virulence differences observed in *Z. tritici* populations are largely based on a combination of different minor Avr-R protein interactions. Similar scenarios were envisioned for other pathosystems, such

as leaf rust in barley and *Magnaporthe grisea* in rice, in which minor gene-for-gene interactions have been described (Zenbayashi-Sawata *et al.*, 2005; Poland *et al.*, 2009; González *et al.*, 2012; Niks *et al.*, 2015).

The closest homologue of Avr3D1 from the species *Z. ardabiliae* was sufficient to induce a strong defence response in wheat when expressed in a virulent *Z. tritici* background. This sister species of *Z. tritici* was isolated from wild grasses and is incapable of infecting wheat (Stukenbrock *et al.*, 2007). The molecular mechanisms involved in host adaptation and speciation of *Z. tritici* are largely unknown, but it is suggested that fixation of adaptive substitutions in genes involved in interaction with the host played a major role. Indeed, genes with signatures of positive selection were shown to be involved in wheat infection and possibly in host specialization of *Z. tritici* (Stukenbrock *et al.*, 2011; Poppe *et al.*, 2015). Function optimization of the effector EpiC1 in *Phytophtora infestans* and *P. mirabilis* towards its target in the respective host species was also demonstrated to be key for host specialization of these two oomycete species (Dong *et al.*, 2014). In addition to function optimization of effectors, it has been predicted that the resistance mechanisms towards host and nonhost pathogens are similar and that accumulation of avirulence factors would lead to the inability of certain pathogens to infect a nonhost (Schulze-Lefert & Panstruga, 2011; Ayliffe & Sørensen, 2019). Recently, it was demonstrated that the recognition of avirulence factors plays a key role in nonhost resistance in *Blumeria graminis* (Bourras *et al.*, 2019) and in specialization of the rice blast fungus to Japonica and Indica rice varieties (Liao *et al.*, 2016). Furthermore, loss of an avirulence factor prompted the emergence of wheat blast (Inoue *et al.*, 2017). Our data on the recognition of an Avr3D1 homologue in wheat also support the role of Avrs in nonhost resistance and we propose that the sister species may harbour several

avirulence genes that impede wheat infection. Therefore, the specialization of *Z. tritici* to its wheat host (Stukenbrock *et al.*, 2007) might have been associated with evasion from Avr recognition.

2.6. Acknowledgements

We thank Jason Rudd for providing the vector pCGEN and Thierry Marcel and Marc-Henri Lebrun for providing wheat seeds. Performance of qPCR was supported by the Genetic Diversity Centre at ETH Zurich. This work was supported by the Swiss National Science Foundation (Grant 31003A_155955 to BAM).

2.7. References

Ayliffe M, Sørensen CK. **2019**. Plant nonhost resistance: paradigms and new environments. *Current Opinion in Plant Biology* **50**: 104–113.

Bettgenhaeuser J, Gardiner M, Spanner R, Green P, Hernández-Pinzón I, Hubbard A, Ayliffe M, Moscou MJ. **2018**. The genetic architecture of colonization resistance in *Brachypodium distachyon* to non-adapted stripe rust (*Puccinia striiformis*) isolates. *PLoS Genetics* **14**: 1–26.

Bourras S, Kunz L, Xue M, Praz CR, Müller MC, Kälin C, Schläfli M, Ackermann P, Flückiger S, Parlange F, *et al.* 2019. The *AvrPm3-Pm3* effector-NLR interactions control both race-specific resistance and host-specificity of cereal mildews on wheat. *Nature Communications* **10**: 2292.

Bourras S, McNally KE, Ben-David R, Parlange F, Roffler S, Praz CR, Oberhaensli S, Menardo F, Stirnweis D, Frenkel Z, *et al.* 2015. Multiple avirulence loci and allele-specific effector recognition control the *Pm3* race-specific resistance of wheat to powdery mildew. *The Plant cell* **27**: 2991–3012.

Bourras S, McNally KE, Müller MC, Wicker T, Keller B. **2016**. Avirulence genes in cereal powdery mildews: the gene-for-gene hypothesis 2.0. *Frontiers in Plant Science* **7**: 241.

Brown JKM, Chartrain L, Lasserre-Zuber P, Saintenac C. **2015**. Genetics of resistance to *Zymoseptoria tritici* and applications to wheat breeding. *Fungal Genetics and Biology* **79**: 33–41.

Brunner PC, McDonald BA. **2018**. Evolutionary analyses of the avirulence effector AvrStb6 in global populations of *Zymoseptoria tritici* identify candidate amino acids involved in recognition. *Molecular Plant Pathology* **19**: 1836–1846.

Chou S, Krasileva K V., Holton JM, Steinbrenner AD, Alber T, Staskawicz BJ. **2011**. *Hyaloperonospora arabidopsidis* ATR1 effector is a repeat protein with distributed recognition surfaces. *Proceedings of the National Academy of Sciences of the United States of America* **108**: 13323–13328.

Cook DE, Mesarich CH, Thomma BPHJ. **2015**. Understanding plant immunity as a surveillance system to detect invasion. *Annual Review of Phytopathology* **53**: 541–563.

Dong S, Stam R, Cano LM, Song J, Sklenar J, Yoshida K, Bozkurt TO, Oliva R, Liu Z, Tian M, *et al.* 2014. Effector specialization in a lineage of the Irish potato famine pathogen. *Science* **343**: 552–555.

Dyrløv Bendtsen J, Nielsen H, von Heijne G, Brunak S. **2004**. Improved prediction of signal peptides: SignalP 3.0. *Journal of Molecular Biology* **340**: 783–795.

Ellis JG, Lawrence GJ, Luck JE, Dodds PN. **1999**. Identification of regions in alleles of the flax rust resistance gene *L* that determine differences in gene-for-gene specificity. *Plant Cell* **11**: 495–506.

Flor HH. **1971**. Current status of the gene-for-gene concept. *Annual Review of Phytopathology* **9**: 275–296.

Fones H, Gurr S. **2015**. The impact of Septoria tritici Blotch disease on wheat: An EU

perspective. *Fungal Genetics and Biology* **79**: 3–7.

Frantzeskakis L, Di Pietro A, Rep M, Schirawski J, Wu CH, Panstruga R. **2019**. Rapid evolution in plant–microbe interactions – a molecular genomics perspective. *New Phytologist*. doi: 10.1111/nph.15966

Fudal I, Ross S, Brun H, Besnard AL, Ermel M, Kuhn ML, Balesdent MH, Rouxel T. **2009**. Repeat-induced point mutation (RIP) as an alternative mechanism of evolution toward virulence in *Leptosphaeria maculans*. *Molecular Plant-Microbe Interactions* **22**: 932–941.

Gilbert B, Bettgenhaeuser J, Upadhyaya N, Soliveres M, Singh D, Park RF, Moscou MJ, Ayliffe M. **2018**. Components of *Brachypodium distachyon* resistance to nonadapted wheat stripe rust pathogens are simply inherited. *PLoS Genetics* **14**: 1–27.

Gilroy EM, Breen S, Whisson SC, Squires J, Hein I, Kaczmarek M, Turnbull D, Boevink PC, Lokossou A, Cano LM, *et al.* 2011. Presence/absence, differential expression and sequence polymorphisms between *PiAVR2* and *PiAVR2*-like in *Phytophthora infestans* determine virulence on *R2* plants. *New Phytologist* **191**: 763–776.

González AM, Marcel TC, Niks RE. **2012**. Evidence for a minor gene-for-minor gene interaction explaining nonhypersensitive polygenic partial disease resistance. *Phytopathology* **102**: 1086–1093.

Goodwin SB, Ben M'Barek S, Dhillon B, Wittenberg AHJ, Crane CF, Hane JK, Foster AJ, Van der Lee TAJ, Grimwood J, Aerts A, *et al.* 2011. Finished genome of the fungal wheat pathogen *Mycosphaerella graminicola* reveals dispensome structure, chromosome plasticity, and stealth pathogenesis. *PLoS Genetics* **7**: e1002070.

Grandaubert J, Bhattacharyya A, Stukenbrock EH. **2015**. RNA-seq-based gene annotation and comparative genomics of four fungal grass pathogens in the genus *Zymoseptoria* identify novel orphan genes and species-specific invasions of transposable elements. *G3: Genes, Genomes, Genetics* **5**: 1323–33.

Hartmann FE, Croll D. **2017**. Distinct trajectories of massive recent gene gains and losses in populations of a microbial eukaryotic pathogen. *Molecular Biology and Evolution* **34**: 2808–2822.

Hartmann FE, Sánchez-Vallet A, McDonald BA, Croll D. **2017**. A fungal wheat pathogen evolved host specialization by extensive chromosomal rearrangements. *The ISME Journal* **11**: 1189–1204.

Hogenhout SA, Van der Hoorn RAL, Terauchi R, Kamoun S. **2009**. Emerging concepts in effector biology of plant-associated organisms. *Molecular Plant-Microbe Interactions* **22**: 115–122.

Van der Hoorn RA., De Wit PJG., Joosten MHA. 2002. Balancing selection favors guarding resistance proteins. *Trends in Plant Science* **7**: 67–71.

Houterman PM, Cornelissen BJC, Rep M. **2008**. Suppression of plant resistance gene-based immunity by a fungal effector. *PLoS Pathogens* **4**: e1000061.

Inoue Y, Vy TTP, Yoshida K, Asano H, Mitsuoka C, Asuke S, Anh VL, Cumagun CJR, Chuma I, Terauchi R, *et al.* 2017. Evolution of the wheat blast fungus through functional losses in a host specificity determinant. *Science* **357**: 80–83.

Jones JDG, Dangl JL. **2006**. The plant immune system. *Nature* **444**: 323–329.

De Jonge R, Van Esse HP, Maruthachalam K, Bolton MD, Santhanam P, Saber MK, Zhang Z, Usami T, Lievens B, Subbarao K V., *et al.* 2012. Tomato immune receptor Ve1 recognizes effector of multiple fungal pathogens uncovered by genome and RNA sequencing. *Proceedings of the National Academy of Sciences of the United States of America* **109**: 5110–5115.

Kanzaki H, Yoshida K, Saitoh H, Fujisaki K, Hirabuchi A, Alaux L, Fournier E, Tharreau D, Terauchi R. **2012**. Arms race co-evolution of *Magnaporthe oryzae AVR-Pik* and rice *Pik* genes driven by their physical interactions. *Plant Journal* **72**: 894–907.

Kema G, Annone J, Sayoud R, Van Silfhout C, Van Ginkel M, De Bree J. **1996**. Genetic variation for virulence and resistance in the wheat-*Mycosphaerella graminicola* pathosystem. 1. Interactions between pathogen isolates and host cultivars. *Phytopathology* **86**: 200–212.

Kollers S, Rodemann B, Ling J, Korzun V, Ebmeyer E, Argillier O, Hinze M, Plieske J, Kulosa D, Ganal MW, *et al.* 2013. Genetic architecture of resistance to Septoria tritici blotch (*Mycosphaerella graminicola*) in European winter wheat. *Molecular Breeding* **32**: 411–423.

Li ZK, Luo LJ, Mei HW, Paterson AH, Zhao XH, Zhong DB, Wang YP, Yu XQ, Zhu L, Tabien R, *et al.* 1999. A 'defeated' rice resistance gene acts as a QTL against a virulent strain of *Xanthomonas oryzae* pv. *oryzae*. *Molecular and General Genetics* **261**: 58–63.

Liao J, Huang H, Meusnier I, Adreit H, Ducasse A, Bonnot F, Pan L, He X, Kroj T, Fournier E, *et al.* 2016. Pathogen effectors and plant immunity determine specialization of the blast fungus to rice subspecies. *eLife* **5**: 1–18.

McNally KE, Menardo F, Lüthi L, Praz CR, Müller MC, Kunz L, Ben-David R, Chandrasekhar K, Dinoor A, Cowger C, *et al.* 2018. Distinct domains of the AVRPM3A2/F2 avirulence protein from wheat powdery mildew are involved in immune receptor recognition and putative effector function. *New Phytologist* **218**: 681–695.

Meile L, Croll D, Brunner PC, Plissonneau C, Hartmann FE, McDonald BA, Sánchez-Vallet A. **2018**. A fungal avirulence factor encoded in a highly plastic genomic region triggers partial resistance to septoria tritici blotch. *New Phytologist* **219**: 1048–1061.

Michelmore R, Coaker G, Bart R, Beattie G, Bent A, Bruce T, Cameron D, Dangl J, Dinesh-Kumar S, Edwards R, *et al.* 2017. Foundational and translational research opportunities to improve plant health. *Molecular Plant-Microbe Interactions* **30**: 515–516.

Motteram J, Lovegrove A, Pirie E, Marsh J, Devonshire J, van de Meene A, Hammond-Kosack K, Rudd JJ. **2011**. Aberrant protein N-glycosylation impacts upon infection-related growth transitions of the haploid plant-pathogenic fungus *Mycosphaerella graminicola*. *Molecular Microbiology* **81**: 415–433.

Niks RE, Qi X, Marcel TC. **2015**. Quantitative resistance to biotrophic filamentous plant pathogens: concepts, misconceptions, and mechanisms. *Annual Review of Phytopathology* **53**: 445–470.

Plissonneau C, Daverdin G, Ollivier B, Blaise F, Degrave A, Fudal I, Rouxel T, Balesdent M-H. **2016a**. A game of hide and seek between avirulence genes *AvrLm4-7*

and *AvrLm3* in *Leptosphaeria maculans*. *New Phytologist* **209**: 1613–1624.

Plissonneau C, Hartmann FE, Croll D. **2018**. Pangenome analyses of the wheat pathogen *Zymoseptoria tritici* reveal the structural basis of a highly plastic eukaryotic genome. *BMC Biology* **16**: 5.

Plissonneau C, Stürchler A, Croll D. **2016b**. The evolution of orphan regions in genomes of a fungal pathogen of wheat. *mBio* **7**: e01231-16.

Poland JA, Balint-Kurti PJ, Wisser RJ, Pratt RC, Nelson RJ. **2009**. Shades of gray: the world of quantitative disease resistance. *Trends in Plant Science* **14**: 21–29.

Poppe S, Dorsheimer L, Happel P, Stukenbrock EH. **2015**. Rapidly evolving genes are key players in host specialization and virulence of the fungal wheat pathogen *Zymoseptoria tritici* (*Mycosphaerella graminicola*). *PLOS Pathogens* **11**: e1005055.

Lo Presti L, Lanver D, Schweizer G, Tanaka S, Liang L, Tollot M, Zuccaro A, Reissmann S, Kahmann R. **2015**. Fungal effectors and plant susceptibility. *Annual Review of Plant Biology* **66**: 513–545.

Qutob D, Patrick Chapman B, Gijzen M. **2013**. Transgenerational gene silencing causes gain of virulence in a plant pathogen. *Nature Communications* **4**: 1349.

Ravensdale M, Bernoux M, Ve T, Kobe B, Thrall PH, Ellis JG, Dodds PN. **2012**. Intramolecular interaction influences binding of the flax L5 and L6 resistance proteins to their AvrL567 ligands. *PLoS Pathogens* **8**.

Rose LE, Bittner-Eddy PD, Langley CH, Holub EB, Michelmore RW, Beynon JL. **2004**. The maintenance of extreme amino acid diversity at the disease resistance gene, *RPP13*, in *Arabidopsis thaliana*. *Genetics* **166**: 1517–1527.

Rouxel T, Penaud A, Pinochet X, Brun H, Gout L, Delourme R, Schmit J, Balesdent MH. **2003**. A 10-year survey of populations of *Leptosphaeria maculans* in France indicates a rapid adaptation towards the *Rlm1* resistance gene of oilseed rape. *European Journal of Plant Pathology* **109**: 871–881.

Sánchez-Vallet A, Fouché S, Fudal I, Hartmann FE, Soyer JL, Tellier A, Croll D. **2018**. The genome biology of effector gene evolution in filamentous plant pathogens. *Annual Review of Phytopathology* **56**: 21–40.

Schneider CA, Rasband WS, Eliceiri KW. **2012**. NIH Image to ImageJ: 25 years of image analysis. *Nature Methods* **9**: 671–675.

Schulze-Lefert P, Panstruga R. **2011**. A molecular evolutionary concept connecting nonhost resistance, pathogen host range, and pathogen speciation. *Trends in Plant Science* **16**: 117–125.

Sperschneider J, Gardiner DM, Dodds PN, Tini F, Covarelli L, Singh KB, Manners JM, Taylor JM. **2016**. EffectorP: predicting fungal effector proteins from secretomes using machine learning. *New Phytologist* **210**: 743–761.

Stergiopoulos I, de Wit PJGM. **2009**. Fungal effector proteins. *Annual Review of Phytopathology* **47**: 233–263.

Stewart EL, Hagerty CH, Mikaberidze A, Mundt CC, Zhong Z, McDonald BA. **2016**. An improved method for measuring quantitative resistance to the wheat pathogen

Zymoseptoria tritici using high-throughput automated image analysis. *Phytopathology* **106**: 782–788.

Stukenbrock EH, Banke S, Javan-Nikkhah M, McDonald BA. **2007**. Origin and domestication of the fungal wheat pathogen *Mycosphaerella graminicola* via sympatric speciation. *Molecular Biology and Evolution* **24**: 398–411.

Stukenbrock EH, Bataillon T, Dutheil JY, Hansen TT, Li R, Zala M, McDonald BA, Wang J, Schierup MH. **2011**. The making of a new pathogen: insights from comparative population genomics of the domesticated wheat pathogen *Mycosphaerella graminicola* and its wild sister species. *Genome research* **21**: 2157–66.

Stukenbrock EH, Quaedvlieg W, Javan-Nikhah M, Zala M, Crous PW, McDonald BA. **2012**. *Zymoseptoria ardabiliae* and *Z. pseudotritici*, two progenitor species of the septoria tritici leaf blotch fungus *Z. tritici* (synonym: *Mycosphaerella graminicola*). *Mycologia* **104**: 1397–1407.

Torriani SFF, Stukenbrock EH, Brunner PC, McDonald BA, Croll D. **2011**. Evidence for extensive recent intron transposition in closely related fungi. *Current Biology* **21**: 2017–2022.

Toruño TY, Stergiopoulos I, Coaker G. **2016**. Plant-pathogen effectors: cellular probes interfering with plant defenses in spatial and temporal manners. *Annual Review of Phytopathology* **54**: 419–441.

Walton JD. **1996**. Host-selective toxins: agents of compatibility. *The Plant cell* **8**: 1723–33.

Wang CIA, Gunčar G, Forwood JK, Teh T, Catanzariti AM, Lawrence GJ, Loughlin FE, Mackay JP, Schirra HJ, Anderson PA, *et al.* 2007. Crystal structures of flax rust avirulence proteins AvrL567-A and -D reveal details of the structural basis for flax disease resistance specificity. *Plant Cell* **19**: 2898–2912.

Wu J, Kou Y, Bao J, Li Y, Tang M, Zhu X, Ponaya A, Xiao G, Li J, Li C, *et al.* 2015. Comparative genomics identifies the *Magnaporthe oryzae* avirulence effector *AvrPi9* that triggers *Pi9* -mediated blast resistance in rice. *New Phytologist* **206**: 1463–1475.

Yates S, Mikaberidze A, Krattinger SG, Abrouk M, Hund A, Yu K, Studer B, Fouche S, Meile L, Pereira D, *et al.* 2019. Precision phenotyping reveals novel loci for quantitative resistance to septoria tritici blotch. *Plant Phenomics* **In press**: 502260.

Yechilevich-Auster M, Levi E, Eyal Z. **1983**. Assessment of interactions between cultivated and wild wheats and *Septoria tritici*. *Phytopathology* **73**: 1077.

Zenbayashi-Sawata K, Ashizawa T, Koizumi S. **2005**. *Pi34-AVRPi34*: A new gene-for-gene interaction for partial resistance in rice to blast caused by *Magnaporthe grisea*. *Journal of General Plant Pathology* **71**: 395–401.

Zhan J, Linde CC, Jurgens T, Merz U, Steinebrunner F, McDonald BA. **2005**. Variation for neutral markers is correlated with variation for quantitative traits in the plant pathogenic fungus *Mycosphaerella graminicola*. *Molecular Ecology* **14**: 2683–2693.

Zhong Z, Marcel TC, Hartmann FE, Ma X, Plissonneau C, Zala M, Ducasse A, Confais J, Compain J, Lapalu N, *et al.* 2017. A small secreted protein in *Zymoseptoria tritici* is responsible for avirulence on wheat cultivars carrying the *Stb6* resistance gene. *New Phytologist* **214**: 619–631.

Zipfel C. **2014**. Plant pattern-recognition receptors. *Trends in Immunology* **35**: 345–351.

Zwiers L-H, De Waard MA. **2001**. Efficient *Agrobacterium tumefaciens*-mediated gene disruption in the phytopathogen *Mycosphaerella graminicola*. *Current Genetics* **39**: 388–393.

2.8. Supporting information

Table S1. Primers used in this study.

Figure S1. Cloning strategy for swapping the coding DNA sequence of *Avr3D1* for ectopic expression.

Figure S2. DNA sequence alignment of homologues of *Avr3D1* identified in different *Zymoseptoria* species**.**

Figure S3. Protein sequence comparison between Avr3D1 and its homologues in different *Zymoseptoria* species.

Figure S4. A homologue of Avr3D1 from a different *Zymoseptoria* species triggers defences in wheat.

Table S1. Primers used in this study. The cloning strategy is further explained in Figure S1.

Primer name (number)	Sequence (5'-3')	Applications	Target	Description
FL_TFC1_F	TGCTCAGATTGTGCGAAGAC	qPCR	*TFC1*	Used to determine the copy number of inserted T-DNA after *Agrobacterium tumefaciens*-mediated transformation of *Zymoseptoria tritici*.
FL_TFC1_R	TCGTAGTCCGATACCATGAGG	qPCR		
GenR_q_F	CTGCTAGATATACCTGTCAGAC	qPCR	*GenR*	Used to determine the copy number of inserted T-DNA after *Agrobacterium tumefaciens*-mediated transformation of *Zymoseptoria tritici*.
GenR_q_R	CGAGCTGGTCACCTGTAATTC	qPCR		
IF-XhoI-581prom_F (97)	TCGCCGTGCCTGGGCT	cloning	*Avr3D1* promoter	Used to amplify the *Avr3D1* promoter from strain 3D1.
IF-581prom_R (98)	GCTGGTGTCGTGGTGTTGTG	cloning		
IF-581prom_R2 (321)	CATTGTGTCGAGGCTGGTGTC	cloning	*Avr3D1* promoter	Used (together with primer 97) to amplify the *Avr3D1* promoter from strain 3D1. The resulting amplicon can be combined by In-Fusion cloning with the amlicon from primer pairs 324/325.
IF-581CDS_F (99)	CACAACACCACGACACCAGC	cloning	*Avr3D1 CDS*	Used to amplify the CDS and intron 1 of *Avr3D1* from strains AUS_1A6, AUS_1B1, ISY_Ar_16h, ISR398, ISY_Ar_19, 3F4, ORE_R.a12_3B3 and AUS_1E5. The resulting amplicon can be combined by In-Fusion cloning with the amlicons from primer pair 97/98
IF-XhoI-581CDS_R (100)	TGGACTCCTTCTCGCTCTCG	cloning		
IF-581CDS_F3 (266)	CACAACACCACGACACCAGCCTCGACACA	cloning	*Avr3D1 CDS*	Used to amplify the CDS and intron 1 of *Avr3D1* from the strain IPO87019.The resulting amplicon can be combined by In-Fusion cloning with the amlicons from primer pair 97/98.
IF-XhoI-581CDS_R3 (267)	TGGACTCCTTCTCGCTCTCGAGCCAGAGCAGGGGAATTTTAC	cloning		
IF_Za_581CDS_F (324)	CACCAGCCTCGACACAATGCGGTCCACTACTACCAC	cloning	*ZaAvr3D1 CDS*	Used to amplify the CDS and intron 1 of a homologue of *Avr3D1* from *Zymoseptoria ardabiliae* strain STIR04 1.1.1. The resulting amplicon can be combined by In-Fusion cloning with the amlicons from primer pair 97/321
IF_Za_581CDS_R (325)	CTCCTTCTCGCTCTCGAGCCAGAGCAGGGGAATTTCAAGCCAAAGCAGGCG	cloning		

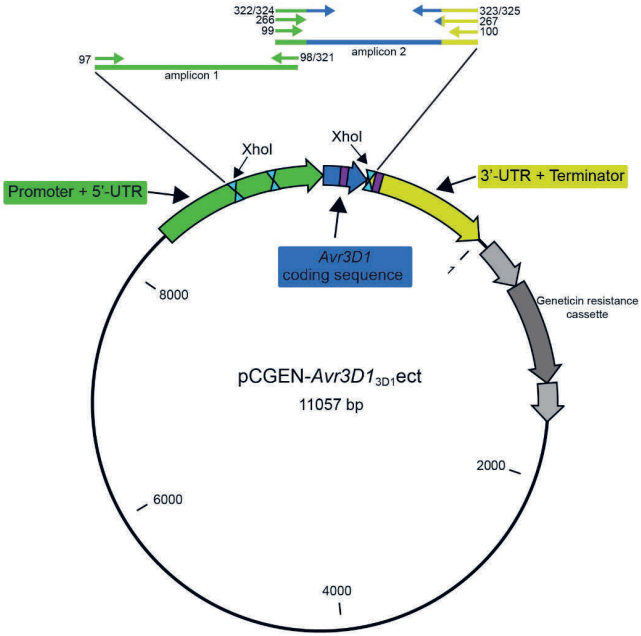

Figure S1. Cloning strategy for swapping the coding DNA sequence of *Avr3D1* for ectopic expression.

Vector map of pCGEN-*Avr3D1*$_{3D1}$ect, which was used for ectopic integration of *Avr3D1* in *Zymoseptoria tritici* and which had been produced for a previous study (Meile *et al*., 2018). Amplicon 1 contains part of the *Avr3D1*$_{3D1}$ promoter and 5'-UTR (both green). Amplicon 2 contains part of the 5'-UTR, the coding DNA sequence (CDS, blue), intron 1 (purple) and the part of the 3'-UTR (yellow). Using seamless cloning, both amplicons were assembled into pCGEN-*Avr3D1*$_{3D1}$ect that had been linearized with the restriction enzyme XhoI (light blue). The resulting plasmid contains a swapped CDS but the original promoter (from strain 3D1). The coloured arrows represent different primers used to amplify the coding sequence of different *Avr3D1* alleles. Primer sequences, indicated by arrows on top of the amplicons, are listed in Table S1.

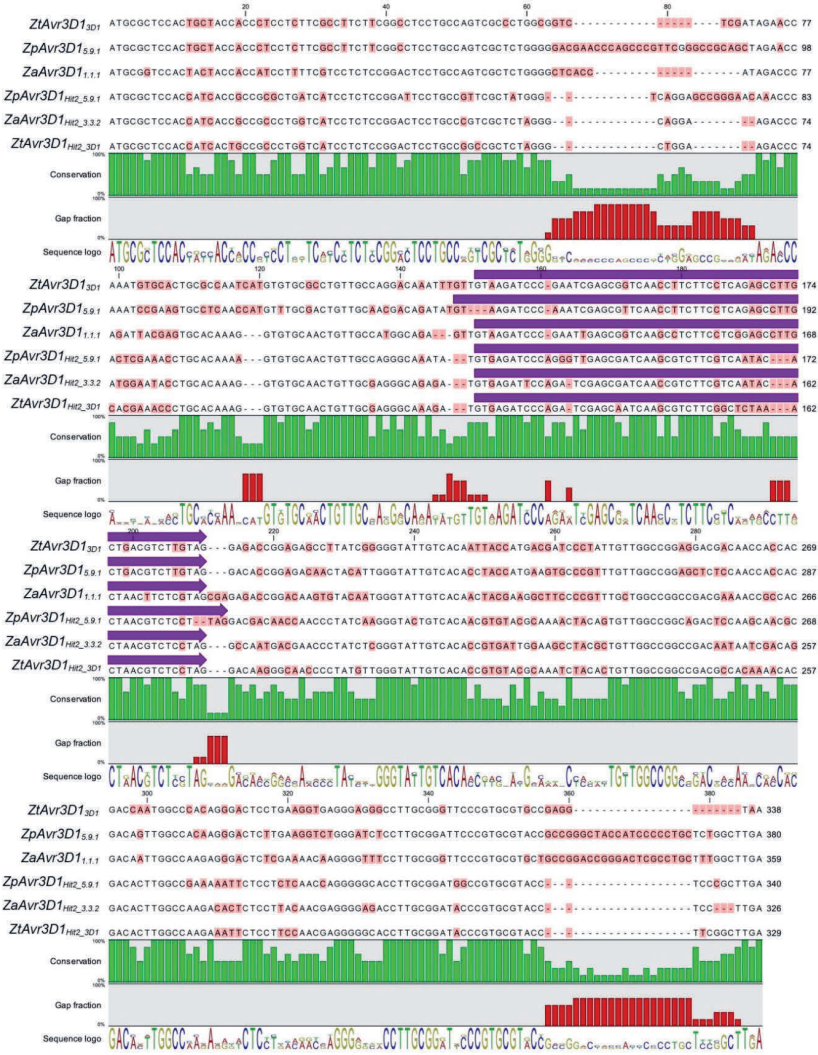

Figure S2. DNA sequence alignment of homologues of *Avr3D1* identified in different *Zymoseptoria* species.

Purple arrows indicate (putative) intron sequences. *Zt*: *Zymoseptoria tritici*; *Zp*: *Zymoseptoria pseudotritici*; *Za*: *Zymoseptoria ardabiliae*. *ZpAvr3D1*$_{5.9.1}$ and *ZaAvr3D1*$_{1.1.1}$ are the closest homologues of *Avr3D1*$_{3D1}$. *ZpAvr3D1*$_{Hit2\_5.9.1}$ and *ZaAvr3D1*$_{Hit2\_3.3.2}$ are more distant homologues of *ZpAvr3D1*. *ZpAvr3D1*$_{Hit2\_3D1}$ is a homologue of *Avr3D1*$_{3D1}$ in *Z. tritici*, which was identified on chromosome 5. The conservation and deletions are represented by green and red bars, respectively.

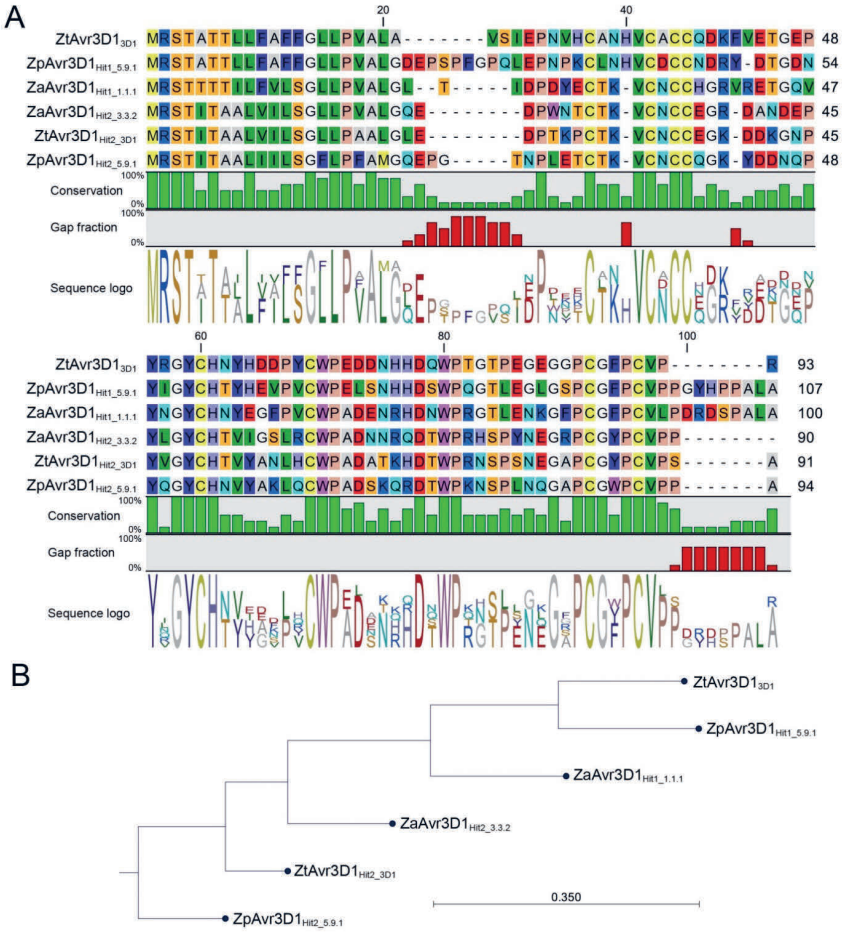

Figure S3. Protein sequence comparison between Avr3D1 and its homologues in different *Zymoseptoria* species.

(A) Protein sequence alignment, conservation (green bars), gap fraction (red bars) and sequence logo. Zt: *Zymoseptoria tritici*; Zp: *Zymoseptoria pseudotritici*; Za: *Zymoseptoria ardabiliae*. ZpAvr3D1$_{5.9.1}$ and ZaAvr3D1$_{1.1.1}$ are the closest homologues of Avr3D1$_{3D1}$. ZpAvr3D1$_{Hit2_5.9.1}$ and ZaAvr3D1$_{Hit2_3.3.2}$ are more distant homologues of Avr3D1$_{3D1}$. ZtAvr3D1$_{Hit2_3D1}$ is a homologue of Avr3D1$_{3D1}$ in *Z. tritici*. **(B)** Maximum-likelihood tree of the sequences shown in (A).

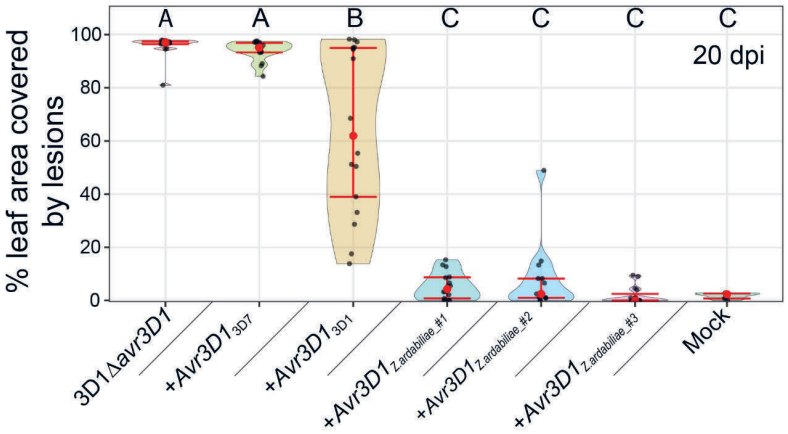

Figure S4. A homologue of Avr3D1 from a different *Zymoseptoria* species triggers defences in wheat.

Violin plots showing the percentage of leaf area covered by lesions of cultivar Runal infected with *Z. tritici* strain 3D1 lacking *Avr3D1* (3D1Δ*avr3D1*) and the same strain harbouring either an ectopic copy of a *Avr3D1* allele from the strain 3D1 or 3D7 (+*Avr3D1*$_{3D1/3D7}$) or an ectopic copy of the closest homologue from *Z. ardabiliae* (*ZaAvr3D1*$_{1.1.1}$). For *ZaAvr3D1*$_{1.1.1}$, three independent transformant lines are shown (#1,2,3). Red dots represent the median, error bars represent the 95% confidence interval of the median and grey dots represent individual data points. Letters indicate statistical groups according to the Kolmogorov-Smirnov test ($p<0.01$). Leaves were phenotyped at 20 days post infection (dpi).

Chapter 3

Chromatin remodeling contributes to the spatio-temporal expression pattern of virulence genes in a fungal plant pathogen

Lukas Meile, Jules Peter, Guido Puccetti, Julien Alassimone, Bruce A. McDonald and Andrea Sánchez-Vallet. 2019.

3.1. Abstract

Dynamic changes in transcription profiles are key for the success of pathogens in colonizing their hosts. In many pathogens, genes associated with virulence, such as effector genes, are located in regions of the genome that are rich in transposable elements and heterochromatin. The contribution of chromatin modifications to gene expression in pathogens remains largely unknown. Here, we show that the heterochromatic environment of effector genes in the fungal plant pathogen Zymoseptoria tritici is a key regulator of their specific spatio-temporal expression patterns. Enrichment in trimethylated lysine 27 and probably also lysine 9 of histone H3 likely dictates the repression of effector genes in the absence of the host. Chromatin remodeling during host colonization, featuring a reduction in these repressive modifications, indicates a major role for epigenetics in effector gene induction. Our results illustrate that host-triggered chromatin decondensation determines the specific expression profile of effector genes at the cellular level and, hence, provide new insights into the regulation of virulence in fungal plant pathogens.

3.2. Introduction

The transition of pathogenic fungi from non-host to host environments requires dynamic changes in gene expression profiles, including the activation of genes with host-specific functions (O'Connell *et al.*, 2012; Gervais *et al.*, 2017; Lanver *et al.*, 2018; Sánchez-Vallet *et al.*, 2018). Recent work has shown that, in addition to classical transcription factors, chromatin structure contributes to the transcriptional control of genes involved in host colonization (Gómez-Díaz *et al.*, 2012; Connolly *et al.*, 2013; Chujo & Scott, 2014; Soyer *et al.*, 2015b). Genomic regions consisting of loosely packed chromatin (euchromatin) are generally conducive for transcription, while densely packed chromatin (heterochromatin) is less accessible and less easily transcribed (Grewal & Jia, 2007). A variety of different proteins associated with chromatin and several epigenetic processes including a complex array of post-translational histone modifications work in concert to shape chromatin structure in eukaryotes and thereby provide an important layer of gene regulation (Strahl & Allis, 2000; Li *et al.*, 2007; Pfluger & Wagner, 2007; van Steensel, 2011). In euchromatin, lysine residues of histones are frequently acetylated, while hypoacetylated histones are associated with heterochromatin and transcriptionally silent genes (Brown *et al.*, 2000). Heterochromatin is further characterized by trimethylation of lysine 9 and/or lysine 27 of histone H3 (H3K9me3 and H3K27me3), which are posttranslational modifications catalyzed by the histone methyltransferases KMT1 and KMT6, respectively (Goodrich *et al.*, 1997; Strahl & Allis, 2000; Galazka & Freitag, 2014; Freitag, 2017). Consequently, de-repression of genes residing in heterochromatic regions requires alteration of histone modifications, acting in conjunction with an active transcription machinery (Nützmann *et al.*, 2011; Collemare & Seidl, 2019).

The genomes of filamentous fungi have been described as compartmentalized into euchromatic gene-rich regions containing housekeeping genes and into heterochromatic regions rich in transposable elements (TEs) and poor in genes (Raffaele & Kamoun, 2012; Galazka & Freitag, 2014; Dong *et al.*, 2015). This compartmentalization has been broadly investigated in plant pathogens and is thought to facilitate different evolutionary rates across the genome (Grandaubert *et al.*, 2014; Seidl *et al.*, 2016). Effector genes, which encode for secreted proteins that modulate the interaction of fungal and oomycete pathogens and symbionts with their hosts, often reside in TE-rich genomic compartments (Hogenhout *et al.*, 2009; Haas *et al.*, 2009; Raffaele & Kamoun, 2012; Lo Presti *et al.*, 2015; Dong *et al.*, 2015; Möller & Stukenbrock, 2017). This non-random distribution of effector genes in the genome suggests that TEs might provide pathogens with an improved capacity to adapt to their host and its immune system (Seidl & Thomma, 2017). TEs are typically associated with repressive epigenetic marks to control their activity. This repression can extend outside of the TEs and affect adjacent genes (Lisch & Bennetzen, 2011; Rebollo *et al.*, 2012; Krishnan *et al.*, 2018). Thus, the expression of many effector genes can be influenced by their proximity to TEs. For instance, in the oil-seed rape pathogen *Leptosphaeria maculans,* effector genes are frequently located in TE-rich regions and have been shown to be under epigenetic control involving H3K9me3 (Soyer *et al.*, 2014; Gervais *et al.*, 2017).

Secondary metabolites are important nonproteinaceous effectors with diverse roles in pathogen-plant interactions and niche colonization (Pusztahelyi *et al.*, 2015; Collemare *et al.*, 2019). Similarly to effector genes, secondary metabolite biosynthetic gene clusters are frequently located in TE-rich regions including subtelomeres (Palmer & Keller, 2010; Collemare & Seidl, 2019) and associated with

heterochromatic histone marks, as shown for filamentous fungi such as *Aspergillus nidulans*, *Epichloë festucae*, *Fusarium fujikorai*, *Fusarium graminearum* and *Colletotrichum higginsianum* (Gacek & Strauss, 2012; Connolly *et al.*, 2013; Chujo & Scott, 2014; Studt *et al.*, 2017; Dallery *et al.*, 2017). Interestingly, different fungal species use different epigenetic mechanisms to control these regions (Reyes-Dominguez *et al.*, 2010; Connolly *et al.*, 2013; Studt *et al.*, 2017), highlighting the high diversity of chromatin architecture found within the fungal kingdom (Erlendson *et al.*, 2017).

Induction of heterochromatic effector and secondary metabolite genes during host colonization is thought to require the remodeling of chromatin (Soyer *et al.*, 2015b; Collemare & Seidl, 2019). However, exactly how, when and where chromatin is reorganized in plant-colonizers to induce interaction-specific genes is largely unknown (Li *et al.*, 2007; Freitag, 2017). In pioneering work, Chujo and Scott found that in *E. festucae*, secondary metabolite gene upregulation during host colonization was associated with a decrease in H3K27me3 and H3K9me3 levels (Chujo & Scott, 2014), highlighting that chromatin remodeling is likely critical for shaping the expression pattern of genes involved in the host interaction.

The wheat pathogen *Zymoseptoria tritici* (formerly *Mycosphaerella graminicola*) is an additional example of a plant pathogenic fungus in which several putative effector genes are associated with TEs and repressive histone modifications (H3K27me3 and H3K9me3) (Schotanus *et al.*, 2015; Soyer *et al.*, 2019). *Z. tritici* is a devastating pathogen that causes necrosis on wheat leaves after an asymptomatic period that lasts more than 7 days (Fones & Gurr, 2015; Sánchez-Vallet *et al.*, 2015; Torriani *et al.*, 2015). During the asymptomatic phase, hyphae from germinated spores on the leaf surface penetrate the stomata and grow in the apoplastic space. Necrotic lesions

on the leaf appear simultaneously with the formation of asexual reproductive structures (Kema *et al.*, 1996; Sánchez-Vallet *et al.*, 2015; Steinberg, 2015). The different stages of infection presumably involve different subsets of effectors. Consequently, putative effector genes have a distinct expression pattern with very low levels in axenic conditions and high induction at various stages of host colonization (Rudd *et al.*, 2015; Palma-Guerrero *et al.*, 2016; Haueisen *et al.*, 2019). For example, a gene encoding a predicted effector with a cellulase domain (*Mycgr3G76589*), which was suggested to be an inducer of the immune response, is specifically expressed during the necrotrophic and saprotrophic phases (Brunner *et al.*, 2013). On the other hand, two validated effector genes (*AvrStb6*, *Avr3D1*) and a predicted one (*QTL7_5*) without any known functional domain are expressed at low levels at early stages of the infection and reach maximum expression levels at the onset of the necrotrophic phase, but are not expressed in the saprotrophic phase (Zhong *et al.*, 2017; Meile *et al.*, 2018). Understanding how the tight regulation of effector gene expression is achieved remains a fundamental question in plant pathology.

In an effort to determine the contribution of epigenetic changes to the tight control of effector genes, we engineered the *Z. tritici* genome with reporter genes that allowed us to distinguish the contributions of the promoter and the genomic environment to effector gene expression. Our data demonstrate that the repressive genomic environment of effector genes shapes their spatio-temporal expression pattern. We additionally showed that de-repression of effector loci requires the activity of strong promoters and is linked with chromatin remodeling, featuring a reduction of H3K27me3 and H3K9me3 levels.

3.3. Results

3.3.1. The genomic environment has a repressive effect on effector gene expression in the absence of the host

To test whether the genomic location contributes to the typically low expression values of effector genes in the absence of the host, we inserted different reporter genes either in the loci of interest or ectopically, i.e. in random positions in the genome of the *Z. tritici* strain 3D7. The effector loci *AvrStb6*, *Avr3D1*, *QTL7_5* and *Mycgr3G76589* were chosen for this approach based on their location in TE-rich regions of the genome (Zhong *et al.*, 2017; Meile *et al.*, 2018, Fig S1) and their stage-specific expression pattern during host colonization (Brunner *et al.*, 2013; Zhong *et al.*, 2017; Stewart *et al.*, 2018; Meile *et al.*, 2018). Insertion of a hygromycin resistance gene (*Hph*) cassette with a constitutive promoter in the loci *AvrStb6*, *Avr3D1* and *QTL7_5* resulted in higher sensitivity to hygromycin B of the recipient strains compared to ectopic integration of the same cassette (Fig 1), suggesting a repressive role of the genomic environment on gene expression at these effector loci. For the non-effector locus *Zt09_7_00577* (Stewart *et al.*, 2018) upstream of *Avr3D1* (Fig S1), a repressive role of the genomic environment on expression of the inserted reporter gene was not observed (Fig1). For *Avr3D1* and *QTL7_5* the same experiment was performed in a different strain, 3D1, with similar results (Fig S2A).

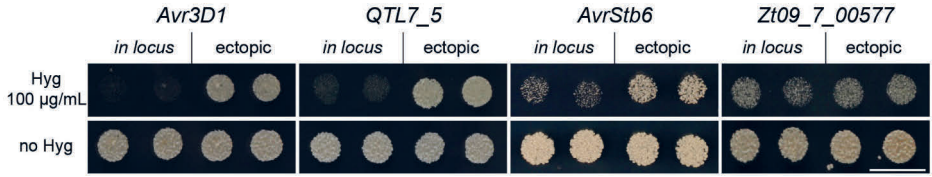

Figure 1. The genomic environment of selected *Zymoseptoria tritici* effector genes is repressive for expression.

Hygromycin B sensitivity assay with 3D7-derived transformants carrying the hygromycin B resistance gene *Hph* under the control of a constitutive promoter either for the loci *Avr3D1*, *QTL7_5* or *AvrStb6* (*in locus*) or at random positions of the genome (ectopic). *Zt09_7_00577* is a non-effector control locus located ~70 kb upstream of Avr3D1 (Fig S1). Two independent transformant lines are shown for each locus. Pictures were taken after 6 days of growth at 18°C on YMS agar plates. Scale bar = 10 mm. Hyg = Hygromycin B.

Using quantitative reverse transcription PCR (qRT-PCR), we confirmed that *in locus* insertion of the *Hph* gene resulted in lower *Hph* transcript levels than ectopic insertions (Fig S2B, left panel). To further characterize repression of *Avr3D1* and *AvrStb6*, an *eGFP* reporter cassette with a constitutive promoter was inserted in these loci. The eGFP fluorescence was lower in *in locus* transformants compared to ectopic transformants in both cases and lower for locus *Avr3D1* compared to *AvrStb6* (Fig S2C), demonstrating that repression at the loci *Avr3D1* and *AvrStb6* is independent of the reporter gene and that different loci can be subjected to different levels of repression.

For *Mycgr3G76589*, we were unable to obtain *in locus* transformants; we therefore generated lines with a second, ectopically inserted copy of *Mycgr3G76589* under the control of the native promoter and compared expression to the wild type using qRT-PCR. Expression levels from ectopic sites were higher than from the native locus (Fig

S2B, right panel), indicating that the *Mycgr3G76589* locus is also epigenetically repressed in axenic culture.

We further tested whether *in locus*-inserted fluorescent reporter genes were also repressed when they were under the control of the native promoters of *AvrStb6* (P*avrStb6*) and *Avr3D1* (P*avr3D1*). To be able to visualize fungal cells, recipient strains expressing either *mTurquiose2* or *mCherry* under the control of a constitutive promoter were used (Fig 2A). In the mTurquoise-3D7 strain, P*avrStb6* was used to control *mCherry* fused to *His1* to localize the reporter to the nucleus and to monitor mCherry levels on a single-cell level. In mCherry-3D7, P*avr3D1* was used to control *mTurquiose2* expression (Fig 2A). In axenic culture, mCherry and mTurquoise2 levels were lower in *in locus* transformants than in ectopic transformants (Fig 2B), suggesting that *AvrStb6* and *Avr3D1* are probably under epigenetic control in the absence of the host.

3.3.2. Effector genes are de-repressed *in planta* and the de-repression pattern is disturbed by ectopic gene relocation.

Since effector genes, including *AvrStb6* and *Avr3D1*, are highly induced during host colonization, we hypothesized that they need to be de-repressed in the presence of the host. The fluorescent reporter genes driven by the native promoters provided a tool to study de-repression of effector genes in detail on a spatial and temporal level. During infection of wheat leaves, strains with P*avrStb6-His1-mCherry* placed in the locus *AvrStb6* showed high mCherry levels mostly in cells that grow inside the host leaf and in cells close to penetration sites but not in cells of hyphae growing epiphytically (Fig 2B).

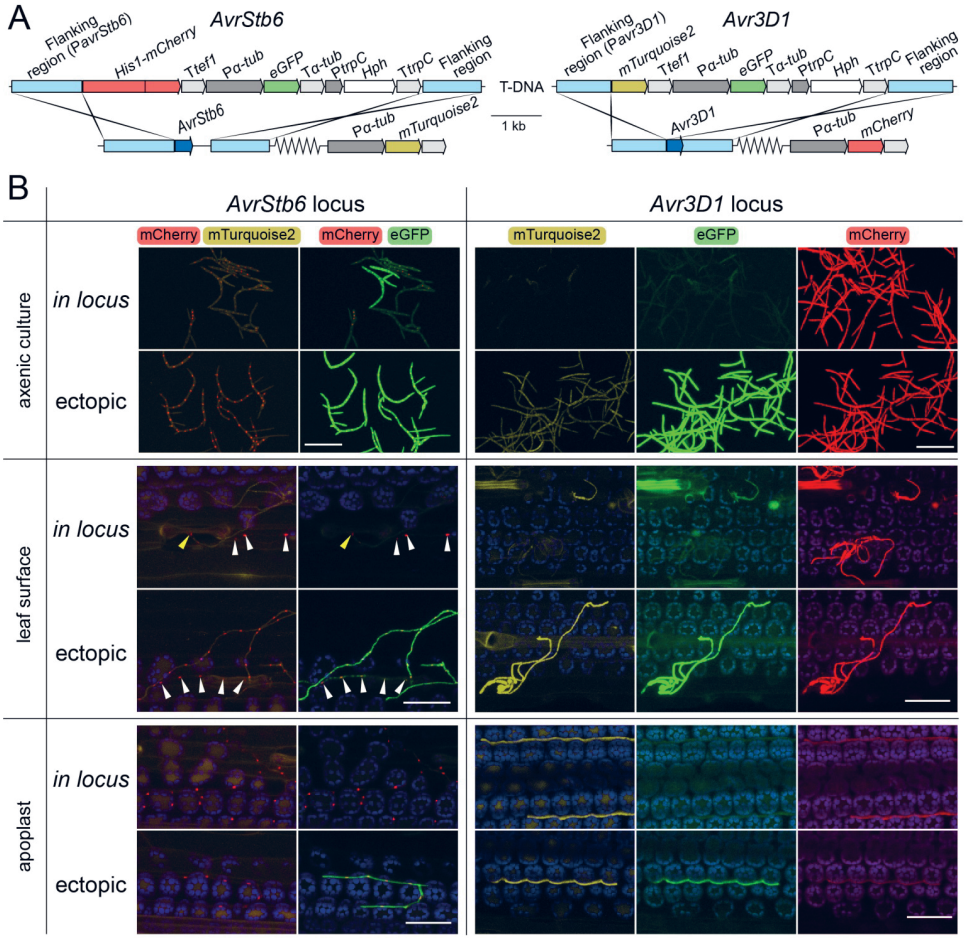
A
AvrStb6
Flanking region (PavrStb6)
His1-mCherry
Ttef1
Pα-tub
eGFP
Tα-tub
PtrpC
Hph
TtrpC
Flanking region
AvrStb6
Pα-tub
mTurquoise2
T-DNA
1 kb
Avr3D1
Flanking region (Pavr3D1)
mTurquoise2
Ttef1
Pα-tub
eGFP
Tα-tub
PtrpC
Hph
TtrpC
Flanking region
Avr3D1
Pα-tub
mCherry
B
AvrStb6 locus
Avr3D1 locus
mCherry
mTurquoise2
mCherry
eGFP
mTurquoise2
eGFP
mCherry
axenic culture
in locus
ectopic
leaf surface
in locus
ectopic
apoplast
in locus
ectopic

Figure 2. *AvrStb6* and *Avr3D1* are silenced in axenic conditions but de-repressed during host colonization (previous page).

(A) Construct design for insertion of three reporter genes into specific effector loci in *Zymoseptoria tritici.* They encode (i) a His1-mCherry fusion protein under the control of the *AvrStb6* promoter (P*avrStb6*, located in the left flanking region of the left construct), (ii) mTurquoise2 under the control of the *Avr3D1* promoter (P*avrStb6,* located in the left flanking region of the right construct) and (iii) eGFP under the control of the constitutive *α-tubulin* promoter (P*α-tub*, present in both constructs). The flanking regions consisted of at least 1.09 kb of sequence identical to the 3D7 genome for homologous recombination. T*tef1* = *Aspergillus nidulans tef1* terminator; T*α-tub* = *Z. tritici α-tubulin* terminator; T*trpC* = *A. nidulans trpC* terminator; P*trpC* = *A. nidulans trpC* promoter; *Hph*= hygromycin phosphostransferase gene. Serrated lines indicate different chromosomal location. **(B)** Fluorescence of mCherry, mTurquoise2 and eGFP of *Z. triciti* strain 3D7 transformed with the constructs described in (A) under axenic conditions, during epiphytic growth on wheat leaves and during colonization of the apoplast. The constructs were either inserted in the locus *AvrStb6* or *Avr3D1* (*in locus*) or in random positions of the genome (ectopic). To be able to visualize fungal cells, the shown mutants were obtained in genetic backgrounds containing either *mTurquiose2* or *mCherry* under the control of the *α-tubulin* promoter. Wheat chloroplasts are highlighted in blue. White arrowheads mark nuclei from cells located in the apoplast and the yellow arrowhead marks a nucleus from a cell in contact with a stomate. In the bottom two image rows (apoplast colonization) all shown hyphae and nuclei are located in the apoplast. Scale bars represent 50 µm.

However, if the same construct was inserted ectopically, the mCherry fluorescence was more uniform and widely detected in hyphae growing on the leaf surface (Fig 2B), suggesting that relocation of *AvrStb6* to a new place in the genome causes misregulation during host colonization and that contact with the host alone is not sufficient for effector gene de-repression in the case of *AvrStb6*. For P*avr3D1*, a similar de-repression pattern was observed during infection; however, compared to P*avrStb6-His1-mCherry,* P*avr3D1-mTurquiose2* was de-repressed in some hyphae shortly after spore germination (2 dpi) on the leaf surface independently of their position relative to stomata (Fig 2B). As in the case of P*avrStb6-His1-mCherry*, mislocation of P*avr3D1-mTurquiose2* led to an early activation of the promoter, since the reporter gene was highly expressed in all observed hyphae already at early stages in epiphytic hyphae (Fig 2B). Genomic location-dependent repression seemed to be restricted to early infection stages, as no expression differences between *in locus* and ectopic transformants could be observed inside the host tissue (Fig 2B). Interestingly, *eGFP* under the control of a constitutive promoter and positioned downstream of P*avrStb6-His1-mCherry* and P*avr3D1-mTurquiose2* remained largely silent in *in locus* transformants during infection, even in hyphae that had undergone effector de-repression (Fig 2B). Thus, de-repression seems to be locally restricted and does not extensively affect neighboring loci in the case of *AvrStb6* and *Avr3D1.*

3.3.3. Histone modifications are involved in effector gene regulation

Given the location of *AvrStb6, Avr3D1, QTL7_5 and Mycgr3G76589* in TE-rich regions of the 3D7 genome, the lack of cytosine methylation (Dhillon *et al.*, 2010) and the enrichment of these genes in the heterochromatin marks histone H3K9me3 and/or H3K27me3 in the reference strain IPO323 (Schotanus *et al.*, 2015; Soyer *et al.*, 2019), we hypothesized that these histone modifications are involved in

repression of these effector genes in axenic culture. The strong and durable silencing phenotype of the *eGFP* reporter cassette with a constitutive promoter inserted at the *Avr3D1* locus provided a tool to investigate the mechanistic basis of effector repression. Based on the described role of histone acetylation as an important determinant of chromatin structure (Strahl & Allis, 2000), we tested whether increased histone acetylation levels are sufficient to rescue the repression phenotype of the *eGFP* cassette in the context of the *Avr3D1* locus. Treatment with the histone deacetylase inhibitors suberoylanilide hydroxamic acid (SAHA) and trichostatin A (TSA) led to an induction of the previously silenced eGFP (Fig S3), highlighting the epigenetic nature of repression at the *Avr3D1* locus and suggesting a role of chromatin structure in this process.

To test whether the four studied effector genes are heterochromatic in the strain 3D7, chromatin immunoprecipitation followed by quantitative PCR (ChIP-qPCR) was performed on axenically grown 3D7 tissue. The enrichment of H3K9me3 and – to a higher extent – H3K27me3 in all four effector genes was higher than in the housekeeping genes *TFC1* and *Actin1* and in the non-effector gene *Zt09_7_00577* located upstream of the *Avr3D1* effector cluster (Fig S4). Based on the upregulation of the four effector genes *in planta,* we hypothesized that the establishment of the interaction would coincide with a reduction of H3K9me3 or H3K27me3 levels, or both. We therefore sought to measure H3K9me3 and H3K27me3 levels during host colonization at the onset of the necrotrophic phase, where we expected the four effector genes to reach high expression levels (Brunner *et al.*, 2013; Stewart *et al.*, 2018; Meile *et al.*, 2018). ChIP-qPCR revealed that, during infection, H3K27me3 levels decreased between 4 (±1) and 100 (±20) fold for all four tested effector genes and, similarly, H3K9me3 levels decreased between 4 (±1) and 16 (±4) fold for all

effector genes except *AvrStb6* (Fig 3). This reduction of heterochromatin marks suggests changes in the chromatin structure during host colonization at specific loci, which might contribute to the specific expression pattern of effector genes.

Considering the dynamic H3K27me3 levels in all four effector genes, we further investigated the role of this histone modification in effector regulation by obtaining a knockout mutant in the gene encoding the histone methyltransferase responsible for

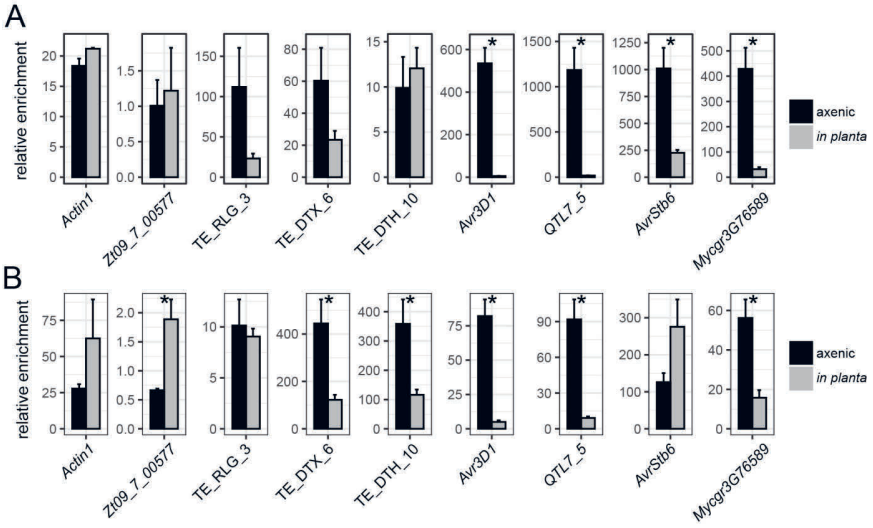

Figure 3. Chromatin is remodelled in effector loci during host colonization.

Relative enrichment of histone H3 lysine 27 trimethylation (A) and histone H3 lysine 9 trimethylation levels (B) of the four effector genes *Avr3D1*, *QTL7_5*, *AvrStb6* and *Mycgr3G76589* during axenic growth and during infection at the beginning of the necrotrophic phase. *Actin1* and *Zt09_7_00577* are genes which are not induced during host colonization. TE_RLG_3, TE_DTX_6 and TE_DTH_10 are transposable elements classified according to Wicker *et al*. (2007): the first letter indicates the class (R, RNA class; D, DNA class); the second letter indicates the order (L, LTR; T, TIR) and the third letter indicates the superfamily (G, Gypsy; H, PIF-Harbinger; X, unknown). The relative enrichment was calculated using a reference housekeeping gene (*TFC1*). Asterisks indicate significant differences between axenic and *in planta* growth (Student's t-test, $p<0.05$).

H3K27 trimethylation, KMT6. The Δ*kmt6* knockout mutant was obtained in the background of a strain harboring a repressed *eGFP* reporter cassette at the locus *Avr3D1* under the control of a constitutive promoter (Fig S2C, right panel). In accordance with a possible role of KMT6 in gene repression, Δ*kmt6* lines exhibited a higher level of eGFP (Figs. 4A & 4B); however, this level was still substantially lower than in lines with an ectopic insertion of the *eGFP* cassette (Fig 4A & 4B), suggesting only a minor contribution of KMT6 to repression of the *Avr3D1* locus in axenic culture. Similarly to the low eGFP fluorescence observed *in planta* (Fig 2B & S2B), *eGFP* transcript levels measured by RT-qPCR only slightly increased during infection in *in locus* transformant lines (Fig 4B). However, loss of KMT6 further contributed to increased *eGFP* expression *in planta*, indicating that colonization can trigger partial de-repression of a silenced but otherwise constitutive promoter located in a heterochromatic region. The transcript levels of *AvrStb6* and *Mycgr3G76589* were higher in Δ*kmt6* compared to the untransformed control in axenic culture (Fig 4C). However, this difference was lost during infection (Fig 4C), suggesting that KMT6 has a repressive effect on these effector genes in the absence of the host but not during their upregulation *in planta*, which is in line with the reduced H3K27me3 levels observed at that stage.

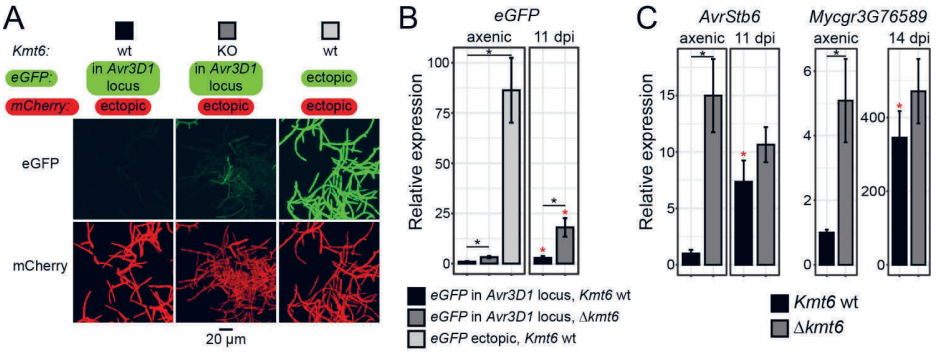

Figure 4. Histone H3 lysine 27 trimethylation is required for effector gene repression.

(A) eGFP fluorescence of *Zymoseptoria tritici* transgenic lines with and without the histone methyltransferase gene *Kmt6 (*wt and KO, respectively), both harbouring the *eGFP* gene under the control of a constitutive promoter in the locus *Avr3D1*. A line harbouring an ectopic copy of the *eGFP* cassette is shown as a control. All lines were obtained in a genetic background containing an *mCherry* reporter cassette for visualization of fungal cells. **(B)** *eGFP* transcript levels in the three transgenic lines described in (A) during axenic growth in rich medium and during plant colonization at 11 days post infection (dpi). **(C)** Transcript levels of *AvrStb6* and *Mycgr3G76589* during axenic growth in rich medium and during plant colonization in *Z. tritici* lines with and without *Kmt6*. Expression levels were normalized to the line with an intact *Kmt6* gene during axenic growth. *Actin1* was used as reference gene for qRT-PCR. Black asterisks indicate differences between strains with and without KMT6 and red asterisks indicate differences between axenic and *in planta* growth of the same mutant line ($p<0.05$, Student's t-test). wt = wild type; KO= knock-out.

3.4. Discussion

A hallmark of fungal and oomycete effector genes is their plant-associated expression pattern. Typically, effectors are highly upregulated during specific stages of host colonization, presumably in accordance with their function during these stages. However, knowledge on the molecular mechanisms governing this tight regulation remains scarce, especially with respect to the role of epigenetics in this process. In this work, we show that the heterochromatic environment of effector genes is crucial for controlling their specific expression in a temporal and spatial manner and thereby provides an important layer of regulation. We propose that de-repression during host colonization is locally confined to effector loci and associated with chromatin remodeling featured by a reduction of H3K27 and/or H3K9 trimethylation levels.

3.4.1. How are effector genes silenced?

The four effector genes *AvrStb6*, *Avr3D1*, *QTL7_5* and *Mycgr3G76589* are silenced under axenic conditions. However, their native promoter sequences were not sufficient to induce repression; instead, the broader genomic context influenced their chromatin state and, consequently, their expression profile. In plant-colonizing organisms, genes involved in host interaction often reside in TE-rich regions (Soyer *et al.*, 2015b, 2019; Schotanus *et al.*, 2015; Seidl & Thomma, 2017; Fouché *et al.*, 2019) and have been shown to be under epigenetic control in plant colonizers such as *F. graminearum* (Connolly *et al.*, 2013), *L. maculans* (Soyer *et al.*, 2014) and *E. festucae* (Chujo & Scott, 2014). TEs are usually silenced as a genome defense mechanism (Selker, 2004; Goll & Bestor, 2005) and TE-associated repressive chromatin modifications are thought to be not locally confined but to spread to nearby

regions, leading to repression of genes therein (Feschotte, 2008; Rebollo *et al.*, 2012; Mita & Boeke, 2016). Although TEs have been emerging as major players in gene regulation, studies on the chromatin-based regulatory role of specific TEs on neighboring genes are still limited, especially in filamentous fungi. A repressive role of TEs on nearby genes has been shown for the basidiomycete *Pleurotus ostreatus* and other fungal species, including the plant symbionts *Laccaria bicolor* and *F. graminearum* (Castanera *et al.*, 2016). In *Z. tritici*, TE-mediated repression of proximal genes was demonstrated by deleting a TE cluster, which resulted in de-repression of a secondary metabolite gene cluster located 1.9 kb downstream (Krishnan *et al.*, 2018). The effector genes investigated in this work reside within a similar distance to upstream TE insertions (distance to start codon between 1.3 and 5.4 kb) and could therefore be subjected to a similar repressive influence. However, the TE insertion present 1.3 kb upstream of *Avr3D1* in strain 3D7 is absent in strain 3D1 (Meile *et al.*, 2018). This TE presence/absence polymorphism does not seem to impact the position effect observed at this locus, since in both strains the *Hph* gene inserted in *Avr3D1* was silenced. Interestingly, *Avr3D1* resides in a genomic region that probably originated from an accessory chromosome. This region is part of the right arm of chromosome 7 and is characterized by high H3K27me3 enrichment and low transcription (Rudd *et al.*, 2015; Schotanus *et al.*, 2015), which are typical features of accessory chromosomes (Schotanus *et al.*, 2015). However, the GC content is similar to the rest of chromosome 7 and even in large (up to 210 kb) segments without TEs inside this peculiar region, H3K27me3 enrichment is uniformly high in the reference strain IPO323 (Schotanus *et al.*, 2015), suggesting that additional features of this region are critical for chromatin structure.

AvrStb6 and *Mycgr3G76589* are located in the proximity of the telomeric repeats, which might also influence their chromatin state. Indeed, telomeric repeats are sufficient for widespread heterochromatin formation in adjacent regions in *Neurospora crassa*, contributing to their epigenetic control (Jamieson *et al.*, 2018). Consequently, subtelomeric regions are frequently heterochromatic (Schotanus *et al.*, 2015; Collemare & Seidl, 2019) and likely influence the expression of genes therein.

By disrupting the gene encoding the histone methyltransferase KMT6, we showed that H3K27me3 has a repressive effect on the investigated effector genes in the absence of the host. However, we observed that in the case of the *Avr3D1* locus, KMT6 had only a minor contribution to repression, suggesting a major role of other histone modifications or chromatin components in this process. Interestingly, all the investigated effector genes exhibited a reduction of H3K27me3 levels during infection. Similarly, with the exception of *AvrStb6*, H3K9me3 levels also decreased during host colonization, suggesting that these modifications might be involved in repression of effector genes. Not only depletion of H3K27me3, but also inhibition of histone deacetylases led to de-repression of the *Avr3D1* locus, indicating that hypoacetylation could also contribute to the silencing of effector genes. In fact, several histone deacetylases are known to target silencing to specific regions of the genome (Wang *et al.*, 2011; Lee & Seo, 2019); similar mechanisms might operate to repress expression of effector genes in the absence of the host. Chromatin structure and dynamics are complex, involving more than 400 known histone post-translational modifications (Zhao & Garcia, 2015) and potentially thousands of interacting proteins (van Steensel, 2011). Thus, it is not surprising that more than one histone modification contributes to the regulation of a specific locus. In line with the high complexity of chromatin architecture and function, the H3K9me3 enrichment pattern

of *AvrStb6* was distinct from the rest of the investigated effector genes; thus, different regulatory mechanisms might operate at different effector loci.

3.4.2. How are effector genes de-repressed?

We show that despite the silenced state of different effector genes in the absence of the host, their de-repression is rapidly induced at specific stages of the infection, in the case of *AvrStb6* even in specialized cells that come into contact with stomata. The *in planta* de-repression was associated with a reduction in H3K27me3 and/or H3K9me3 levels, similar to what was observed for secondary metabolite gene clusters in *E. festucae* (Chujo & Scott, 2014). Interestingly, during host colonization, H3K9me3 levels in the *AvrStb6* locus remained high despite high expression levels during this stage, suggesting that the removal of this H3K9me3 mark is not always necessary for de-repression. The specific de-repression of effector genes *in planta* suggests an environmental or developmental trigger, which remains unknown for the *Z. tritici*-wheat interaction. Interestingly, *Avr3D1* and an additional 16 out of 238 (Plissonneau *et al.*, 2018) candidate effector genes predicted by EffectorP (Sperschneider *et al.*, 2016), are co-upregulated in four strains during infection and hyphal growth in axenic culture (Francisco *et al.*, 2019). This raises the possibility that hyphal growth is involved in effector de-repression, since *Z. tritici* grows mainly as hyphae on the leaf surface before penetrating. However, most of the hyphal growth-induced effector genes including *Avr3D1* are upregulated *in planta* compared to axenic hyphal growth (Francisco *et al.*, 2019) and our de-repression assays showed that *Avr3D1* and *AvrStb6* are still largely repressed in most individuals on the leaf surface despite growing as hyphae, suggesting that dimorphic switching alone is not sufficient to de-repress effector genes.

The spatio-temporal de-repression patterns of effector genes and the associated local changes in the chromatin state were investigated using fluorescent reporters that informed us about the accessibility of effector loci for the transcription machinery. The promoter sequences of *Avr3D1* and *AvrStb6* but not a constitutive promoter were sufficient for *in planta* de-repression of a reporter construct inserted in both loci. Based on these results, we predict that sequence-specific DNA-binding proteins contribute to chromatin decondensation at these loci. Transcription factors have been shown to recruit other factors that promote changes in the chromatin structure and thereby regulate transcription (Weiste & Dröge-Laser, 2014). For example, the transcription factor PfSIP2 from *Plasmodium falciparum* binds to a conserved recognition sequence in heterochromatic domains and promotes silencing of virulence genes (Flueck *et al.*, 2010). Even transcription by RNA polymerase II can further change chromatin structure and organization (Kireeva *et al.*, 2002; van Steensel & Furlong, 2019). Interestingly, the relatively small distance (1.6 kb between stop and start codon) between genes that were de-repressed *in planta* and the downstream gene that largely remained silent at the same time suggests that only a few nucleosomes are affected by locus-specific chromatin remodeling or that post-transcriptional gene silencing is acting at neighboring loci. In line with this hypothesis, Fouché and colleagues found that expression of the closest retrotransposon upstream of *Avr3D1* in strain 3D7 remained low in a susceptible cultivar (Fouché *et al.*, 2019) despite the high induction of *Avr3D1*. Locally confined chromatin remodeling could reflect the necessity to avoid broad-scale de-repression of TE-rich regions, reducing deleterious effects associated with TE activation.

3.4.3. Is an epigenetic layer of regulation needed?

In numerous plant pathogens, the genomic distribution of effector genes is non-random and shows an enrichment in TE-rich subtelomeric and heterochromatic regions. It is assumed that this particular genomic environment acts as a driver for accelerated evolution due to increased mutation/recombination rates. Therefore, the question arises whether chromatin-based regulation is a mere side-effect of the spatial association of effector genes with heterochromatin or whether this additional layer of regulation is functionally relevant and might even contribute to compartmentalization as an evolutionary force.

Although effectors generally have a major role in pathogenicity, misexpression may have fatal consequences for the pathogen for various reasons. First, some effectors may trigger host defense responses through direct or indirect recognition by host resistance proteins, which was shown for both AvrStb6 and Avr3D1. Tight regulation of these avirulence effectors could limit the host immune responses, which may be especially relevant for avirulence factors such as Avr3D1 that induce only partial resistance (Meile *et al.*, 2018). The location of effector genes in heterochromatic regions might also make them more prone to epiallelic variation, which provides a reversible mechanism to escape avirulence effector recognition (Kasuga & Gijzen, 2013; Gijzen *et al.*, 2014). Second, especially in hemibiotrophic pathogens, which require living host tissue for a certain period of time, effectors that are involved in the transition to the necrotrophic infection stage might induce early necrosis if expressed too early and thereby disturb the hemibiotrophic lifestyle. Some necrotrophic effectors may also induce host defense responses through their functions; for example, secreted cell wall degrading enzymes (CWDEs) produce degradation products that can trigger defense responses (Kohorn *et al.*, 2009; Souza *et al.*, 2017). Therefore, in

hemibiotrophs, such as *Z. tritici*, premature induction necrotrophic effectors including CWDEs might have fatal consequences due to early induction of host defenses, highlighting the need for a tight regulation. Third, some effectors function as toxins. Although many necrotrophic effectors have plant-specific targets (Wolpert et al., 2002), others act as non-specific toxins (Wang et al., 2014; Kettles et al., 2018) and it is possible that some of them exhibit autotoxicity that could be reduced by tight regulation. Fourth, given the typically high expression levels of effector genes during infection (Rudd *et al.*, 2015; Evangelisti *et al.*, 2017; Lanver *et al.*, 2018; Courville *et al.*, 2019), it cannot be excluded that an extra layer of regulation is relevant to reduce the metabolic costs associated with leaky expression at stages when effectors are not needed.

In summary, we hypothesize that the epigenetic layer of gene regulation observed in our experiments provides a key element for regulation of effector genes, contributing to transcriptional inactivity when not needed and thereby reducing the self-damage caused by secreted enzymes or toxins and the consequences of host defenses induced upon effector perception. Epigenetic mechanisms may also enable stage-specific gene induction that can operate together with or as an alternative to classical transcriptional activators and repressors. Our experiments on the *AvrStb6* and *Avr3D1* loci showed that de-repression is highly local and likely does not occur without sequence-specific factors as well as one or more host-related triggers, both of which remain to be discovered.

3.5. Materials & Methods

3.5.1. Fungal and bacterial strains, culture conditions and genome resources

The Swiss *Zymoseptoria tritici* strains ST99CH_3D7 and ST99CH_3D1 (Linde *et al.*, 2002, abbreviated as 3D7 and 3D1, respectively) and mutants in these backgrounds were used in this study. To assess the proximity of selected effector genes and transposable elements (TEs), we used the 3D7 genome assembly and TE annotations that were previously published (Plissonneau *et al.*, 2016). For all experiments involving 3D7Δ*kmt6* mutants, blastospores were grown on yeast-peptone-dextrose agar (YPD; 1% yeast extract, 2% peptone, 2% dextrose, 1.5% agar). For all other experiments, either yeast-sucrose broth (YSB; 1% yeast extract, 1% sucrose) or yeast-malt-sucrose agar (YMS; 0.4% yeast extract, 0.4% malt extract, 0.4% sucrose, 1.5% agar) was used if not stated otherwise. For all axenic cultures of *Z. tritici*, media were supplemented with kanamycin sulfate (50 µg/mL). Molecular cloning and plasmid propagation were performed with the *Escherichia coli* strain HST08 (Takara Bio, Shiga, Japan). For *Agrobacterium tumefaciens*-mediated transformation of *Z. tritici*, the *A. tumefaciens* strain AGL-1 was used.

3.5.2. Generation of *Z. tritici* mutant lines

All constructs for targeted or ectopic insertion mutagenesis were generated with the In-Fusion HD Cloning Kit (Takara Bio Inc., Shiga, Japan) as previously described (Meile *et al.*, 2018). All constructs and fragments from which they were assembled are listed in Table S1. Constitutive promoters, terminators, selection markers and fluorescent reporter genes were amplified from the plasmids pES1, pES6 (plasmids for fungal transformation; Eva. H. Stukenbrock, Christian-Albrechts-University of Kiel,

unpublished), pFC332 (Nødvig *et al.*, 2015), pCGEN (Motteram *et al.*, 2011), pCmCherry (Schuster *et al.*, 2015) and pCZtGFP (Kilaru *et al.*, 2015b). The fluorescent reporter gene *mTurquoise2* was designed based on the codon-optimized *eGFP* sequence present in pCZtGFP and its dsDNA sequence (File S1) was purchased from IDT (Coralville, IA, USA). *Z. tritici* was transformed by *Agrobacterium tumefaciens*-mediated transformation as described before (Zwiers & De Waard, 2001; Meile *et al.*, 2018). Strain 3D7 harboring the *mCherry* gene under the control of the *Z. tritici α-tubulin* promoter was obtained by S. Kilaru and G. Steinberg using targeted ectopic integration (Kilaru *et al.*, 2015a). For targeted insertion mutants, the position of the insertion was verified by PCR using a primer specific for the insert sequence combined with a primer specific for the genomic region adjacent to the point of insertion. For all mutants, the copy number of the inserted transgenes was determined by qPCR on genomic DNA and transformant lines with more than one insert copy were excluded from further experiments.

3.5.3. Hygromycin sensitivity assays

Z. tritici blastospores were grown for 5-7 days in YSB medium. The spore suspension was filtered through cheese cloth and centrifuged (3273 g, 15 min, 4°C). Spores were resuspended in water and the spore concentration was determined using KOVA Glasstic counting chambers (Hycor Biomedical, Inc., Garden Grove, CA, USA). The concentration was adjusted to 10^6 spores/mL and 2.5-5 µL were placed on YMS agar with and without Hygromycin B (100 µg/mL). Hygromycin sensitivity was assessed after 6 days of growth at 18°C.

3.5.4. RNA isolation and quantitative reverse transcription PCR

To obtain RNA from infected leaf tissue, wheat seedlings (cultivar Runal) were infected with *Z. tritici* blastospores as previously described (Meile *et al.*, 2018), except for experiments involving Δ*kmt6* mutant lines, for which blastospores were grown on YPD agar at 18°C for 3-5 days, washed off the agar surface with water by scraping with a pipette tip to create a spore suspension and filtered through a 100-µm nylon mesh. Infected leaves were harvested as described (Meile *et al.*, 2018) and for each biological replicate, at least two leaves were pooled. To obtain RNA from axenically grown tissue, fungal blastospores were grown on YPD agar and harvested as described above for the preparation of infection inoculum (in case of experiments involving the Δ*kmt6* mutant*)* or they were grown in liquid YSB medium at 18°C for 4-6 days (all other experiments). In both cases, tissue was harvested by centrifugation at 4°C and flash-frozen in N_2.

RNA isolation was performed as described (Meile *et al.*, 2018) and cDNA was synthesized with the RevertAid First Strand cDNA Synthesis Kit (Thermo Fisher Scientific, Waltham, MA, USA) following the manufacturer's instructions using oligo$(dT)_{18}$ primers and up to 1000 ng RNA per reaction. Quantitative reverse transcription PCR (qRT-PCR) was performed on a LightCycler 480 (Roche Diagnostics International AG, Rotkreuz, ZG, Switzerland). Each 10-µL reaction consisted of 250 nM of each primer, template cDNA generated from up to 25 ng of RNA and 1x HOT FIREPol EvaGreen qPCR Mix Plus mastermix (Solis BioDyne, Tartu, Estonia). The amplification reactions were performed with at least three technical replicates. Primers used for qRT-PCR are listed in Table S2. Primer efficiency was determined using 5-fold serial dilutions of genomic DNA or cDNA (in case of *AvrStb6* primers) and used for efficiency-corrected calculations of the relative

expression (Pfaffl, 2001) with *Actin1* as reference gene, if not stated otherwise. The expression values of ectopic copies of the *Mycgr3G76589* gene were calculated by subtracting the value of the native gene measured in the wildtype strain from the total expression values in the ectopic insertion mutants. The mean relative expression and standard error of the mean was calculated using RStudio v.1.2.1335 (RStudio Team, 2015).

3.5.5. Histone deacetylase inhibition assay

The *Z. tritici* lines used for the histone deacetylase inhibition assays carried the following transgenes: (i) *eGFP* under the control of the constitutive *α-tubulin* promoter inserted in the locus *Avr3D1* or ectopically and (ii) *mCherry* under the control of the same *α-tubulin* promoter in an ectopic position (Kilaru *et al.*, 2015a). For trichostatin A (TSA) treatments, 1 mL YSB medium containing 0.5 µg/mL TSA (Selleckchem, Houston, TX, USA) was inoculated with blastospores from glycerol stocks in a 12-well cell culture plate. Cultures were incubated at 18°C under gentle agitation for three days. For suberoylanilide hydroxamic acid (SAHA) treatments, 600 µL Minimal Medium (Vogel & J., 1956) containing 1 mM SAHA (Cayman Chemical, Ann Arbor, MI, USA) were inoculated with blastospores from glycerol stocks in a 24-well cell culture plate. Cultures were incubated at 18°C under gentle agitation for 11 days. All treatments were performed with three biological replicates. De-repression of the *eGFP* cassette was assessed with a Leica DM2500 fluorescence microscope equipped with a Leica DFC3000 G greyscale camera (Leica Microsystems, Wetzlar, Germany) and the filter blocks L5 for GFP (480/40 nm excitation, 527/30 nm emission) and mCherry (580/20 nm excitation, 632/60 nm emission). All images were processed in the same way using the Fiji platform of ImageJ (Schneider *et al.*, 2012).

3.5.6. Confocal laser scanning microscopy

Confocal laser scanning microscopy was performed on an inverted Zeiss LSM 780 confocal microscope using a multi-tracking acquisition setup and the following detection settings: 490.33 - 534.72 nm for the eGFP channel, 623.51 - 641.26 nm for the mCherry channel, 656.01 - 681.98 nm for the chloroplast channel and 459.95 - 490.07 nm for the mTurquoise2 channel. A DPSS (561 nm) and an argon (488 nm) laser were used for Track 1 (eGFP, mCherry and chloroplast channels) and a diode laser (405 nm) was used for Track 2 (mTurquiose2 channel). Axenically grown fungal material was suspended in 0.02 % Tween20 (when grown on solid medium) or directly observed in liquid medium. For *in planta* observations, plants were infected as described previously (Meile *et al.*, 2018) and infected 2nd leaves were harvested immediately before observation. The top 3 cm of each leaf was discarded and the adaxial side of the adjacent section of approx. 2 cm was observed in 0.02 % Tween20. Images were processed using the Fiji platform of ImageJ (Schneider *et al.*, 2012). Processing included cropping, adjusting brightness and contrast, adding scalebars and generation of maximum intensity z-projections. 3D reconstruction enabled us to differentiate between hyphae on the leaf surface and hyphae growing in the apoplastic space.

3.5.7. Fixation of fungal and infected plant tissue for chromatin extraction

Fixation of axenically grown fungal cells of *Z. tritici* strain 3D7 was performed as described (Soyer *et al.*, 2015a) with the following modifications: A 5-day-old preculture was used to inoculate a 100-mL YMS culture with a starting OD_{600} of 0.225. This culture was grown for 38 hours to an OD_{600} between 0.79 and 0.85. Cells were fixed by adding formaldehyde to a final concentration of 0.5% and shaking for

15 min. Formaldehyde was quenched by adding glycine to a final concentration of 50 mM. Cells were washed with phosphate buffered saline (PBS, Sigma-Aldrich, St. Louis, MO, USA), harvested by centrifugation (1 min, 800 *g*) and flash-frozen in N_2.

Infected 2nd leaves of cultivar Runal (spray-inoculated as described but with $5x10^6$ spores/mL) were harvested for chromatin preparations when the first necrosis symptoms appeared (10-11 days post infection; Fig S5). The top 2 cm of the leaves was discarded and the adjacent 8.5 cm sections were used for fixation. Leaf sections were cut in half, pooled (n= 45-60) and vacuum-infiltrated with 55-80 mL fixation buffer modified from Chujo and Scott (Chujo & Scott, 2014) [0.4 M sucrose, 10 mM Tris-HCl (pH 8.0), 1 mM EDTA, 1 mM phenylmethylsulphonyl fluoride (PMSF), 0.5% (w/v) formaldehyde and 0.02% (v/v) Triton X-100] in a 250-mL beaker for 15 min under constant stirring. During fixation, the vacuum was released several times. Formaldehyde was quenched by adding glycine to a final concentration of 100 mM followed by vacuum-infiltration for 5 min under constant stirring, releasing the vacuum several times during incubation. The leaf sections were washed twice with PBS and once with water before drying them on paper towels and flash-freezing them in N_2.

3.5.8. Chromatin preparations, immunoprecipitation and ChIP-qPCR

Frozen fungal or infected leaf tissue was ground using mortar and pestle. Between 150 and 233 mg of tissue were used for each chromatin extraction, which was performed similarly as described (Soyer *et al.*, 2015a): Lysis buffer [50 mM HEPES-NaOH (pH 7.5), 20 mM NaCl, 1 mM Na-EDTA (pH 8.0), 1% (v/v) Triton X-100; 0.1% (w/v) Na-deoxycholate] supplied with proteinase inhibitors (1 µg/mL leupeptin, 1 µg/mL E-64, 0.5 µg/mL pepstatin A, 1 mM PMSF and 2 µg/mL aprotinin) was added in a ratio of 5 µl to 1 mg of ground tissue in Eppendorf tubes. $CaCl_2$ (1 M stock) was

added to a final concentration of 2 mM and chromatin was fragmented with micrococcal nuclease (M0247S; New England Biolabs, Ipswich, MA, USA) at a concentration of 10 gel units/µL for 15 min at 37°C. Tubes were vortexed several times during incubation. The reaction was stopped by placing the tubes on ice and adding EGTA and EDTA (final concentration 4 mM each). Additional NaCl (stock solution: 5 M) was added to a final concentration of 130 mM and SDS [stock solution: 10 % (w/v)] was added to a final concentration of 0.1%. Samples were incubated on ice for 5 min, vortexed several times during incubation and subsequently cleared by centrifugation (4°C, 5 min, 1500 *g*). For axenically grown tissue, clearing was repeated 3 times (4°C, 5 min, 4000 *g*). Immunoprecipitation and de-crosslinking was performed as described (Soyer *et al.*, 2015a) using 8.75 µg anti-histone H3K27me3 (Cat# 39155; Active Motif, Carlsbad, CA, USA) or anti-histone H3K9me3 (Active Motif Cat# 39161) antibodies and 52.5 µL Dynabeads™ protein A (Thermo Fisher Scientific) per mL chromatin.

qPCR was carried out on a LightCycler480 (Roche) in technical duplicates using HOT FIREPol EvaGreen qPCR Mix Plus mastermix (Solis BioDyne, Tartu, Estonia) and the primers shown in Table S2. The relative enrichment of each target gene compared to the reference gene *TFC1* was calculated using enrichment = $\text{eff.TFC1}^{\text{Cp.TFC1}}/\text{eff.Target}^{\text{Cp.Target}}$, where eff.TFC1 and eff.Target are the primer efficiency for *TFC1* and the target gene, respectively, and Cp.TFC1 and Cp.Target the crossing point of *TFC1* and the target gene, respectively. The crossing point values were determined using the LightCylcer480 software. The % input (ratio of immunoprecipitated DNA relative to the chromatin before immunoprecipitation) was also calculated for *in vitro* immunoprecipitations.

3.6. Acknowledgments

We thank Sreedhar Kilaru and Gero Steinberg for providing pCmCherry, pCZtGFP and the strain 3D7 expressing *mCherry*, Eva Stukenbrock for providing pES1 and pES6, Uffe Mortensen for providing pFC332 and Jason Rudd for providing pCGEN. qPCR reactions were performed in collaboration with the Genetic Diversity Centre (GDC), ETH Zurich. Confocal laser scanning microscopy experiments were supported by the Scientific Center for Optical and Electron Microscopy (ScopeM), ETH Zurich. We are grateful for technical assistance by Ziqi Shen and for fruitful discussions with Olivier Voinnet and Thomas Grentzinger. This research was supported by the Swiss National Science Foundation (Grant 31003A_155955 to BAM).

3.7. References

Brown CE, Lechner T, Howe LA, Workman JL. **2000**. The many HATs of transcription coactivators. *Trends in Biochemical Sciences* **25**: 15–19.

Brunner PC, Torriani SFF, Croll D, Stukenbrock EH, McDonald BA. **2013**. Coevolution and life cycle specialization of plant cell wall degrading enzymes in a hemibiotrophic pathogen. *Molecular Biology and Evolution* **30**: 1337–1347.

Castanera R, López-Varas L, Borgognone A, LaButti K, Lapidus A, Schmutz J, Grimwood J, Pérez G, Pisabarro AG, Grigoriev I V., *et al.* 2016. Transposable elements versus the fungal genome: impact on whole-genome architecture and transcriptional profiles. *PLOS Genetics* **12**: e1006108.

Chujo T, Scott B. **2014**. Histone H3K9 and H3K27 methylation regulates fungal alkaloid biosynthesis in a fungal endophyte-plant symbiosis. *Molecular Microbiology* **92**: 413–434.

Collemare J, O'Connell R, Lebrun M. **2019**. Nonproteinaceous effectors: the *terra incognita* of plant–fungal interactions. *New Phytologist* **223**: 590–596.

Collemare J, Seidl MF. **2019**. Chromatin-dependent regulation of secondary metabolite biosynthesis in fungi: is the picture complete? *FEMS Microbiology Reviews*.

Connolly LR, Smith KM, Freitag M. **2013**. The Fusarium graminearum histone H3 K27 methyltransferase KMT6 regulates development and expression of secondary metabolite gene clusters. *PLoS Genetics* **9**: e1003916.

Courville KJ, Frantzeskakis L, Gul S, Haeger N, Kellner R, Heßler N, Day B, Usadel B, Gupta YK, Esse HP, *et al.* 2019. Smut infection of perennial hosts: the genome and the transcriptome of the Brassicaceae smut fungus *Thecaphora thlaspeos* reveal functionally conserved and novel effectors. *New Phytologist* **222**: 1474–1492.

Dallery J-F, Lapalu N, Zampounis A, Pigné S, Luyten I, Amselem J, Wittenberg AHJ, Zhou S, de Queiroz M V., Robin GP, *et al.* 2017. Gapless genome assembly of *Colletotrichum higginsianum* reveals chromosome structure and association of transposable elements with secondary metabolite gene clusters. *BMC Genomics* **18**: 667.

Dhillon B, Cavaletto JR, Wood K V., Goodwin SB. 2010. Accidental amplification and inactivation of a methyltransferase gene eliminates cytosine methylation in *Mycosphaerella graminicola*. *Genetics* **136**: 789–802.

Dong S, Raffaele S, Kamoun S. 2015. The two-speed genomes of filamentous pathogens: waltz with plants. *Current Opinion in Genetics & Development* **35**: 57–65.

Erlendson AA, Friedman S, Freitag M. 2017. A matter of scale and dimensions: chromatin of chromosome landmarks in the fungi. *Microbiology Spectrum* **5**.

Evangelisti E, Gogleva A, Hainaux T, Doumane M, Tulin F, Quan C, Yunusov T, Floch K, Schornack S. 2017. Time-resolved dual transcriptomics reveal early induced *Nicotiana benthamiana* root genes and conserved infection-promoting *Phytophthora palmivora* effectors. *BMC Biology* **15**: 39.

Feschotte C. 2008. Transposable elements and the evolution of regulatory networks. *Nature Reviews Genetics* **9**: 397–405.

Flueck C, Bartfai R, Niederwieser I, Witmer K, Alako BTF, Moes S, Bozdech Z, Jenoe P, Stunnenberg HG, Voss TS. 2010. A major role for the *Plasmodium falciparum* ApiAP2 protein PfSIP2 in chromosome end biology. *PLoS Pathogens* **6**: e1000784.

Fones H, Gurr S. 2015. The impact of Septoria tritici Blotch disease on wheat: An EU perspective. *Fungal Genetics and Biology* **79**: 3–7.

Fouché S, Badet T, Oggenfuss U, Plissonneau C, Francisco CS, Croll D. 2019. Stress-driven transposable element de-repression dynamics and virulence evolution in a fungal pathogen. *Molecular Biology and Evolution*.

Francisco CS, Ma X, Zwyssig MM, McDonald BA, Palma-Guerrero J. 2019. Morphological changes in response to environmental stresses in the fungal plant pathogen *Zymoseptoria tritici*. *Scientific Reports* **9**: 9642.

Freitag M. 2017. Histone methylation by SET domain proteins in fungi. *Annual Review of Microbiology* **71**: 413–439.

Gacek A, Strauss J. 2012. The chromatin code of fungal secondary metabolite gene clusters. *Applied Microbiology and Biotechnology* **95**: 1389–1404.

Galazka JM, Freitag M. 2014. Variability of chromosome structure in pathogenic fungi — of 'ends and odds'. *Current Opinion in Microbiology* **20**: 19–26.

Gervais J, Plissonneau C, Linglin J, Meyer M, Labadie K, Cruaud C, Fudal I, Rouxel T, Balesdent MH. 2017. Different waves of effector genes with contrasted genomic location are expressed by *Leptosphaeria maculans* during cotyledon and stem

colonization of oilseed rape. *Molecular Plant Pathology* **18**: 1113–1126.

Gijzen M, Ishmael C, Shrestha SD. **2014**. Epigenetic control of effectors in plant pathogens. *Frontiers in Plant Science* **5**: 638.

Goll MG, Bestor TH. **2005**. Eukaryotic cytosine methyltransferases. *Annual Review of Biochemistry* **74**: 481–514.

Gómez-Díaz E, Jordà M, Peinado MA, Rivero A. **2012**. Epigenetics of host–pathogen interactions: the road ahead and the road behind. *PLoS Pathogens* **8**: e1003007.

Goodrich J, Puangsomlee P, Martin M, Long D, Meyerowitz EM, Coupland G. **1997**. A Polycomb-group gene regulates homeotic gene expression in *Arabidopsis*. *Nature* **386**: 44–51.

Grandaubert J, Balesdent M-H, Rouxel T. **2014**. Evolutionary and adaptive role of transposable elements in fungal genomes. *Advances in Botanical Research* **70**: 79–107.

Grewal SIS, Jia S. **2007**. Heterochromatin revisited. *Nature Reviews Genetics* **8**: 35–46.

Haas BJ, Kamoun S, Zody MC, Jiang RHY, Handsaker RE, Cano LM, Grabherr M, Kodira CD, Raffaele S, Torto-Alalibo T, *et al.* 2009. Genome sequence and analysis of the Irish potato famine pathogen *Phytophthora infestans*. *Nature* **461**: 393–398.

Haueisen J, Möller M, Eschenbrenner CJ, Grandaubert J, Seybold H, Adamiak H, Stukenbrock EH. **2019**. Highly flexible infection programs in a specialized wheat pathogen. *Ecology and Evolution* **9**: 275–294.

Hogenhout SA, Van der Hoorn RAL, Terauchi R, Kamoun S. **2009**. Emerging concepts in effector biology of plant-associated organisms. *Molecular Plant-Microbe Interactions* **22**: 115–122.

Jamieson K, McNaught KJ, Ormsby T, Leggett NA, Honda S, Selker EU. **2018**. Telomere repeats induce domains of H3K27 methylation in Neurospora. *eLife* **7**.

Kasuga T, Gijzen M. **2013**. Epigenetics and the evolution of virulence. *Trends in Microbiology* **21**: 575–582.

Kema G, Yu D, Rijkenberg F. **1996**. Histology of the pathogenesis of *Mycosphaerella graminicola* in wheat. *Phytopathology* **86**: 777–786.

Kettles GJ, Bayon C, Sparks CA, Canning G, Kanyuka K, Rudd JJ. **2018**. Characterization of an antimicrobial and phytotoxic ribonuclease secreted by the fungal wheat pathogen *Zymoseptoria tritici*. *New Phytologist* **217**: 320–331.

Kilaru S, Schuster M, Latz M, Das Gupta S, Steinberg N, Fones H, Gurr SJ, Talbot NJ, Steinberg G. **2015a**. A gene locus for targeted ectopic gene integration in *Zymoseptoria tritici*. *Fungal Genetics and Biology* **79**: 118–124.

Kilaru S, Schuster M, Studholme D, Soanes D, Lin C, Talbot NJ, Steinberg G. **2015b**. A codon-optimized green fluorescent protein for live cell imaging in *Zymoseptoria tritici*. *Fungal Genetics and Biology* **79**: 125–131.

Kireeva ML, Walter W, Tchernajenko V, Bondarenko V, Kashlev M, Studitsky VM. **2002**. Nucleosome remodeling induced by RNA polymerase II: loss of the H2A/H2B dimer

during transcription. *Molecular Cell* **9**: 541–552.

Kohorn BD, Johansen S, Shishido A, Todorova T, Martinez R, Defeo E, Obregon P. **2009**. Pectin activation of MAP kinase and gene expression is WAK2 dependent. *The Plant Journal* **60**: 974–982.

Krishnan P, Meile L, Plissonneau C, Ma X, Hartmann FE, Croll D, McDonald BA, Sánchez-Vallet A. **2018**. Transposable element insertions shape gene regulation and melanin production in a fungal pathogen of wheat. *BMC Biology* **16**: 78.

Lanver D, Müller AN, Happel P, Schweizer G, Haas FB, Franitza M, Pellegrin C, Reissmann S, Altmüller J, Rensing SA, *et al.* 2018. The biotrophic development of Ustilago maydis studied by RNA-seq analysis. *The Plant Cell* **30**: 300–323.

Lee HG, Seo PJ. **2019**. MYB96 recruits the HDA15 protein to suppress negative regulators of ABA signaling in *Arabidopsis*. *Nature Communications* **10**: 1713.

Li B, Carey M, Workman JL. **2007**. The role of chromatin during transcription. *Cell* **128**: 707–719.

Linde CC, Zhan J, McDonald BA. **2002**. Population structure of *Mycosphaerella graminicola*: from lesions to continents. *Phytopathology* **92**: 946–955.

Lisch D, Bennetzen JL. **2011**. Transposable element origins of epigenetic gene regulation. *Current Opinion in Plant Biology* **14**: 156–161.

Meile L, Croll D, Brunner PC, Plissonneau C, Hartmann FE, McDonald BA, Sánchez-Vallet A. **2018**. A fungal avirulence factor encoded in a highly plastic genomic region triggers partial resistance to septoria tritici blotch. *New Phytologist* **219**: 1048–1061.

Mita P, Boeke JD. **2016**. How retrotransposons shape genome regulation. *Current Opinion in Genetics & Development* **37**: 90–100.

Möller M, Stukenbrock EH. **2017**. Evolution and genome architecture in fungal plant pathogens. *Nature Reviews Microbiology* **15**: 756–771.

Motteram J, Lovegrove A, Pirie E, Marsh J, Devonshire J, van de Meene A, Hammond-Kosack K, Rudd JJ. **2011**. Aberrant protein N-glycosylation impacts upon infection-related growth transitions of the haploid plant-pathogenic fungus *Mycosphaerella graminicola* . *Molecular Microbiology* **81**: 415–433.

Nødvig CS, Nielsen JB, Kogle ME, Mortensen UH. **2015**. A CRISPR-Cas9 system for genetic engineering of filamentous fungi. *PLOS ONE* **10**: e0133085.

Nützmann HW, Reyes-Dominguez Y, Scherlach K, Schroeckh V, Horn F, Gacek A, Schümann J, Hertweck C, Strauss J, Brakhage AA. **2011**. Bacteria-induced natural product formation in the fungus *Aspergillus nidulans* requires Saga/Ada-mediated histone acetylation. *Proceedings of the National Academy of Sciences of the United States of America* **108**: 14282–14287.

O'Connell RJ, Thon MR, Hacquard S, Amyotte SG, Kleemann J, Torres MF, Damm U, Buiate EA, Epstein L, Alkan N, *et al.* 2012. Lifestyle transitions in plant pathogenic *Colletotrichumy* fungi deciphered by genome and transcriptome analyses. *Nature Genetics* **44**: 1060–1065.

Palma-Guerrero J, Torriani SFF, Zala M, Carter D, Courbot M, Rudd JJ, McDonald BA,

Croll D. **2016**. Comparative transcriptomic analyses of *Zymoseptoria tritici* strains show complex lifestyle transitions and intraspecific variability in transcription profiles. *Molecular plant pathology* **17**: 845–859.

Palmer JM, Keller NP. **2010**. Secondary metabolism in fungi: does chromosomal location matter? *Current Opinion in Microbiology* **13**: 431–436.

Pfaffl MW. **2001**. A new mathematical model for relative quantification in real-time RT-PCR. *Nucleic acids research* **29**: e45.

Pfluger J, Wagner D. **2007**. Histone modifications and dynamic regulation of genome accessibility in plants. *Current Opinion in Plant Biology* **10**: 645–652.

Plissonneau C, Hartmann FE, Croll D. **2018**. Pangenome analyses of the wheat pathogen *Zymoseptoria tritici* reveal the structural basis of a highly plastic eukaryotic genome. *BMC Biology* **16**: 5.

Plissonneau C, Stürchler A, Croll D. **2016**. The evolution of orphan regions in genomes of a fungal pathogen of wheat. *mBio* **7**: e01231-16.

Lo Presti L, Lanver D, Schweizer G, Tanaka S, Liang L, Tollot M, Zuccaro A, Reissmann S, Kahmann R. **2015**. Fungal effectors and plant susceptibility. *Annual Review of Plant Biology* **66**: 513–545.

Pusztahelyi T, Holb IJ, Pócsi I. **2015**. Secondary metabolites in fungus-plant interactions. *Frontiers in Plant Science* **6**: 573.

Raffaele S, Kamoun S. **2012**. Genome evolution in filamentous plant pathogens: why bigger can be better. *Nature Reviews Microbiology* **10**: 417–430.

Rebollo R, Romanish MT, Mager DL. **2012**. Transposable elements: an abundant and natural source of regulatory sequences for host genes. *Annual Review of Genetics* **46**: 21–42.

Reyes-Dominguez Y, Bok JW, Berger H, Shwab EK, Basheer A, Gallmetzer A, Scazzocchio C, Keller N, Strauss J. **2010**. Heterochromatic marks are associated with the repression of secondary metabolism clusters in *Aspergillus nidulans*. *Molecular Microbiology* **76**: 1376–1386.

RStudio Team. **2015**. RStudio: integrated development for R. *RStudio, Inc., Boston, MA. http://www.rstudio.com*.

Rudd JJ, Kanyuka K, Hassani-Pak K, Derbyshire M, Andongabo A, Devonshire J, Lysenko A, Saqi M, Desai NM, Powers SJ, *et al.* 2015. Transcriptome and metabolite profiling of the infection cycle of Zymoseptoria tritici on wheat reveals a biphasic interaction with plant immunity involving differential pathogen chromosomal contributions and a variation on the hemibiotrophic lifestyle def. *Plant Physiology* **167**: 1158–1185.

Sánchez-Vallet A, Fouché S, Fudal I, Hartmann FE, Soyer JL, Tellier A, Croll D. **2018**. The genome biology of effector gene evolution in filamentous plant pathogens. *Annual Review of Phytopathology* **56**: 21–40.

Sánchez-Vallet A, McDonald MC, Solomon PS, McDonald BA. **2015**. Is *Zymoseptoria tritici* a hemibiotroph? *Fungal Genetics and Biology* **79**: 29–32.

Schneider CA, Rasband WS, Eliceiri KW. **2012**. NIH Image to ImageJ: 25 years of image analysis. *Nature Methods* **9**: 671–675.

Schotanus K, Soyer JL, Connolly LR, Grandaubert J, Happel P, Smith KM, Freitag M, Stukenbrock EH. **2015**. Histone modifications rather than the novel regional centromeres of *Zymoseptoria tritici* distinguish core and accessory chromosomes. *Epigenetics & Chromatin* **8**: 41.

Schuster M, Kilaru S, Guo M, Sommerauer M, Lin C, Steinberg G. **2015**. Red fluorescent proteins for imaging *Zymoseptoria tritici* during invasion of wheat. *Fungal Genetics and Biology* **79**: 132–140.

Seidl MF, Cook DE, Thomma BPHJ. **2016**. Chromatin biology impacts adaptive evolution of filamentous plant pathogens. *PLOS Pathogens* **12**: e1005920.

Seidl MF, Thomma BPHJ. **2017**. Transposable elements direct the coevolution between plants and microbes. *Trends in Genetics* **33**: 842–851.

Selker EU. **2004**. Genome defense and DNA methylation in Neurospora. *Cold Spring Harbor Symposia on Quantitative Biology* **69**: 119–24.

Souza C de A, Li S, Lin AZ, Boutrot F, Grossmann G, Zipfel C, Somerville SC. **2017**. Cellulose-derived oligomers act as damage-associated molecular patterns and trigger defense-like responses. *Plant Physiology* **173**: 2383–2398.

Soyer JL, El Ghalid M, Glaser N, Ollivier B, Linglin J, Grandaubert J, Balesdent M-H, Connolly LR, Freitag M, Rouxel T, *et al.* 2014. Epigenetic control of effector gene expression in the plant pathogenic fungus *Leptosphaeria maculans*. *PLoS Genetics* **10**: e1004227.

Soyer JL, Grandaubert J, Haueisen J, Schotanus K, Stukenbrock EH. **2019**. *In planta* chromatin immunoprecipitation in *Zymoseptoria tritici* reveals chromatin-based regulation of putative effector gene expression. *bioRxiv*: 544627.

Soyer JL, Möller M, Schotanus K, Connolly LR, Galazka JM, Freitag M, Stukenbrock EH. **2015a**. Chromatin analyses of *Zymoseptoria tritici*: methods for chromatin immunoprecipitation followed by high-throughput sequencing (ChIP-seq). *Fungal Genetics and Biology* **79**: 63–70.

Soyer JL, Rouxel T, Fudal I. **2015b**. Chromatin-based control of effector gene expression in plant-associated fungi. *Current Opinion in Plant Biology* **26**: 51–56.

Sperschneider J, Gardiner DM, Dodds PN, Tini F, Covarelli L, Singh KB, Manners JM, Taylor JM. **2016**. EffectorP: predicting fungal effector proteins from secretomes using machine learning. *New Phytologist* **210**: 743–761.

van Steensel B. **2011**. Chromatin: constructing the big picture. *The EMBO Journal* **30**: 1885–1895.

van Steensel B, Furlong EEM. **2019**. The role of transcription in shaping the spatial organization of the genome. *Nature Reviews Molecular Cell Biology* **20**: 327–337.

Steinberg G. **2015**. Cell biology of *Zymoseptoria tritici*: Pathogen cell organization and wheat infection. *Fungal Genetics and Biology* **79**: 17–23.

Stewart E l., Croll D, Lendenmann MH, Sanchez-Vallet A, Hartmann FE, Palma-

Guerrero J, Ma X, McDonald BA. **2018**. Quantitative trait locus mapping reveals complex genetic architecture of quantitative virulence in the wheat pathogen *Zymoseptoria tritici*. *Molecular Plant Pathology* **19**: 201–216.

Strahl BD, Allis CD. **2000**. The language of covalent histone modifications. *Nature* **403**: 41–45.

Studt L, Janevska S, Arndt B, Boedi S, Sulyok M, Humpf H-U, Tudzynski B, Strauss J. **2017**. Lack of the COMPASS component Ccl1 reduces H3K4 trimethylation levels and affects transcription of secondary metabolite genes in two plant–pathogenic *Fusarium* species. *Frontiers in Microbiology* **07**: 2144.

Torriani SFF, Melichar JPE, Mills C, Pain N, Sierotzki H, Courbot M. **2015**. *Zymoseptoria tritici*: A major threat to wheat production, integrated approaches to control. *Fungal Genetics and Biology* **79**: 8–12.

Vogel, J. H. **1956**. A convenient growth medium for *Neurospora* (medium N). *Microb. Genet. Bull.* **13**: 42–43.

Wang X, Jiang N, Liu J, Liu W, Wang G-L. **2014**. The role of effectors and host immunity in plant–necrotrophic fungal interactions. *Virulence* **5**: 722–732.

Wang S-S, Zhou BO, Zhou J-Q. **2011**. Histone H3 lysine 4 hypermethylation prevents aberrant nucleosome remodeling at the *PHO5* promoter. *Molecular and cellular biology* **31**: 3171–81.

Weiste C, Dröge-Laser W. **2014**. The *Arabidopsis* transcription factor bZIP11 activates auxin-mediated transcription by recruiting the histone acetylation machinery. *Nature Communications* **5**: 3883.

Wolpert TJ, Dunkle LD, Ciuffetti LM. **2002**. Host-selective toxins and avirulence determinants: what's in a name? *Annual Review of Phytopathology* **40**: 251–285.

Zhao Y, Garcia BA. **2015**. Comprehensive catalog of currently documented histone modifications. *Cold Spring Harbor Perspectives in Biology* **7**: a025064.

Zhong Z, Marcel TC, Hartmann FE, Ma X, Plissonneau C, Zala M, Ducasse A, Confais J, Compain J, Lapalu N, *et al.* 2017. A small secreted protein in *Zymoseptoria tritici* is responsible for avirulence on wheat cultivars carrying the *Stb6* resistance gene. *New Phytologist* **214**: 619–631.

Zwiers L-H, De Waard MA. **2001**. Efficient *Agrobacterium tumefaciens*-mediated gene disruption in the phytopathogen *Mycosphaerella graminicola*. *Current Genetics* **39**: 388–393.

3.8. Supporting information

Figure S1. The genomic context of selected *Zymoseptoria tritici* effector genes.

Figure S2. The genomic environment of selected *Zymoseptoria tritici* effector genes is repressive for expression.

Figure S3. Repression of the Avr3D1 locus is chromatin-based.

Figure S4. Effector genes are enriched in histone H3 lysine 27 and lysine 9 trimethylation.

Figure S5. Phenotype of infected leaf samples used for in planta chromatin immunoprecipitation.

Table S1. Plasmid constructs used in this study.

Table S2. Primers used in this study.

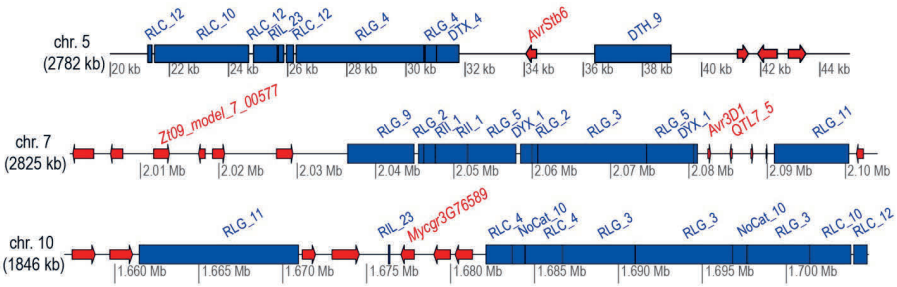

Figure S1. The genomic context of selected *Zymoseptoria tritici* effector genes.

The effector genes *AvrStb6*, *Avr3D1*, *QTL7_5* and *Mycgr3G76589* reside in transposable element (TE)-rich regions of the genome of strain 3D7. Red arrows represent genes from their start to their stop codons and blue blocks represent TEs. Gene and TE annotations are based on Plissonneau et al., 2016. TEs were classified according to Wicker *et al*. (2007): the first letter indicates the class (R, RNA class; D, DNA class); the second letter indicates the order (L, LTR; I, Line; T, TIR; Y, Crypton); and the third letter indicates the superfamily (C, Copia; G, Gypsy; L, L1; I, I; H, PIF-Harbinger; M, Mutator; X, unknown; NoCat, no category). chr.: chromosome.

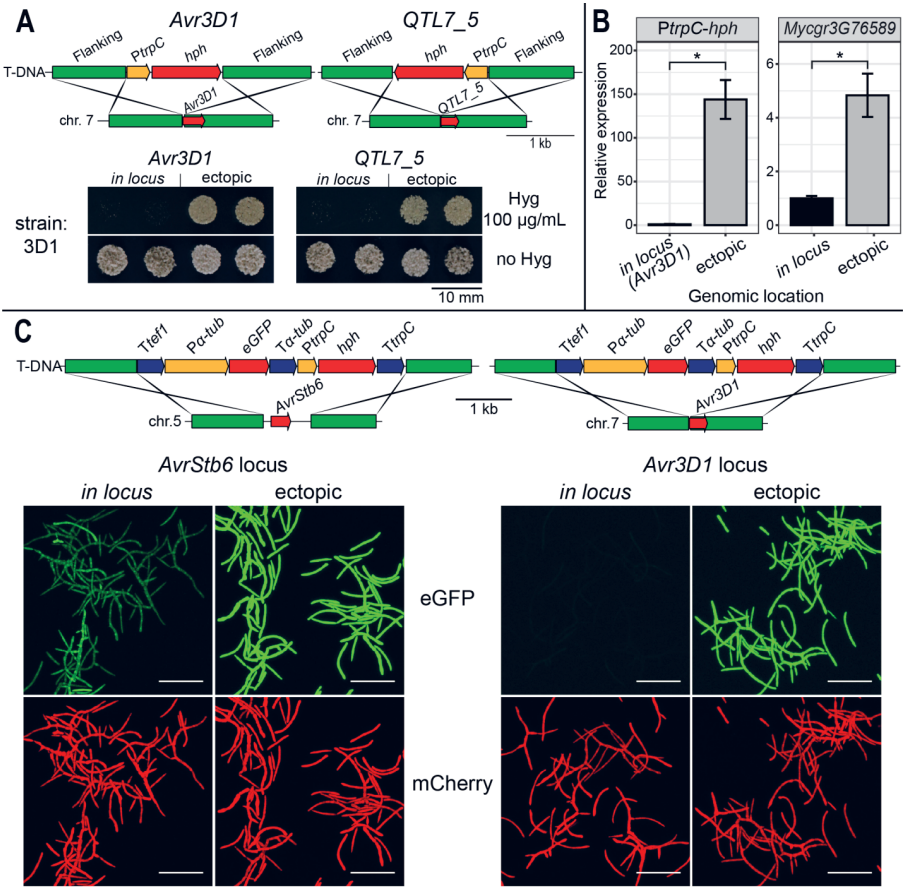

Figure S2. The genomic environment of selected *Zymoseptoria tritici* effector genes is repressive for expression.

(A) Top: Construct design for insertion of the *Hph* gene encoding the hygromycin B phosphotransferase used as a reporter for the epigenetic state in the loci *Avr3D1* (left) and *QTL7_5* (right). Bottom: Hygromycin B sensitivity assay with mutants in the background of strain 3D1 carrying the hygromycin B resistance gene *Hph* either in one of the loci *Avr3D1* or *QTL7_5* (*in locus*) or in random positions of the genome (ectopic). Two independent transformant lines are shown. **(B)** Left panel: Relative expression of the *Hph* gene inserted ectopically compared to the same gene inserted at locus *Avr3D1* (*in locus*) in strain 3D1 under axenic conditions (YSB medium). The

number of replicates was: n_{in_locus} =4, $n_{ectopic}$=2. *18S* was used as a reference and relative expression was calculated without efficiency correction. Right panel: Relative expression of the effector gene *Mycgr3G76589* inserted ectopically compared to the endogenous gene (*in locus*) in strain 3D7 under axenic conditions (YPD liquid medium). n_{in_locus} =3, $n_{ectopic}$=6. Bars represent the means and error bars represent the standard error of the mean. Asterisks represent statistical differences ($p<0.05$, Student's t-test). **(C)** Top: Construct design for insertion of the *eGFP* reporter cassette in the loci *AvrStb6* (left) and *Avr3D1* (right) to assess the influence of the genomic context on gene expression. Bottom: eGFP fluorescence in transformants harboring the *eGFP* cassette either in the locus *AvrStb6* or *Avr3D1* (*in locus*) or in a random position of the genome (ectopic). The transformants were obtained in a 3D7-derived strain carrying the *mCherry* reporter gene at a euchromatic region under the control of the same promoter as the *eGFP* reporter gene (*α-tubulin* promoter). T*tef1* = *Aspergillus nidulans tef1* terminator; T*α-tub* = *Z. tritici α-tubulin* terminator; T*trpC* = *A. nidulans trpC* terminator; P*trpC* = *A. nidulans trpC* promoter; *Hph*= hygromycin phosphostransferase gene. White scale bar: 50 µm.

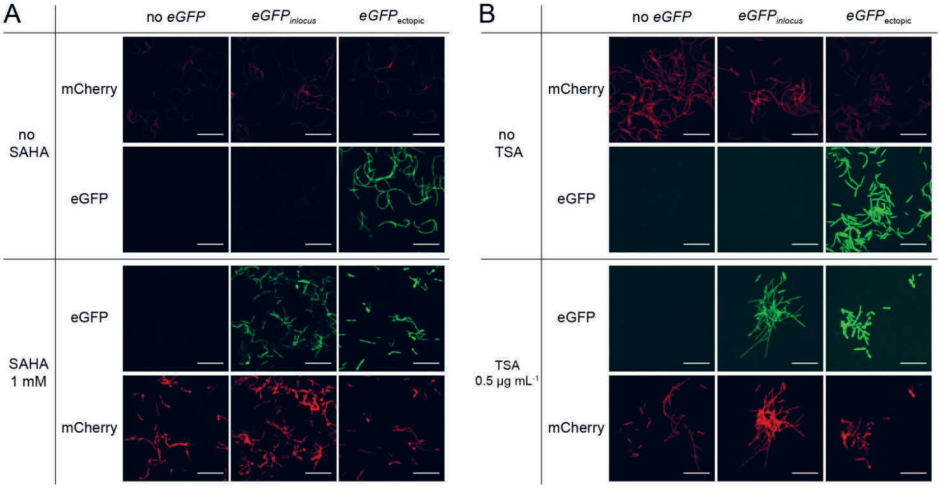

Figure S3. Repression of the *Avr3D1* locus is chromatin-based.

Histone deacetylase inhibition assay with *Zymoseptoria tritici* transformants harbouring the *eGFP* reporter gene under the constitutive *α-tubulin* promoter either in the locus *Avr3D1 (eGFP*$_{\text{inlocus}}$*)* or in an ectopic location (eGFP$_{\text{ectopic}}$). Transformants were grown axenically and treated with the histone deacetylase inhibitors suberoylanilide hydroxamic acid (SAHA) or trichostatin A (TSA). All transformants contain the *mCherry* gene under the control of the *α-tubulin* promoter, allowing visualization of living cells regardless of their eGFP levels. A transformant line harboring only *mCherry* but no *eGFP* is also shown (no *eGFP*). SAHA-treated cells were grown in liquid minimal medium and observed after 11 days. TSA-treated cells were grown in liquid YSB medium and observed after four days. Scale bars represent 50 µm.

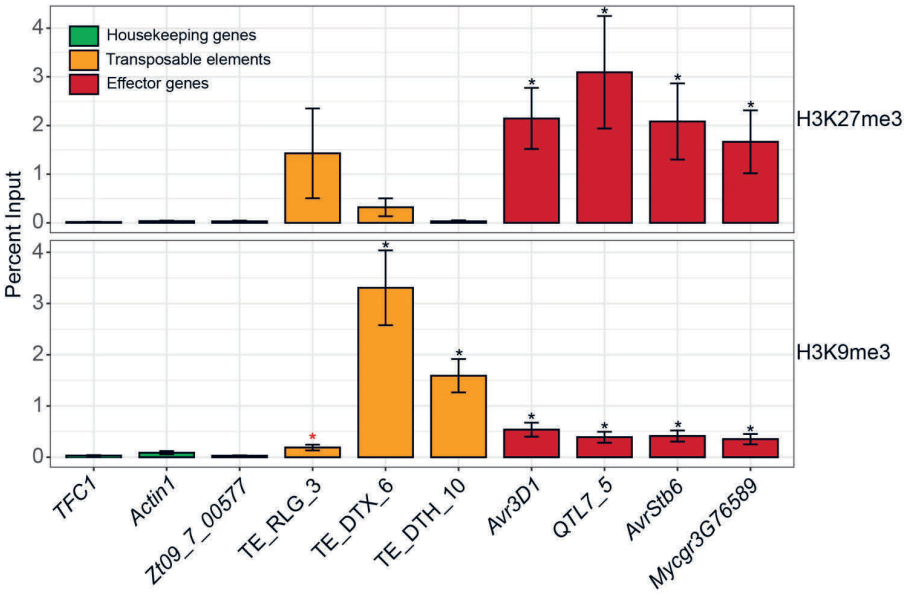

Figure S4. Effector genes are enriched in histone H3 lysine 27 and lysine 9 trimethylation.

Enrichment of histone lysine 27 and lysine 9 trimethylation levels (upper and lower panel, respectively) as measured by the percent input method. Shown are the enrichments for the two housekeeping genes *TFC1* and *Actin1* (green bars), the cell wall protein-encoding gene *Zt09_7_00577* residing upstream of the *Avr3D1* effector cluster, three transposable elements (orange bars) and the four effector genes *Avr3D1*, *QTL7_5*, *AvrStb6* and *Mycgr3G76589* (red bars). The transposable elements were classified according to Wicker *et al*. (2007): the first letter indicates the class (R, RNA class; D, DNA class); the second letter indicates the order (L, LTR; T, TIR) and the third letter indicates the superfamily (G, Gypsy; H, PIF-Harbinger; X, unknown). Black asterisks indicate significantly higher enrichments compared to *TFC1* and *Actin1*; the red asterisk indicates a significantly higher enrichment compared to *TFC1* only.

Figure S5. Phenotype of infected leaf samples used for *in planta* chromatin immunoprecipitation.

Shown are approximately one third of the leaves used for chromatin preparations on the day when the first necrotic symptoms appeared. Repl. = independent biological replicate consisting of 45-60 2nd leaves.

Table S1. Plasmid constructs used in this study (next page).

P*trpC* = *Aspergillus nidulans TrpC* promoter; *Hph* = hygromycin phosphotransferase gene; T*trpC* = *A. nidulans TrpC* terminator; P*α-tub* = *Zymoseptoria tritici α-tubulin* promoter; P*α-tub* = *Z. tritici α-tubulin* terminator; P*gpd1* = *Cochliobolus heterostrophus Gpd1* promoter, *Gen* = geneticin resistance gene, T*β-tub* = *Neurospora crassa β-tubulin* terminator.

Plasmid	Description	Backbone	Linearization	Inserts	Description insert	Primer pair	Template	Application	Resulting mutants
pLM1	pES1-*Ttef-PtrpC-Hph-Ttrpc*	pES1	KpnI, SbfI	A	*PtrpC-Hph*	LMP_25/26	pES6	Template for further cloning	-
				B	*Ttef*	LMP_148/149	pFC332		
				C	*TtrpC*	LMP_150/151	pES1		
pLM2	pES1-*Ttef-Pα-tub-eGFP-Tα-tub-PtrpC-Hph-Ttrpc*	pLM1	SnaBI	A	*Pα-tub-eGFP-Tα-tub*	LMP_152/153	pCZtGFP	Template for further cloning	-
pLM2-Flanking$_{DOWN_AvrStb6}$	pES1-*Ttef-Pα-tub-eGFP-Tα-tub-PtrpC-Hph-Ttrpc*-Flanking$_{DOWN}$	pLM2	SbfI	A	Flanking$_{DOWN}$	LMP_183/185	3D7 gDNA	Template for further cloning	-
pLM2-Δ*AvrStb6*	pES1- Flanking$_{UP}$- *Ttef-Pα-tub-eGFP-Tα-tub-PtrpC-Hph-Ttrpc*- Flanking$_{DOWN}$	pLM2-Flanking$_{DOWN_AvrStb6}$	EcoRV	A	Flanking$_{UP}$	LMP_181/182	3D7 gDNA	Insertion of hygromycin resistance cassette and *eGFP* cassette in locus *AvrStb6* or ectopically	3D7-GFP-HygR$_{in\text{-}locus_AvrStb6}$, 3D7-GFP-HygR $_{ect\_AvrStb6}$
pES1-Δ*Avr3D1*$_{3D7}$	pES1-Flanking$_{UP}$-*PtrpC-Hph*-Flanking$_{DOWN}$	pES1	KpnI, PstI	A	*PtrpC-Hph*	LMP_25/26	pES6	Insertion of hygromycin resistance cassette in locus *Avr3D1* or ectopically	3D7-HygR$_{in\text{-}locus_Avr3D1}$, 3D7-HygR$_{ect_Avr3D1}$
				B	Flanking$_{UP}$	LMP_36/37	3D7 gDNA		
				C	Flanking$_{DOWN}$	LMP_38/39	3D7 gDNA		
pES1-Δ*QTL7_5*$_{3D7}$	pES1-Flanking$_{UP}$-*PtrpC-Hph*-Flanking$_{DOWN}$	pES1	KpnI, PstI	A	*PtrpC-Hph*	LMP_25/26	pES6	Insertion of hygromycin resistance cassette in locus *QTL7_5* or ectopically	3D7-HygR$_{in\text{-}locus_QTL7_5}$, 3D7-HygR$_{ect_QTL7_5}$
				B	Flanking$_{UP}$	LMP_40/41	gDNA		
				C	Flanking$_{DOWN}$	LMP_42/43	gDNA		
pES1-Δ*00577*$_{3D7}$	pES1-Flanking$_{UP}$-*PtrpC-Hph*-Flanking$_{DOWN}$	pES1	KpnI, PstI	A	*PtrpC-Hph*	LMP_25/26	pES6	Insertion of hygromycin resistance cassette in locus Zt09_7_*00577* or ectopically	3D7-HygR$_{in\text{-}locus_00577}$, 3D7-HygR$_{ect_00577}$
				B	Flanking$_{UP}$	LMP_21/22	gDNA		
				C	Flanking$_{DOWN}$	LMP_23/24	gDNA		
pES1-Δ*Avr3D1*$_{3D1}$	pES1-Flanking$_{UP}$-*PtrpC-Hph*-Flanking$_{DOWN}$	pES1	KpnI, PstI	A	*PtrpC-Hph*	LMP_25/26	pES6	Insertion of hygromycin resistance cassette in locus *Avr3D1* or ectopically	3D1-HygR$_{in\text{-}locus_Avr3D1}$, 3D1-HygR$_{ect_Avr3D1}$
				B	Flanking$_{UP}$	LMP_36/37	3D1 gDNA		
				C	Flanking$_{DOWN}$	LMP_38/39	3D1 gDNA		
pES1-Δ*QTL7_5*$_{3D1}$	pES1-Flanking$_{UP}$-*PtrpC-Hph*-Flanking$_{DOWN}$	pES1	KpnI, PstI	A	*PtrpC-Hph*	LMP_25/26	pES6	Insertion of hygromycin resistance cassette in locus *QTL7_5* or ectopically	3D1-HygR$_{in\text{-}locus_QTL7_5}$, 3D1-HygR$_{ect_QTL7_5}$
				B	Flanking$_{UP}$	LMP_40/41	3D1 gDNA		
				C	Flanking$_{DOWN}$	LMP_42/43	3D1 gDNA		
pLM2-Δ*Avr3D1*$_{3D7}$	pES1-Flanking$_{UP}$-*Ttef-Pα-tub-eGFP-Tα-tub-PtrpC-Hph-Ttrpc*-Flanking$_{DOWN}$	pES1	KpnI, SbfI	A	*Pα-tub-eGFP-Tα-tub-PtrpC-Hph-Ttrpc*	LMP_154/155	pLM2	Insertion of *eGFP* cassette in locus *Avr3D1* or ectopically	3D7-eGFP$_{in\text{-}locus_Avr3D1}$, 3D7-eGFP$_{ect_Avr3D1}$
				B	Flanking$_{UP}$	LMP_36/156	3D7 gDNA		
				C	Flanking$_{DOWN}$	LMP_157/39	3D7 gDNA		
pCGEN-*76589*$_{3D7\_ect}$	pCGEN-*Mycgr3G76589*	pCGEN	KpnI	A	*Mycgr3G76589*$_{3D7}$	LMP_319/320	3D7 gDNA	Insertion of an ectopic copy of *Mycgr3G76589*	3D7-76589$_{ect}$
pLM2-*Pavr3D1-mTurq2*	pES1-Flanking$_{UP}$-*Pavr3D1-mTurquoise2-Ttef-Pα-tub-eGFP-Tα-tub-PtrpC-Hph-Ttrpc*-Flanking$_{DOWN}$	pLM2	EcoRI	A	*Pavr3D1*$_{3D7}$	LMP_188/189	pLM2-Δ*Avr3D1*$_{3D7}$	Insertion of *mTurq2* under the control of the native *Avr3D1* promoter and the *eGFP* cassette in locus *Avr3D1* or ectopically	3D7-P$_{nat}$mTurq-eGFP$_{inlocus_Avr3D1}$, 3D7-P$_{nat}$mTurq-eGFP$_{ect_Avr3D1}$
				B	*mTurquoise2*	LMP_190/191	*mZtTurq2* dsDNA		
				C	*Ttef-Pα-tub*$_{partial}$	LMP_192/193	pLM2-Δ*Avr3D1*$_{3D7}$		
pCGEN-mTurq2$_{ect}$	pCGEN-*Pα-tub-mTurquoise2-Tα-tub*	pCGEN	KpnI	A	*Pα-tub*	LMP_140/ oJA_002	pCZGFP	Generation of a 3D7-derived strain labelled with cytosolic mTurquoise2	3D7-mTurq$_{ect}$
				B	*mTurquoise2*	oJA_001/003	*mZtTurq2* dsDNA		
				C	*Tα-tub*	LMP_141/ oJA_004	pCZtGFP		
pLM2-*PavrStb6-His1-mCherry*	pES1-Flanking$_{UP}$-*PavrStb6-His1-mCherry-Ttef-Pα-tub-eGFP-Tα-tub-PtrpC-Hph-Ttrpc*-Flanking$_{DOWN}$	pLM2-Δ*AvrStb6*	EcoRI	A	*PavrStb6*	LMP_226/227	3D7 gDNA	Insertion of *His1-mCherry* under the control of the native *AvrStb6* promoter and the *eGFP* cassette in locus *AvrStb6* or ectopically	3D7-P$_{nat}$mChe-GFP$_{in\text{-}locus_Avr3D1}$, 3D7-P$_{nat}$mChe-GFP$_{ect_Avr3D1}$
				B	*His1*	LMP_228/229	3D7 gDNA		
				C	*mCherry*	LMP_230/231	pCmCherry		
				D	*Ttef-Pα-tub*$_{partial}$	LMP_232/233	pLM2-Δ*AvrStb6*		
pES1Δ*kmt6*	pES1-Flanking$_{UP}$-*PtrpC-Hph*-Flanking$_{DOWN}$	pES1	KpnI, PstI	A	*Pgpd1-Gen-Tβ-tub*	LMP_128/107	pCGEN	Generation of *Kmt6* knockout mutant	3D7-GFP$_{in\text{-}locus_Avr3D1\Delta kmt6}$
				B	Flanking$_{UP}$	LMP_108/109	3D7 gDNA		
				C	Flanking$_{DOWN}$	LMP_110/111	3D7 gDNA		

Table S2. Primers used in this study.

Primer name	Sequence (5'-3')	Application	Target
LMP_25	CGGCTTTGATATTGAAGGAGC	cloning	
LMP_26	GATGGCTAGCAGATCTCTATTCC	cloning	
LMP_148	TAATTAAGATATCGAGCTCGAGGCGGACATT CGATTTATGC	cloning	
LMP_149	CTCCTTCAATATCAAAGCCGTACGTATTGGG ATGAATTTTGTATGC	cloning	
LMP_150	ATAGAGATCTGCTAGCCATCGTTCATTTGTC CAAGCAGCA	cloning	
LMP_151	CAGTGCCAAGCTTGCATGCCTGCAGGCCTT CTGGGTAAACGACTCATAGG	cloning	
LMP_183	AGTCGTTTACCCAGAAGGCCGTCATCAACTT CCTCTCAACCATTCACACTCTTCTCTGGACT CCT	cloning	
LMP_185	CAGTGCCAAGCTTGCATGCCTAGTCGTTGA ACTCGCCACTC	cloning	
LMP_181	TACGAATTCTTAATTAAGATGTCCGCTACCC TTATAATAACGA	cloning	
LMP_182	GGCATAAATCGAATGTCCGTGGAAAGAAGT GTGGAAGATGTG	cloning	
LMP_36	TAATTAAGATATCGAGCTCGGACTTCTTCCG ACGACTTCC	cloning	
LMP_37	CTCCTTCAATATCAAAGCCGCATTGTGTCGA GGCTGGTG	cloning	
LMP_38	ATAGAGATCTGCTAGCCATCCTCCTCTTCGC CTTCTTCGG	cloning	
LMP_39	CAGTGCCAAGCTTGCATGCCAATAATCCCAT CCTACCTCGCC	cloning	
LMP_40	CAGTGCCAAGCTTGCATGCCACTGCCAGAT GTGTTCCTCAG	cloning	
LMP_41	ATAGAGATCTGCTAGCCATCCATTGTTGTGG ATGGGTTGC	cloning	
LMP_42	CTCCTTCAATATCAAAGCCGGTTTCGCCATC TTCGCTGC	cloning	
LMP_43	TAATTAAGATATCGAGCTCGGGCTTTCGTTC AGTCAACTCG	cloning	
LMP_21	AAGATATCGAGCTCGGTACCACAACTCCAC TCGCATTGAG	cloning	
LMP_22	TCAATATCAAAGCCGACTTGTACCTCTTCGT CCTCG	cloning	

LMP_23	GATCTGCTAGCCATCATGTATATCCCGTCCC TGCTG	cloning	
LMP_24	CCAAGCTTGCATGCCTGCATTAACCGCCTC ATTCGTCAG	cloning	
LMP_154	GCGGACATTCGATTTATGC	cloning	
LMP_155	TTCTGGGTAAACGACTCATAGG	cloning	
LMP_156	GGCATAAATCGAATGTCCGCATTGTGTCGA GGCTGGTG	cloning	
LMP_157	TATGAGTCGTTTACCCAGAACTCCTCTTCGC CTTCTTCGG	cloning	
LMP_319	GCGCGCCGAATTCGAGCTCGGAACAACAAG GATGAACGC	cloning	
LMP_320	CCAACATGGTGGAGTGAGGGTGAATGCCAT TGTCCGTG	cloning	
LMP_188	CTATGACATGATTACGAATTCGACTTCTTCC GACGACTTCC	cloning	
LMP_189	AGCTCCTCGCCCTTGGAGACCATTGTGTCG AGGCTGGTG	cloning	
LMP_190	GTCTCCAAGGGCGAGGAGC	cloning	
LMP_191	TTACTTGTAGAGCTCGTCCATGC	cloning	
LMP_140	GCCGAATTCGAGCTCGCGCCAGATGATGGC TGAGAG	cloning	
LMP_141	ACATGGTGGAGTGAGGGTACGACCGAGCT GAAGAGG	cloning	
oJA002	CCTCGCCCTTGGAGACCATGGCGATGGTGG TATGCGGATG	cloning	
oJA001	ATGGTCTCCAAGGGCGAGG	cloning	
oJA003	TTACTTGTAGAGCTCGTCC	cloning	
oJA004	GGACGAGCTCTACAAGTAAGCGACGACGGA CGAGGACAGG	cloning	
LMP_226	CTATGACATGATTACGAATTCGTCCGCTACC CTTATAATAACGAG	cloning	
LMP_227	GTGACTTTCTTGGGAGGCATCTTCGTTGAAT TCGAAAGGCA	cloning	
LMP_228	ATGCCTCCCAAGAAAGTCA	cloning	
LMP_229	TGCCTTCTTGGGAGTGG	cloning	
LMP_230	CCGCCACTCCCAAGAAGGCAATGGTGAGCA AGGGCGAG	cloning	
LMP_231	CGGCATAAATCGAATGTCCGTTACTTGTACA GCTCGTCCATGC	cloning	
LMP_232	CGGACATTCGATTTATGCCGTTA	cloning	
LMP_233	TGATAGCAACCCACCGAATTCTG	cloning	

LMP_128	CCCGCTTGACGACATTCC	cloning	
LMP_107	CGACGCCAGCAGTAGACAC	cloning	
LMP_108	TAATTAAGATATCGAGCTCGCCTCTTCATCT ATGCCTCCT	cloning	
LMP_109	TCGGAATGTCGTCAAGCGGGAACTGCCGTG CTACTTTCTG	cloning	
LMP_110	AGTGTCTACTGCTGGCGTCGAGTAGGTAGA TGTCTCTTTCGT	cloning	
LMP_111	CAGTGCCAAGCTTGCATGCCTACCACTCAA AGCCGTCCTC	cloning	
LMP_220	AGGGCATCGACTTCAAGGAG	RT-qPCR	*eGFP*
LMP_221	GTGTTCTGCTGGTAGTGGTC	RT-qPCR	
LMP_292	GTTCCGCTTCCAGTGGTTC	RT-qPCR	*Mycgr3G76589*
LMP_293	ATCCACTCCTGCTCACCAAG	RT-qPCR	
FL_act1_F	TGCCAATCTACGAGGGTTTC	RT-qPCR	*Actin1*
FL_act1_R	GGATCTCCTGCTCAAAGTCG	RT-qPCR	
FL2_18344	CCAGCAAATCCTTCGATCTC	RT-qPCR	*18S*
FL2_18344	CCACTTTGACATTTCCACACC	RT-qPCR	
LMP_254	AAGGCGGGTCCTAGTTGCT	RT-qPCR	*AvrStb6*
LMP_255	AAGCTGCTGTGATGGAGAGC	RT-qPCR	
ASVP_9	CGTCTGCTGCTCCATACAAG	RT-qPCR	*Hph*
ASVP_10	CTCGATGAGCTGATGCTTTG	RT-qPCR	
LMP_160	AGAGGGGTCCGTTCATCTCA	ChIP-qPCR	*TFIIIC*
LMP_161	GTCGAAGCAGTAGAGGCGTT	ChIP-qPCR	
FL_act1_F	TGCCAATCTACGAGGGTTTC	ChIP-qPCR	*Actin1*
LMP_308	GAGGTAGTCGGTCAAATCACG	ChIP-qPCR	
LMP_166	CGAGGACGAAGAGGTACAAGTAT	ChIP-qPCR	*Zt09_7_00577*
LMP_167	AGTGGTTGTAGAAAACGAGTGAATG	ChIP-qPCR	
LMP_306	TAAAGGCATTGTCTCCGACAG	ChIP-qPCR	TE_RLG_
LMP_307	GGTCACATGCGATTCCCAAC	ChIP-qPCR	element3
LMP_300	ATTAGTGTCTCTGTCGCCGTC	ChIP-qPCR	TE_DTX_
LMP_301	TCGCAATCTCCCTTATTATCTCC	ChIP-qPCR	element6
LMP_296	GTTAATATCCTCCGTAGCCGAAT	ChIP-qPCR	TE_DTH_
LMP_297	CACTACTACCGCTATAACTACCCT	ChIP-qPCR	element10
LMP_170	AGCATTCGACGACTGTTGGT	ChIP-qPCR	*Avr3D1*
LMP_171	GGTGGCTAGCTTGGAACTGT	ChIP-qPCR	
LMP_309	AATGGATTCGGCGACAGGT	ChIP-qPCR	*AvrStb6*
LMP_310	TTAGGTCATCAACTTCCTCTCAAC	ChIP-qPCR	

LMP_174	AATTGAGCCGAGGACCAAGG	ChIP-qPCR	*QTL7_5*
LMP_175	CGATGTGGGAGGCAGATGAA	ChIP-qPCR	
LMP_286	GTCTGGAGTAGATTAGCCTCGC	ChIP-qPCR	*Mycgr3G76589*
LMP_287	CACCAACGAAAGTCACGAAAC	ChIP-qPCR	

General discussion and outlook

Overview

Effectors produced by plant-colonizing microbes are widely recognized as key components of the interaction with the host due to their various functions in promoting colonization but also due to their role as elicitors of host defences and, consequently, as crucial determinants of host specificity (Bent & Mackey, 2007). However, in many plant-pathosystems, including important crop diseases, the role of effectors in host specificity and virulence is understudied. In this thesis, I used the most important fungal wheat pathogen in Europe, *Zymoseptoria tritici*, to study how effectors and effector diversity contribute to host specificity and how they are employed by the pathogen.

In chapter 1, I discovered and characterized a fungal effector, Avr3D1, which triggers partial resistance in certain wheat lines upon recognition. Quantitative virulence differences between a highly virulent strain and less virulent strain could be largely explained by sequence polymorphism in this avirulence factor. I further investigated its sequence diversity and found 30 different isoforms in 132 *Z. tritici* strains as well as signs of diversifying selection. This chapter highlights that quantitative phenotypic differences in virulence can be controlled by avirulence factor polymorphisms in *Z. tritici*.

In chapter 2, I further investigated the diversity of the avirulence factor discovered in chapter 1 by functionally characterizing the avirulence activity of different naturally occurring protein isoforms. I showed that at least three different mutation events led to the complete escape from recognition by the wheat host and I identified several

amino acid residues in Avr3D1 that additively contribute to host evasion, extending our knowledge on how avirulence factor diversity can shape different shades of partial resistance. In addition, by including a homologue of *Avr3D1* from a sister species of *Z. tritici* in the functional analysis, I provide first evidence for a possible role of avirulence factors in nonhost resistance against wild relatives of *Z. tritici*.

In chapter 3, I investigated the role of the genomic environment on the regulation of *Avr3D1* and other effector genes. This work demonstrated that the location of effector genes in heterochromatic regions of *Z. tritici* has functional consequences on their expression regulation. Effector genes were epigenetically silenced under axenic conditions but rapidly de-repressed during wheat infection. Several histone modifications were identified as key regulatory components and some of these modifications exhibited a highly dynamic behaviour during host colonization. Fluorescent reporter genes allowed the monitoring of de-repression during host infection at the single-cell level, identifying stomata as hot spots for effector de-repression. This study provides novel insights on how the genome compartmentalization of pathogenic fungi might functionally contribute to effector deployment.

Why are *Avr* genes maintained in pathogen populations?

The first cloned fungal effector genes were identified because of their avirulence activity (de Wit, 1992, 2016). Only years later it was realized that some of these avirulence factors also have intrinsic functions in promoting infection in susceptible hosts, explaining why they might be maintained in pathogen populations (de Wit, 2016). However, for many of the cloned avirulence genes, including *Avr3D1* and *AvrStb6*, as well as for many predicted effectors without a known avirulence activity,

an intrinsic function is still unknown (chapter 1, Skamnioti & Ridout, 2005). Although it is intriguing that pathogen populations maintain apparently dispensable effectors which can be highly detrimental on a subset of hosts when recognized by the immune system (chapters 1 & 2), several factors that could explain this discrepancy have to be taken into account and will be discussed in the following paragraphs.

First, the selection pressure that is exerted on an avirulence gene also depends on how frequently the corresponding resistance gene is used (Bent & Mackey, 2007). Low resistance gene frequency, especially combined with high gene flow on the pathogen side, might explain why avirulence factors are maintained in pathogen populations.

Second, even highly avirulent pathogen strains may still be able to sexually reproduce, as recently demonstrated for avirulent *Z. tritici* strains carrying a highly avirulent allele of *AvrStb6* (Kema *et al.*, 2018). This might reduce the selection pressure on avirulence genes in the field, especially if their encoded avirulence factors only trigger partial resistance, such as observed for Avr3D1 (chapters 1 and 2), allowing also a certain level of asexual reproduction.

Third, apparently dispensable avirulence factors might in reality be conditionally and/or partially dispensable for host colonization and their function might not be adequately assessed in many cases. For example, not only the avirulence activity but also the virulence function of effectors can be strain- and host-specific (Rep *et al.*, 2005; Friesen *et al.*, 2008; Kombrink *et al.*, 2017). A striking example is the effector Six1 in *Fusarium oxysporum* f. sp. *Lycopersici*, which has a role in virulence only in certain strain-host combinations (Rep *et al.*, 2005). In addition, the plant growth stage can influence virulence (Kema & van Silfhout, 1997) and, consequently, might also

be critical for effector validation. Nevertheless, infection assays are usually conducted at the seedling stage for simplicity, which could hinder the discovery and characterization of effectors that mainly promote virulence in adult plants. Furthermore, it has been suggested that non-ideal infection conditions can facilitate the characterization of effector functions (Rep *et al.*, 2004, 2005) and, thus, can help dealing with the dubious dispensability of avirulence factors.

Despite the apparent dispensability of *Avr3D1* and *AvrStb6*, these two genes are likely to have a function, which remains to be identified. Several possible new roles of effector genes are discussed below and could also apply to *Avr3D1* and *AvrStb6*.

Future opportunities for effector discovery and characterization

Effectors of plant pathogens represent fascinating innovations of evolution. The identification of their functions and plant targets not only has the potential to reveal new principles of molecular plant pathology but can also shed light into basic processes of plant biology, such as hormone signalling, vesicle trafficking and development (Bray Speth *et al.*, 2007; Toruño *et al.*, 2016). The understanding of effector functions has even yielded tools for biotechnology, such as the transcription activator-like effector nucleases (TALENs), which allow site-directed mutagenesis of plants based on the sequence-specific DNA binding capacities of bacterial TAL effectors (Perez-Quintero & Szurek, 2019). Despite the recent advances in the –omics approaches, the identification and the functional characterization of candidate effectors remains a challenging task. The new concepts, discoveries and technologies discussed below might help overcoming these challenges.

Many candidate effectors lack sequence homology to known genes, which not only complicates their functional characterization but also their proper annotation in the first place because many gene prediction tools also benefit from sequence homology detection (Haas *et al.*, 2011). In this context, it is noteworthy that *Avr3D1* would not even have been classified as a candidate effector without its manual reannotation (chapter 1). In all previously published genome annotations (Goodwin *et al.*, 2011; Grandaubert *et al.*, 2015; Plissonneau *et al.*, 2016, 2018), a different ATG codon on a different reading frame was considered to be the start codon and the corresponding protein did not contain a predicted signal peptide as a consequence. A possible explanation for this incorrect prediction could be that in our manually corrected gene model, the stop codon is located on the second last exon (57 bp upstream of the last intron; chapter 1), while in all automatic annotation models, it is located on the last exon (Goodwin *et al.*, 2011; Grandaubert *et al.*, 2015; Plissonneau *et al.*, 2016, 2018). The location of a stop codon more than 55 bp upstream of an intron is generally thought to induce nonsense-mediated mRNA decay (NMD), which is a control mechanism that prevents the translation of aberrant mRNA with premature stop codons (Zhang & Sachs, 2015). Therefore, the correct gene model might have been rejected because it was considered a pseudogene. Interestingly, also the stop codon of *AvrStb6* is located on the second last exon (Kema *et al.*, 2018) and this gene was not predicted in some published genome annotations (Goodwin *et al.*, 2011; Grandaubert *et al.*, 2015) or annotated in a way that the stop codon would be located on the last exon as a consequence of incorrectly predicting the intron sequences (Plissonneau *et al.*, 2016). These incorrect predictions may indicate that the parameters for the identification of premature stop codons could generally be too strict, at least for *Z. tritici*, hampering the identification of important effector genes. In line with this, new perspectives on introns in 3'-UTRs suggest that misconceptions

around these introns are responsible for common but spurious classifications of functional genes as pseudogenes (Bicknell *et al.*, 2012).

Once identified as candidate effector genes, their functional characterization also comes with several challenges. Pathogen genomes can harbour several hundred putative effector genes and redundancy between some of them has been suggested (Mirzadi Gohari *et al.*, 2015), possibly as a way to compensate effector loss, e.g. driven by a host resistance protein (Birch *et al.*, 2008; Sánchez-Vallet *et al.*, 2018). To cope with redundancy in functional studies, multi-gene mutants could be obtained, which would be a promising approach to study the roles of *Avr3D1* and *AvrStb6*, since both of these genes have at least one homologue present in the *Z. tritici* genome, possibly with a similar function. However, obtaining multi-gene knockouts has its limitations due to the limited amount of available selection markers. New technologies like CRISPR-Cas9-mediated gene disruption can overcome these limitations because several genes can simultaneously be disrupted without the need for many selection markers. This technology has been emerging more and more as a promising tool for different filamentous fungi and oomycetes, including many filamentous pathogens (Schuster & Kahmann, 2019), and is likely going to accelerate advances in effector biology in the near future.

Possible new roles of effectors

Although many effectors directly interact with the host, e.g. by interfering with plant defences and development, other possible functions that are not directly connected to the host plant should not be overlooked. Effectors may provide a fitness advantage at various points in the life cycle of a pathogen, which is neglected by only scoring

symptoms in infection assays under conditions that are optimal for the pathogen. For example, standard greenhouse experiments neither account for high day-night differences in temperature and humidity that pathogens are exposed to under field conditions nor for rain and wind, which might represent stress conditions that could potentially be counteracted by the use of secreted proteins with a role in protecting from desiccation and attaching spores and hyphae to the leaf surface prior to host invasion. Effectors are secreted by definition; therefore, they possibly do not only interact with the plant but also with other co-existing microorganisms including other plant colonizers (Rovenich *et al.*, 2014). Recently, the characterization of the *Z. tritici* effector Zt6, which is highly upregulated at the initial stage of infection and has a toxic effect on other microorganisms, highlighted the possibility that effectors have targets beyond the host plant (Snelders *et al.*, 2018; Kettles *et al.*, 2018). Similarly, saprophytes can interact with soil microbes via the secretion of effectors (Kombrink *et al.*, 2019). As microbiomes associated with plants under laboratory conditions can be different from plants grown under field conditions (Ottesen *et al.*, 2016), functional validation of effectors that interact with microbes might be challenging. However, key interactors of pathogens may be identified in the microbiome, as shown for *Z. tritici* and the wheat endophytes *Acremonium sclerotigenum, Penicillium olsonii, Acremonium alternatum* and *Alternaria alternata* (Latz *et al.*, 2019), which could aid the characterization of effectors with an microbe interaction-related function by introducing these interactors in infection assays.

Can effector regulation provide information on effector function?

Expression patterns of effector genes are generally thought to be related to effector function (Mirzadi Gohari *et al.*, 2015). For example, effector genes with a peak of expression during the necrotrophic switch might be suspected to act as inducers of

necrosis in *Z. tritici*. Measuring gene expression by RNA sequencing (RNA-seq) has become the standard method to study transcriptional dynamics of pathogens during host colonization (Palma-Guerrero *et al.*, 2016; Gervais *et al.*, 2017; Evangelisti *et al.*, 2017; Lanver *et al.*, 2018; Courville *et al.*, 2019). Although such transcriptomic studies are very powerful tools because they cover the full transcriptome, they usually cannot resolve gene expression at the single-cell level. For example, if *Z. tritici* is subjected to RNA-seq during wheat infection, the extracted RNA of fungal cells inside the leaf and fungal cells on the leaf surface will be pooled and the resulting expression values averaged, although these two stages probably represent distinct environments and developmental stages for the pathogen. Our single-cell expression analysis of *AvrStb6* and *Avr3D1* using fluorescent reporter genes has shown that there is a substantial expression difference between cells on the leaf surface and cells in the apoplast at a given time point. Therefore, a peak of expression at the switch to necrotrophy, as observed for both Avr proteins (Zhong *et al.*, 2017; Meile *et al.*, 2018), might be a result of a higher ratio of cells in the apoplast compared to cells on the leaf surface as host colonization progresses and not a result of a higher expression over time in individual cells inside the host. This example illustrates that expression peaks do not necessarily reflect the real cell biological context of gene regulation and therefore could lead to misinterpretations about possible effector functions. Similarly, by using a fluorescent reporter gene under the control of a native effector promoter, specialized hyphae were suggested to act as effector delivery hubs during the biotrophic phase of *Colletotrichum higginsianum* infections (O'Connell *et al.*, 2012). Therefore, single-cell expression analyses in combination with other approaches like protein-protein interaction assays and/or biochemical activity assays are likely to accelerate the characterization of effector functions and of key moments during the life cycle of pathogens.

Can advances in effector biology improve agriculture?

Molecular insights into the interaction of effectors and their targets and plant R proteins not only provide fundamental knowledge on plant and fungal biology but also tools to improve disease resistance in crops. Since effectors are often involved in suppressing defence, the identification of effector targets might reveal new components of the host immune system, which could be applied using biotechnological approaches (Lacombe *et al.*, 2010; Vleeshouwers & Oliver, 2014). The discovery of effector targets might also yield new plant susceptibility genes, which then could exploited in the breeding process (Gawehns *et al.*, 2013). The identification of virulence targets is also of great importance with respect to *R* genes that operate through the guard model because these *R* genes will only work in hosts that harbour the target/guardee, setting limits for transgenic approaches (Van der Hoorn *et al.*, 2002).

Effectors are generally easier to identify than resistance genes because pathogens are easier to manipulate and their genomes are generally smaller and easier to sequence (Van de Wouw & Idnurm, 2019). Using effector-guided breeding, effectors have already been proven to be useful for *R*-gene discovery and improving crops (Vleeshouwers & Oliver, 2014; Lenman *et al.*, 2016; Giesbers *et al.*, 2017; Van de Wouw & Idnurm, 2019). Thanks to modern biotechnological tools and marker-assisted breeding, many *R* genes can potentially be combined in a single crop variety without the need of extensive phenotyping (Barabaschi *et al.*, 2016). Alternatively, cultivar mixtures can be used with cultivars that have different repertoires of *R* genes (McDonald & Linde, 2002; Mundt, 2002). However, in-depth knowledge will be required to not only discover new sources of genetic resistance, but also to improve durability by making smart choices on which (combinations of) *R* genes to use and by

taking the evolutionary potential of pathogens into account (McDonald & Linde, 2002). The identification of the molecular bases involved in broad-spectrum resistance, the identification of *R* genes against conserved and presumably indispensable effectors, the discovery of allelic series of *R* genes to optimize the resistance spectrum and the assessment of the vulnerabilities of R proteins are important steps towards more durable disease resistance.

References

Barabaschi D, Tondelli A, Desiderio F, Volante A, Vaccino P, Valè G, Cattivelli L. 2016. Next generation breeding. *Plant Science* **242**: 3–13.

Bent AF, Mackey D. 2007. Elicitors, effectors, and *R* genes: the new paradigm and a lifetime supply of questions. *Annual Review of Phytopathology* **45**: 399–436.

Bicknell AA, Cenik C, Chua HN, Roth FP, Moore MJ. 2012. Introns in UTRs: Why we should stop ignoring them. *BioEssays* **34**: 1025–1034.

Birch PR, Boevink PC, Gilroy EM, Hein I, Pritchard L, Whisson SC. 2008. Oomycete RXLR effectors: delivery, functional redundancy and durable disease resistance. *Current Opinion in Plant Biology* **11**: 373–379.

Bray Speth E, Lee YN, He SY. 2007. Pathogen virulence factors as molecular probes of basic plant cellular functions. *Current Opinion in Plant Biology* **10**: 580–586.

Courville KJ, Frantzeskakis L, Gul S, Haeger N, Kellner R, Heßler N, Day B, Usadel B, Gupta YK, Esse HP, *et al.* 2019. Smut infection of perennial hosts: the genome and the transcriptome of the Brassicaceae smut fungus *Thecaphora thlaspeos* reveal functionally conserved and novel effectors. *New Phytologist* **222**: 1474–1492.

Evangelisti E, Gogleva A, Hainaux T, Doumane M, Tulin F, Quan C, Yunusov T, Floch K, Schornack S. 2017. Time-resolved dual transcriptomics reveal early induced *Nicotiana benthamiana* root genes and conserved infection-promoting *Phytophthora palmivora* effectors. *BMC Biology* **15**: 39.

Friesen TL, Faris JD, Solomon PS, Oliver RP. 2008. Host-specific toxins: effectors of necrotrophic pathogenicity. *Cellular Microbiology* **10**: 1421–1428.

Gawehns F, Cornelissen BJC, Takken FLW. 2013. The potential of effector-target genes in breeding for plant innate immunity. *Microbial Biotechnology* **6**: 223–229.

Gervais J, Plissonneau C, Linglin J, Meyer M, Labadie K, Cruaud C, Fudal I, Rouxel T, Balesdent MH. 2017. Different waves of effector genes with contrasted genomic location are expressed by *Leptosphaeria maculans* during cotyledon and stem

colonization of oilseed rape. *Molecular Plant Pathology* **18**: 1113–1126.

Giesbers AKJ, Pelgrom AJE, Visser RGF, Niks RE, Van den Ackerveken G, Jeuken MJW. 2017. Effector-mediated discovery of a novel resistance gene against *Bremia lactucae* in a nonhost lettuce species. *New Phytologist* **216**: 915–926.

Goodwin SB, Ben M'Barek S, Dhillon B, Wittenberg AHJ, Crane CF, Hane JK, Foster AJ, Van der Lee TAJ, Grimwood J, Aerts A, *et al.* 2011. Finished genome of the fungal wheat pathogen *Mycosphaerella graminicola* reveals dispensome structure, chromosome plasticity, and stealth pathogenesis. *PLoS Genetics* **7**: e1002070.

Grandaubert J, Bhattacharyya A, Stukenbrock EH. 2015. RNA-seq-based gene annotation and comparative genomics of four fungal grass pathogens in the genus *Zymoseptoria* identify novel orphan genes and species-specific invasions of transposable elements. *G3: Genes, Genomes, Genetics* **5**: 1323–33.

Haas BJ, Zeng Q, Pearson MD, Cuomo CA, Wortman JR. 2011. Approaches to fungal genome annotation. *Mycology* **2**: 118–141.

Van der Hoorn RA., De Wit PJG., Joosten MHA. 2002. Balancing selection favors guarding resistance proteins. *Trends in Plant Science* **7**: 67–71.

Kema GHJ, Mirzadi Gohari A, Aouini L, Gibriel HAY, Ware SB, van den Bosch F, Manning-Smith R, Alonso-Chavez V, Helps J, Ben M'Barek S, *et al.* 2018. Stress and sexual reproduction affect the dynamics of the wheat pathogen effector AvrStb6 and strobilurin resistance. *Nature Genetics* **50**: 375–380.

Kema GHJ, van Silfhout CH. 1997. Genetic variation for virulence and resistance in the wheat- *Mycosphaerella graminicola* pathosystem III. Comparative seedling and adult plant experiments. *Phytopathology* **87**: 266–272.

Kettles GJ, Bayon C, Sparks CA, Canning G, Kanyuka K, Rudd JJ. 2018. Characterization of an antimicrobial and phytotoxic ribonuclease secreted by the fungal wheat pathogen *Zymoseptoria tritici*. *New Phytologist* **217**: 320–331.

Kombrink A, Rovenich H, Shi-Kunne X, Rojas-Padilla E, van den Berg GCM, Domazakis E, de Jonge R, Valkenburg D-J, Sánchez-Vallet A, Seidl MF, *et al.* 2017. *Verticillium dahliae* LysM effectors differentially contribute to virulence on plant hosts. *Molecular Plant Pathology* **18**: 596–608.

Kombrink A, Tayyrov A, Essig A, Stöckli M, Micheller S, Hintze J, van Heuvel Y, Dürig N, Lin C, Kallio PT, *et al.* 2019. Induction of antibacterial proteins and peptides in the coprophilous mushroom *Coprinopsis cinerea* in response to bacteria. *The ISME Journal* **13**: 588–602.

Lacombe S, Rougon-Cardoso A, Sherwood E, Peeters N, Dahlbeck D, van Esse HP, Smoker M, Rallapalli G, Thomma BPHJ, Staskawicz B, *et al.* 2010. Interfamily transfer of a plant pattern-recognition receptor confers broad-spectrum bacterial resistance. *Nature Biotechnology* **28**: 365–369.

Lanver D, Müller AN, Happel P, Schweizer G, Haas FB, Franitza M, Pellegrin C, Reissmann S, Altmüller J, Rensing SA, *et al.* 2018. The biotrophic development of *Ustilago maydis* studied by RNA-seq analysis. *The Plant Cell* **30**: 300–323.

Latz MAC, Jensen B, Collinge DB, Jørgen Lyngs Jørgensen H. 2019. Identification of two endophytic fungi that control Septoria tritici blotch in the field, using a structured

screening approach. *Biological Control*: 104128.

Lenman M, Ali A, Mühlenbock P, Carlson-Nilsson U, Liljeroth E, Champouret N, Vleeshouwers VGAA, Andreasson E. **2016**. Effector-driven marker development and cloning of resistance genes against *Phytophthora infestans* in potato breeding clone SW93-1015. *Theoretical and Applied Genetics* **129**: 105–115.

McDonald BA, Linde C. **2002**. Pathogen population genetics, evolutionary potential, and durable resistance. *Annual Review of Phytopathology* **40**: 349–379.

Meile L, Croll D, Brunner PC, Plissonneau C, Hartmann FE, McDonald BA, Sánchez-Vallet A. **2018**. A fungal avirulence factor encoded in a highly plastic genomic region triggers partial resistance to septoria tritici blotch. *New Phytologist* **219**: 1048–1061.

Mirzadi Gohari A, Ware SB, Wittenberg AHJ, Mehrabi R, Ben M'Barek S, Verstappen ECP, van der Lee TAJ, Robert O, Schouten HJ, de Wit PPJGM, *et al.* 2015. Effector discovery in the fungal wheat pathogen *Zymoseptoria tritici*. *Molecular Plant Pathology* **16**: 931–945.

Mundt CC. **2002**. Use of multiline cultivars and cultivar mixtures for disease management. *Annual Review of Phytopathology* **40**: 381–410.

O'Connell RJ, Thon MR, Hacquard S, Amyotte SG, Kleemann J, Torres MF, Damm U, Buiate EA, Epstein L, Alkan N, *et al.* 2012. Lifestyle transitions in plant pathogenic *Colletotrichumy* fungi deciphered by genome and transcriptome analyses. *Nature Genetics* **44**: 1060–1065.

Ottesen AR, Gorham S, Reed E, Newell MJ, Ramachandran P, Canida T, Allard M, Evans P, Brown E, White JR. **2016**. Using a control to better understand phyllosphere microbiota. *PLOS ONE* **11**: e0163482.

Palma-Guerrero J, Torriani SFF, Zala M, Carter D, Courbot M, Rudd JJ, McDonald BA, Croll D. **2016**. Comparative transcriptomic analyses of *Zymoseptoria tritici* strains show complex lifestyle transitions and intraspecific variability in transcription profiles. *Molecular plant pathology* **17**: 845–859.

Perez-Quintero AL, Szurek B. **2019**. A decade decoded: spies and hackers in the history of TAL effectors research. *Annual Review of Phytopathology* **57**: 459–481.

Plissonneau C, Hartmann FE, Croll D. **2018**. Pangenome analyses of the wheat pathogen *Zymoseptoria tritici* reveal the structural basis of a highly plastic eukaryotic genome. *BMC Biology* **16**: 5.

Plissonneau C, Stürchler A, Croll D. **2016**. The evolution of orphan regions in genomes of a fungal pathogen of wheat. *mBio* **7**: e01231-16.

Rep M, Van Der Does HC, Meijer M, Van Wijk R, Houterman PM, Dekker HL, De Koster CG, Cornelissen BJC. **2004**. A small, cysteine-rich protein secreted by *Fusarium oxysporum* during colonization of xylem vessels is required for *I-3*-mediated resistance in tomato. *Molecular Microbiology* **53**: 1373–1383.

Rep M, Meijer M, Houterman PM, van der Does HC, Cornelissen BJC. **2005**. *Fusarium oxysporum* evades *I-3*-mediated resistance without altering the matching avirulence gene. *Molecular Plant-Microbe Interactions* **18**: 15–23.

Rovenich H, Boshoven JC, Thomma BP. **2014**. Filamentous pathogen effector functions:

of pathogens, hosts and microbiomes. *Current Opinion in Plant Biology* **20**: 96–103.

Sánchez-Vallet A, Fouché S, Fudal I, Hartmann FE, Soyer JL, Tellier A, Croll D. **2018**. The genome biology of effector gene evolution in filamentous plant pathogens. *Annual Review of Phytopathology* **56**: 21–40.

Schuster M, Kahmann R. **2019**. CRISPR-Cas9 genome editing approaches in filamentous fungi and oomycetes. *Fungal Genetics and Biology* **130**: 43–53.

Skamnioti P, Ridout CJ. **2005**. Microbial avirulence determinants: Guided missiles or antigenic flak? *Molecular Plant Pathology* **6**: 551–559.

Snelders NC, Kettles GJ, Rudd JJ, Thomma BPHJ. **2018**. Plant pathogen effector proteins as manipulators of host microbiomes? *Molecular plant pathology* **19**: 257–259.

Toruño TY, Stergiopoulos I, Coaker G. **2016**. Plant-pathogen effectors: cellular probes interfering with plant defenses in spatial and temporal manners. *Annual Review of Phytopathology* **54**: 419–441.

Vleeshouwers VGAA, Oliver RP. **2014**. Effectors as tools in disease resistance breeding against biotrophic, hemibiotrophic, and necrotrophic plant pathogens. *Molecular Plant-Microbe Interactions* **27**: 196–206.

de Wit PJGM. **1992**. Molecular characterization of gene-for-gene systems in plant-fungus interactions and the application of avirulence genes in control of plant pathogens. *Annual Review of Phytopathology* **30**: 391–418.

de Wit PJGM. **2016**. Apoplastic fungal effectors in historic perspective; a personal view. *New Phytologist* **212**: 805–813.

Van de Wouw AP, Idnurm A. **2019**. Biotechnological potential of engineering pathogen effector proteins for use in plant disease management. *Biotechnology Advances* **37**: 107387.

Zhang Y, Sachs MS. **2015**. Control of mRNA stability in fungi by NMD, EJC and CBC factors through 3'UTR introns. *Genetics* **200**: 1133–48.

Zhong Z, Marcel TC, Hartmann FE, Ma X, Plissonneau C, Zala M, Ducasse A, Confais J, Compain J, Lapalu N, *et al.* 2017. A small secreted protein in *Zymoseptoria tritici* is responsible for avirulence on wheat cultivars carrying the *Stb6* resistance gene. *New Phytologist* **214**: 619–631.

Acknowledgements

This thesis is the result of a concerted effort involving many people who supported me in various ways during several years. I would like to especially thank the following key people:

Dr. Andrea Sánchez Vallet for all kinds of support and all the time you invested in our project. Without your dedication and passion for original and authentic research, the outcome of this thesis would without doubt be dramatically different, both in content and quality. Your scientific and mental support and your empathy were crucial for me not only to overcome difficult times but also to confidently tackle the high-risk subprojects that made my PhD so thrilling.

Prof. Dr. Bruce McDonald for providing the excellent opportunity to join the Plant Pathology Group, for all the support, advice and for trusting even in unexpected projects that emerged from the original one.

Prof. Dr. Olivier Voinnet for your interest in my project and several useful discussions, for accepting to be a co-examiner and for giving me the opportunity to connect with your team.

Prof. Dr. Antonio Di Pietro for agreeing to be a co-examiner and to come all the way to Zürich and for the fruitful discussion during your previous visit to the group.

Jules Peter, Zoe Bernasconi, Guido Puccetti and Zacharie Ngamenie for your amazing contributions to several projects that resulted from your work.

Ziqi Shen, Anna Spescha, Barryette Oberholzer, Susanne Meile, Tiziana Vonlanthen, Julie Gasser, Claudia Fuchs, Natasa Radulovic for your much appreciated technical assistance.

The (former) members of the Plant Pathology Group, especially Julien Alassimone, Marcello Zala, Parvathy Krishnan, Alessio Bernasconi, Clémence Plissonneau and Daniel Croll for all your help,advice and the great time I had in this Group.

Finally, my family and all my friends from LFW and from Züri Oberland for all the fun we had and hopefully will have in the future.

Curriculum Vitae

Lukas Meile

Born 25th May 1989

Citizen of Mosnang (SG), Switzerland

2015 – 2019 Doctor of Sciences (Dr. Sc. ETH Zurich)

ETH Zurich

Plant Pathology Group; Institute of Integrative Biology

Title: Functional analyses of candidate QTL genes involved in fungal virulence

Supervisor: Prof. Dr. Bruce McDonald

2013-2014 Master of Science ETH in Biology (MSc ETH Biology)

ETH Zurich

Specialisation: Plant Biology

Thesis Title: Characterisation of candidate resistance and susceptibility genes in cassava cultivars of contrasting resistance to cassava bacterial blight.

Supervisors: Dr. Hervé Vanderschuren & Dr. Emily McCallum. Plant Biotechnology Group.

2009-2013 Bachelor of Science ETH in Biology (BSc ETH Biology)

ETH Zurich

Scientific contributions

Published articles

Meile L, Croll D, Brunner PC, Plissonneau C, Hartmann FE, McDonald BA, Sánchez-Vallet A. 2018. A fungal avirulence factor encoded in a highly plastic genomic region triggers partial resistance to septoria tritici blotch. *New Phytologist* **219**: 1048–1061.

Krishnan P, **Meile L**, Plissonneau C, Ma X, Hartmann FE, Croll D, McDonald BA, Sánchez-Vallet A. 2018. Transposable element insertions shape gene regulation and melanin production in a fungal pathogen of wheat. *BMC Biology* **16**: 78.

Yates S, Mikaberidze A, Krattinger SG, Abrouk M, Hund A, Yu K, Studer B, Fouche S, **Meile L**, Pereira D, Karisto P, McDonald BA. 2019. Precision phenotyping reveals novel loci for quantitative resistance to septoria tritici blotch. Plant Phenomics **2019**: 1–11.

Inglin RC, Stevens MJA, **Meile L**, Lacroix C, Meile L. 2015. High-throughput screening assays for antibacterial and antifungal activities of *Lactobacillus* species. Journal of Microbiological Methods 114: 26–29.

Oral Presentations

Epigenetic control of effector genes in the wheat pathogen *Zymoseptoria tritici*. 30th Fungal Genetics Conference, Pacific Grove, CA, USA, March 2019.

Epigenetic control of effector gene expression in *Zymoseptoria tritici*. Host-Microbe Genomics Meeting. Zürich, Switzerland, September 2018.

Isolate-specific recognition triggers quantitative resistance in wheat. Zurich Mycology Symposium, Zürich, Switzerland, January 2018.

Recognition of a highly polymorphic avirulence gene in *Zymoseptoria tritici* contributes to resistance in wheat. Host-Microbe Genomics Meeting. Neuchâtel, Switzerland, September 2017.

Recognition of a highly polymorphic avirulence gene in *Zymoseptoria tritici* contributes to resistance in wheat. *Zymoseptoria tritici* Community Meeting. Kiel, Germany, September 2017.

Poster presentations

Epigenetic control of effector genes in the wheat pathogen *Zymoseptoria tritici*. 30th Fungal Genetics Conference, Pacific Grove, CA, USA, March 2019.

Epigenetic control of effector gene expression in *Zymoseptoria tritici*. Host-Microbe Genomics Meeting. Zürich, Switzerland, September 2018.